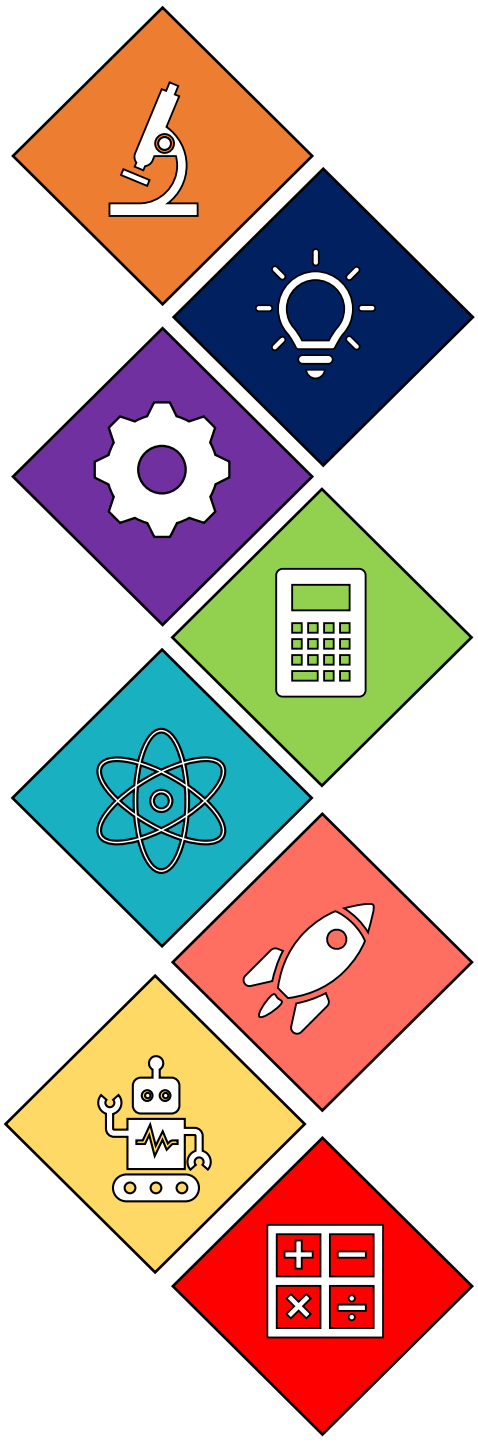

OFFICE OF UNDERGRADUATE RESEARCH
LAMAR UNIVERSITY

WELCOMES YOU

to the Tenth Annual

Texas STEM Conference

Science
Technology
Engineering
Mathematics
Medical

Archer Building

November 5th, 2022

LAMAR UNIVERSITY

Message from Lamar University's Dean of College of Arts and Sciences Dr. Lynn Maurer

The College of Arts and Sciences is proud of the research undertaken by its outstanding students in collaboration with our committed faculty. Together your partnerships advance the wealth of knowledge that grows from the breadth of our disciplines from natural sciences to behavioral sciences and humanities. Students who participate in Undergraduate Research at Lamar University graduate among the best prepared in Texas and the nation. I am proud of all of the awards which have been won, but in addition every research project which has been undertaken through OUR reflects your excellence in collaboration and discovery. Enjoy your time today and know that the College of Arts and Sciences is honored by the research of its scholars, students and faculty alike!

LAMAR UNIVERSITY
MEMBER THE TEXAS STATE UNIVERSITY SYSTEM™

YOUR Moment IS HERE

Message from Lamar University's Dean of Engineering Dr. Brian Craig

On behalf of the Lamar University College of Engineering, I welcome all Lamar University students, faculty, mentors and staff, students from other universities and colleges around the country, and our distinguished panel of speakers to the 10th Annual Texas STEM Conference. What a great event to share the results of your hard work on your projects! Each of your projects look amazing and I look forward to hearing many of your talks. I applaud you for undertaking undergraduate research. It truly gives you insight into a whole different side of learning that most of your fellow students are not exposed to. I hope each of you enjoy the fun and fellowship of the 10th Annual Texas STEM conference!

LAMAR UNIVERSITY
MEMBER THE TEXAS STATE UNIVERSITY SYSTEM™

YOUR Moment IS HERE

Welcome to the 10th Annual Texas STEM Conference at Lamar University

Dr. Cristian Bahrim - Director of O.U.R.

This year the Texas STEM conference celebrates its tenth edition with a plethora of special guests. The participation to this conference grew every year. For this edition, we had a more diverse content than ever before, with eleven schools outside Lamar presenting through their undergraduate and graduate students, including Ph.D. candidates and professionals. Several Lamar alumni joined us and presented the richness of their research efforts. We welcomed young researchers from UT Austin, Rice University, UT Arlington and UTMB-Galveston from Texas, University of Arkansas-Fayetteville, Cornell University, Colorado School of Mines, Auburn University, LSU, Arizona State University. The Lamar alumni were invited guests, but students from UTMB and UT Arlington, as well as Dr. Okafor, a Research Scholar from the University of Arkansas-Fayetteville, requested to present at our conference with their direct submission through the conference portal, simply because they knew about the quality of our event from previous editions. We always hoped and worked to increase Lamar's visibility through fine research conducted and disseminated by our students. This year, we had three special guest speakers: Dr. Jay Prigmore, a Lamar alumnus, cohort of 2010, is an accomplished Electrical Quality Engineer and Technical Manager at Google Inc. Dr. Prigmore talked about the key role of circuit breakers in protecting high power systems. Mr. Alexander Bahrim, a recent electrical engineering graduate, who is now Systems Engineer at NASA – Johnson Space Flight Center has presented the newest NASA project "Artemis – Back to the Moon". Mr. Monir Hossain, is a Sr. Engineer at Entergy, and presented the challenges faced by one of the major Energy Companies in the United States. With this edition, our conference got an international dimension, by having as invited speaker Dr. Raktim Haldar, an Alexander von Humboldt fellow from Leibniz University of Hannover, Germany, who talked about quantum photonic entanglement, a topic which has received great attention with the most recent Nobel Prize in Physics awarded just one month ago. But more important than the two exceptional focused sessions on Bioengineering and Medical Research, and Material Sciences and Applications tracks, which offered top notch research done in all those top universities listed above, we have been very proud to welcome seven SURF students who presented their summer research experience here, at Lamar, 14 undergraduate and 15 graduate presentations offered in poster or breakout sessions. 25 out these 29 presentations were offered by our Lamar students, from all the STEM academic areas. For the first time we welcome both Beck fellows presenting exciting research developed in Belize (Ms. Angel Flowers) and University of Ottawa (Mr. Zaid Mohammed) during the past summer. This year more than 150 people attended in-person and online during a marathon conference of twelve non-stop hours full of quality research. Eleven worthy Lamar students (7 undergrads and 4 grads) have received awards for their fine research and quality presentations.

Office Information:

Chemistry Suite 115
Dr. Cristian Bahrim – Chem 115B / Ms. Jenna Erwin – Chem 115A
cbahrim@lamar.edu - ext. 8290 / jerwin6@lamar.edu - ext. 8430

The Office of Undergraduate Research - Advisory Board

Dr. Stefan Andrei – Professor of Computer Science

Dr. Robert Kelley Bradley – Assistant Professor of Industrial Engineering

Dr. Bianca Easterly – Associate Professor of Political Science

Dr. Gina Hale – Associate Professor of Nursing

Dr. Matthew Hoch - Associate Professor of Biology

Dr. Alyse Jordan – Head of Research, Engagement & Learning at the Mary and Gray Library

Dr. Edythe Kirk - Associate Professor of Psychology

Dr. Nicki Michalski – Associate Professor of Communication

Dr. Lekeitha Morris – Associate Professor of Speech and Hearing

Dr. Gevorg Sargsyan – Assistant Professor of Finance

Dr. Thinesh Selvaratnam – Assistant Professor of Civil and Environmental Engineering

Dr. Mamta Singh – Associate Professor of Teacher Education

Dr. Freddie Titus – Associate Professor of Teacher Education, Vice President for Diversity Inclusion and Community Relations at Lamar University

Dr. Chun-Wei Yao – Associate Professor of Mechanical Engineering

Mr. Juan Zabala – Vice President for University Advancement and Chief Officer of the Lamar University Foundation

Co-Chairs of the 10th Texas STEM Conference

Dr. Stefan Andrei – Professor of Computer Science

Dr. Robert Kelley Bradley – Assistant Professor of Industrial Engineering

Dr. Matthew Hoch - Associate Professor of Biology

Dr. Thinesh Selvaratnam – Assistant Professor of Civil and Environmental Engineering

Dr. Chun-Wei Yao – Associate Professor of Mechanical Engineering

OFFICE OF UNDERGRADUATE RESEARCH
LAMAR UNIVERSITY

WELCOME TO THE 10th ANNUAL TEXAS STEM CONFERENCE

All events will take place on Zoom platform with **ID: 879-918-4160** *and* **password 88888**

8:00 AM	Registration Opens in Archer-Physics bldg.
8:20 – 8:50 AM	Poster Session 1 (*co-Chairs Dr. Selvaratnam and Dr. He*)
8:50 AM	Welcoming Remarks Dr. Cristian Bahrim, Director of O.U.R.
9:00 AM	Introduction of Our Guest Speaker, Dr. Jay Prigmore Electrical Quality Engineer and Technical Program Manager at Google Inc.
9:50 AM	Recognition of Dr. Jay Prigmore
9:50 – 10:00 AM	**Coffee Break**

O.U.R. Sponsored Research
2022 Summer Undergraduate Research Fellowship (SURF)
Chair: Dr. Cristian Bahrim

10:00 AM	**Melissa Tan** – Major in Civil and Environmental Engineering Major in Civil and Environmental Engineering Mentor: **Dr. Thinesh Selvaratnam** Department of Civil and Environmental Engineering "Removal of Heavy Metals from Municipal Landfill Leachate using *Galdieria sulphuraria*"
10:15 AM	**David Matherne** Major in Biology Mentors: **Dr. Evgeny Romashets** and **Dr. Cristian Bahrim** Department of Physics "Heliospheric Storms"

10:30 AM	**Kiley Mazdra** – Major in Mechanical Engineering Mentors: **Dr. Evgeny Romashet**s and **Dr. Cristian Bahrim** Department of Physics "The Physics of Active Longitudes and Their Impact on Earth through the Interplanetary Coronal Mass Ejection They Produce."
10:45 AM	**Ian Sisson** – Major in Chemistry Mentor: **Dr. Paul Bernazzani** Department of Chemistry and Biochemistry "Iron-Cellulose Bioplastic Nanocomposite Research."
11:00 AM	**Jacob WilliamSmith** – Major in Mechanical Engineering Mentor: **Dr. Sushil Doranga** Department of Mechanical Engineering "Evaluation of Pin Fretting in the Electronic Connectors Using the Vibration Shaker."
11:15 AM	**Lily Yoder** – Major in Psychology Mentor: **Dr. Edythe Kirk** Department of Psychology "The Effects of Positive Mood and Stereotype Threat on Memory Recall."
11:30 AM	**Rafael Gutierrez** – Major in Mechanical Engineering and Physics Mentor: **Dr. Rafael de la Madrid** Department of Physics "Dynamic Wetting and Dewetting in Non-Uniform Solids."
11:45 – 12:00 PM	**Special Invited Speaker – Dr. Raktim Haldar** Alexander von Humboldt (AvH) Postdoctoral Fellow, (Leibniz University) Raman-Charpak Fellow (RCF), (CNRS, Univ. Paris-Saclay), Postdoc at Photonics Quantum Technologies Group, Hannover Centre for Optical Technologies, Leibniz Universität Hannover, Nienburger Straße 17, 30167 Hannover, Germany "*Fully on-chip Electrically-pumped Laser-integrated Two and High-dimensional Entangled Photon Pair Source for Quantum Information Processing*."
12:00 – 12:30 PM	**Lunch Break** – **Group photo at 12:15pm in the Quad**

Poster Session II 12:30 – 1:00 PM

Chair: Dr. Berna Eren Tokgoz and Dr. Stefan Andrei

David Beck Fellow Session

Chair: Dr. Matthew Hoch

1:00 PM **Angel Flowers –** Beck Fellow 2022 – Major in Biology – Lamar University
Mentor: Dr. Matthew Hoch

"*Tardigrades in Belize*."

1:15 PM **Zaid Mohammed –** Beck Fellow 2022 – Major in Biology – Lamar University
Mentor: Dr. Ian Lian

"*The Role of Autophagy Receptors in Cancer*."

Focus Session 1 – Modern Trends in Bioengineering and Medical Science

Chair: Dr. Lauren Richardson

1:30 PM **Kayla Meyers** – Major in Biomedical Engineering – UT Arlington
Mentor: Dr. Young-Tae Kim - Department of Biomedical Engineering, College of Engineering

"Melanoma Chemotherapy Treatment using Modified Cellulose-Based Injectable Hydrogels Combined with Temozolomide."

1:45 PM **Alexus Locke** – Clinical Research Coordinator on the Pediatric Emergency Medicine (PEM) Research Team at Children's Healthcare of Atlanta, GA

"Unraveling the Role of Tumor Extracellular Vesicles in Angiogenesis to Inform the Design of Biomimetic Electronic Devices."

Research done at Cornell University, Robert Frederick Smith School of Chemical and Biomolecular Engineering

2:00 PM **Ben Morales** – Ph.D. candidate at Louisiana State University, LA

"*Biomechanics Research from Lamar to LSU.*"

2:15 – 2:25 PM **Coffee Break**

OFFICE OF UNDERGRADUATE RESEARCH
LAMAR UNIVERSITY

Focus Session 2 – Trends in Material Science and Engineering

Chair: Dr. Chun-Wei Yao

2:25 PM **Dr. Okafor Ekene Gabriel** – Research Scholar at University of Arkansas –Fayetteville, AR
Supervisor: Dr. David Ryan Huitink, Department of Mechanical Engineering

"*Laminated Transcient Liquid Phase Preform and Bond Fabrication and Characterization for High Temperature Power Electronics Application*."

2:45 PM **Nurul Azam** – Ph. D. candidate at Auburn University, AL

"*Laser-based Bottom-Up Synthesis of Monolayer 2D Crystals with Tunable.*"

3:00 PM **Dylan Palmer** – Ph. D. candidate at Colorado School of Mines, CO

"*Thermal Fatigue of Secondary Cooling Support Rolls during Continuous Casting*."

3:15 PM **Daniel Quispe** – Ph. D. candidate at Northwestern University, IL
Supervisor: Dr. Mel Ulmer – Lab of Ulmer Research Group,
Department of Physics and Astronomy.

"*Magnetic Smart Materials*."

3:30 PM **Tyler Nelson** – Ph. D. candidate at Rice University, TX

"*Construction and Validation of a Multimodal 3D Single-Molecule Super-Resolution Microscope for Whole Cell Imaging*."

3:45 PM **David Quispe** – Ph. D. candidate at Arizona State University, AZ

"*Solar Cells Efficiency with Perovskite Materials.*"

4:00 – 4:15 PM **Coffee Break**

OFFICE OF UNDERGRADUATE RESEARCH
LAMAR UNIVERSITY

Poster Session III 4:00 – 4:30 PM

Chair: Dr. Stefan Andrei and Dr. Ian Lian

Breakout Session 1 4:30 – 5:30 p.m.

Chair: Dr. Kelley Bradley

Archer 108

4:30 PM

Rebekah Schilberg
University of Texas at Austin

"*Ergonomic Design Process of the Austin Formula SAE*."

4:45 PM

Rahagir Ridwan Anik
Co-Author: Kalen Baker
Mentor: **Dr. Ping He**
Department of Mechanical Engineering, Lamar University

"*An Explanation of Wetting Transitions between Cassie-Baxter and Wenzel States on Reentrant Micropatterned Surfaces*."

5:00 PM

Rishi Bharadwaj[1]
Mentor: **Dr. Cristian Bahrim**[2]
[1]Phillip Drayer Department of Electrical Engineering
[2]Opto-Electronics Laboratory, Department of Physics, Lamar University

"*Comparison of the Interference Patterns between Non-Coherent and Coherent Laser Beams Illuminating the Same Dielectric Surface*."

5:15 PM

Hari Lal Kharel
Mentor: **Dr. Thinesh Selvaratnam**
Department of Civil and Environmental Engineering, Lamar University

"*Bioremediation of Lead Using Galdieria sulphuraria.*"

OFFICE OF UNDERGRADUATE RESEARCH
LAMAR UNIVERSITY

Breakout Session 2 4:30 – 5:30 p.m.

Chair: Dr. Matthew Hoch

Archer 107

4:30 PM

Negar Saraei
Mentors: **Dr. Thinesh Selvaratnam**[1] and **Dr. Berna Tokgoz**[2]
[1]Department of Civil and Environmental Engineering
[2]Industrial and System Engineering, Lamar University

"*Developing a Resilience Framework for Jefferson County, Texas."*

4:45 PM

Nader Madkour[1]
Co-author: **Dr. Reda Amer** and **Dr. Berna Eren Tokgoz**[2]
Mentor: **Dr. Berna Eren Tokgoz**[1]
[1]Department of Industrial and Systems Engineering, Lamar University
[2]Department of Earth and Space Sciences, Lamar University

"*A Critical Approach Towards a Change Detection Framework for Assessing Soil Degradation Rates."*

5:00 PM

Prasad Pawar[1,2]
Mentor: **Dr. Clayton Jeffryes**[1,2,3]
[1]Nanobiomaterials and Bioprocessing Laboratory (NABLAB),
Dan F. Smith Department of Chemical Engineering, Lamar University
[2]Center for Midstream Management and Science, Lamar University
[3]Center for Advances in Water & Air Quality, Lamar University

"*Demulsification of Tight Crude Oil-Water Emulsions Under Microwave Radiation in Presence of Chemical Demulsifiers*."

5:15 PM

Premkumar Ravishankar[1]
Co-Authors: **Dr. Seokyon Hwang**[3] and **Dr. Jing Zhang**[2]
Mentor: **Dr. Berna Eren-Tokgoz**[1]
[1]Department of Industrial and Systems Engineering
[2]Department of Computer Science
[3]Construction Management Program
Lamar University

"*Increasing The Oil and Gas Pipeline Resiliency using Image Processing Algorithm*."

5:30 – 5:40 PM **Coffee Break**

Keynote Speaker

The 10th Annual Texas STEM Conference

Archer – Physics Building

November 5, 2022

9:00 – 10:00 a.m.

Dr. Jay Prigmore

Electrical Quality Engineer
Technical Program Manager
at Google Inc.

Biography

Dr. Jay Prigmore received his bachelor's degree in electrical engineering from Lamar University and his M.S. and Ph.D. degrees in electrical engineering from Arizona State University. His research focus for all three degrees was in Power Engineering.

He is presently employed at Google Inc. as an Electrical Quality Engineer - Technical Program Manager (TPM) but began his Google employment as an Electrical Field Reliability - TPM. Prior to his employment at Google Inc., he was employed by Exponent Inc. and performed numerous failure analysis and root cause investigations on electrical power equipment. Upon graduation he was employed at G&W Electric Company where he was responsible for short-circuit protection devices, their manufacture, and applications.

Dr. Prigmore developed a peer-reviewed arc flash mitigation device which won the "product of the year" in electrical safety. He is a founding and principal member of NFPA 78 and 1078 which provide guidance on performing electrical inspections and the qualifications of electrical inspectors, respectively. Dr. Prigmore has published more than 20 peer-reviewed articles and has written two book chapters. He is actively involved in IEEE standards meetings, NFPA committees, and CIGRE workgroups. Dr. Prigmore is a licensed professional engineer in various states, and he is certified to climb wind turbines.

Keynote Speaker

The 10th Annual Texas STEM Conference

Archer – Physics Building

November 5, 2022

9:00 – 10:00 a.m.

Dr. Jay Prigmore

Electrical Quality Engineer
Technical Program Manager
at Google Inc.

Solid-State Circuit Breakers - An Introduction to Their Technical, Operational and Application Benefits

Solid-state circuit breakers (SSCBs) recently entered the marketplace for certain low-voltage applications and have multiple attractive technical and performance improvements over their mechanical counterparts. These performance improvements are achieved primarily by the SSCB's microsecond switching speed as compared to a mechanical circuit breaker's (MCB's) switching speed in milliseconds. Their speed advantage is due to the solid state circuit breaker breaking the circuit path with a semiconductor switch. However, there are operational trade-offs to utilizing a SSCB instead of a MCB. For example, heat generation through the semiconductor switch is greater than that of mechanical circuit breaker contacts which results in increased power losses. However, in certain applications, the benefits of using a SSCB may outweigh the disadvantages making the SSCB a viable option to consider for industrial applications - especially as the technology matures.

Keynote Speaker

The 10th Annual Texas STEM Conference

Archer – Physics Building

November 5, 2022

11:45 a.m. – 12:00 p.m.

Dr. Raktim Haldar

Institute of Photonics (IOP), Leibniz University Hannover, Germany Hannover Centre for Optical Technologies (HOT), Leibniz Univ. Hannover, Germany

Biography

Dr. Raktim Haldar was born in Kolkata, India. He is currently a postdoctoral researcher at the Institute of Photonics, Leibniz Universität Hannover since 2020, and an Alexander von Humboldt Fellow at the same place since 2021. His research interests include integrated and silicon photonics, fiber-optics, nanophotonics and plasmonics, nonlinear optics, quantum photonic technologies, quantum neural network, etc. Previously, in September 2022, he was a visiting scientist at Paris Centre for Quantum Computing, Sorbonne University. In 2017-18, he was a Raman-Charpak Fellow and worked on quantum guidonics at CNRS/C2N, University Paris-Saclay, France. He obtained his Ph.D. and M. Tech. from Electronics and Electrical Communication department, Indian Institute of Technology Kharagpur in 2019 and 2013, respectively. He is a reviewer of *Nature Photonics*, *Phys. Rev. Lett.*, *Phys. Rev. Research*, *Phys. Rev. X.*, *Phys. Rev. A.*, *Phys. Rev. Applied*, *Applied Optics*, *Optics Express*, *JOSA B*, *Photonic Research*, *IEEE Photonics Journal*, *SPIE journal Optical Engineering*, *MDPI journal Micromachines*, etc. He is a life member of SPIE, OSA, IEEE. He served as the President of IITKGP OSA Student Chapter from 2018 to 2019.

In his spare time, Dr. Haldar is a painter, photographer, and a science enthusiast. He writes popular science articles, stories, and columns in Bengali and English to disseminate interesting scientific facts and knowledge among children.

Keynote Speaker

The 10th Annual Texas STEM Conference

Archer – Physics Building

November 5, 2022

11:45 a.m. – 12:00 p.m.

Dr. Raktim Haldar

Institute of Photonics (IOP), Leibniz University Hannover, Germany Hannover Centre for Optical Technologies (HOT), Leibniz Univ. Hannover, Germany

Fully on-chip Electrically Pumped Laser-integrated Two and High-dimensional Entangled Photon Pair Source for Quantum Information Processing

Integrated photonics has recently become a leading platform for the realization and processing of optical entangled quantum states in compact, robust and scalable chip formats with applications in long-distance quantum-secured communication, quantum-accelerated information processing, and non-classical metrology. However, the quantum light sources developed so far have relied on external bulky excitation lasers making them impractical, not reproducible prototype devices, hindering scalability and the transfer out of the lab into real-world applications. Here we demonstrate a fully integrated quantum light source, which overcomes these challenges through the combined integration of a laser cavity, a highly efficient tunable noise suppression filter 55 dB exploiting the Vernier effect, and a nonlinear microring for entangled photon pair generation through spontaneous four-wave mixing. The hybrid quantum source employs an electrically pumped InP gain section and a Si3N4 low-loss microring filter system, and demonstrates high performance parameters, i.e., a pair emission over four resonant modes in the telecom band (bandwidth ~1 THz), and a remarkable pair detection rate of ~620 Hz at a high coincidence-to-accidental ratio of ~80. The source directly creates high-dimensional frequency-bin entangled quantum states (qubits/qudits), verified by quantum interference measurements with visibilities up to 96% (violating Bell-inequality) and by density matrix reconstruction through state tomography showing fidelities of up to 99%. Our approach, leveraging a hybrid photonic platform, enables commercial-viable, low-cost, compact, lightweight, and field-deployable entangled quantum sources, quintessential for practical, out-of-lab applications, e.g., in quantum processors and quantum satellite communications systems.

Invited Speaker 5:40 – 6:00 PM

Mr. Alexander Bahrim

NASA Systems Engineering – Johnson Space Flight Center

Invited Speaker 6:00 – 6:30 PM

Mr. Monir Hossain

Senior Power Systems Engineering at Entergy

Awards Ceremony 6:30 – 7:00 PM

OFFICE OF UNDERGRADUATE RESEARCH
LAMAR UNIVERSITY

Awards and Prizes

At The 10th Texas STEM Conference

Best SURF STEM Project for year 2022:

- **First place: $200**
- **Runner-up: $150**

Best SURF STEM Presentation at the Texas STEM Conference: $200

Best Poster Presentation for Undergraduate Research:

- **First place: $200**
- **Second place: $150**
- **Third place: $100**

Best Poster Presentation at Master level: $200

Best Poster Presentation at Doctoral level: $200

Best Talk at Undergraduate Level for non-OUR Sponsored Research: $200

Best Talk at Doctoral Level:

- **First place: $200**
- **Runner-up: $150**

10th Texas STEM Award Winners

Best SURF STEM Projects for Year 2022

Winner:
Lily Yoder – major in Psychology
Research in Human Behavior
"The Effects of Positive Mood and Stereotype Threat on Memory Recall."
Mentor: Dr. Edythe Kirk

Runner Up:
Ian Sisson – major in Chemistry
Research in Sustainable Materials – Polymers
"Iron-Cellulose Bioplastic Nanocomposite Research."
Mentor: Dr. Paul Bernazzani

Best SURF STEM Presentation at the Texas STEM Conference

Winner:
Ian Sisson – major in Chemistry
Research in Sustainable Materials – Polymers
"Iron-Cellulose Bioplastic Nanocomposite Research."
Mentor: Dr. Paul Bernazzani

Best Poster Presentation for Undergraduate Research

First place:
David Matherne – major in Biology
Research in Geo-space Sciences
"Interplanetary Magnetic Cloud of April 17, 1999."
Mentors: Dr. Evgeny Romashets and Dr. Cristian Bahrim

Second place:
Tarin Hill – major in Chemistry
Research in Chemistry
"Exploiting the hydrogen storage properties of ammonia borane with the addition of polyacrylic acid and calcium chloride: Thermal and kinetic studies."
Mentor: Dr. Ozge Gunaydin

Third place:
Ian Sisson – major in Chemistry
Research in Sustainable Materials – Polymers
"Iron-Cellulose Nanocomposites: A Potential Replacement for High Strength Plastics."
Mentor: Dr. Paul Bernazzani

10th Annual Texas STEM Award Winners

Best Poster Presentation at Master Level

Winner:
Elizabeth Claire Alexander – Master candidate in Biology
Research in Biology
"CBD Mechanisms of Action at the Human 5-HT1A Receptor."
Mentor: Dr. Mariam Vasefi

Best Poster Presentation at Doctoral Level

Winner:
Rishi Bharadwaj – Doctoral candidate in Electrical Engineering
Research in Optoelectronics
"Comparison of the Interference Patterns between Non-Coherent and Coherent Laser Beams Illuminating the Same Dielectric Surface."
Mentor: Dr. Cristian Bahrim

Best Talk at Undergraduate Level for non-OUR Sponsored Research

Winner:
Zaid Mohammed – major in Biology
Research in Medicine
"Role of Autophagy Receptors in Cancer."
Mentor: Dr. Ian Lian

Best Talk at Doctoral Level

Winner:
Premkumar Ravishaker - Doctoral candidate in Industrial and Systems Engineering
Research in Oil Industry
"Increasing The Oil and Gas Pipeline Resiliency Using Image Processing Algorithm."
Mentor: Dr. Berna Eren-Tokgoz

Runner Up:
Prasad Pawar – Ph.D. candidate in Chemical Engineering
Research in Bioprocessing
"Demulsification of Tight Crude Oil-Water Emulsions Under Microwave Radiation in Presence of Chemical Demulsifiers."
Mentor: Dr. Clayton Jeffryes

OFFICE OF UNDERGRADUATE RESEARCH
LAMAR UNIVERSITY

10th Annual Texas STEM Conference – November 5th, 2022

Beck Fellow Speaker

Research in Ecology and Biodiversity

Angel Flowers

Mentors: Dr. Matthew Hoch[1], Dr. Latha Thomas[2], Dr. Kathy Jackson[3], and Dr William R. Miller[4]

[1]Department of Biology, Lamar University, Beaumont, TX
[2]Department of Biology, University of Belize, Belmopan, Belize
[3]Department of Biology, McNeese State University, Lake Charles, LA
[4]Department of Biology and Chemistry, Baker University, Baldwin City, KS

Talk in Archer Auditorium – Plenary Session from 1:00 to 1:15 p.m.

Tardigrades of Belize

Tardigrades are aquatic invertebrates found in marine, freshwater, and moist terrestrial habitats across almost every ecosystem on earth. Most closely related to arthropods and onychophorans, the phylum Tardigrada encompasses over 1400 species to date. It is thought that only one-tenth of species have been discovered and described in the literature. The biogeographic relationships between North, South, and Central American tardigrades have received little attention due to the paucity of sampling in Central America. Based on limited collections mostly from Costa Rica, many tardigrade species from Central America appear unique and specific, while North and South America share some species, suggesting more complex biogeographic processes in Central America than explained by the Great American Biotic Interchange hypothesis alone. One country with no previous record of tardigrades is Belize, a beautiful, rich, tropical country situated on the Yucatan Peninsula facing the Caribbean Sea. This research serves to increase the knowledge of tardigrade biogeography in Central America and to further understand the drivers of species distributions.

Moss and lichen samples were collected in June 2022 from moist habitat types across Belize: cliff faces, waterfalls, cave entrances, and along forest trails. These were located within four different regions of Central Belize: Mountain Pine Ridge Forest Reserve, Chiquibul National Park, Cockscomb Basin Wildlife Sanctuary, and Monkey Bay Wildlife Sanctuary. Samples were obtained by scrapping the moss or

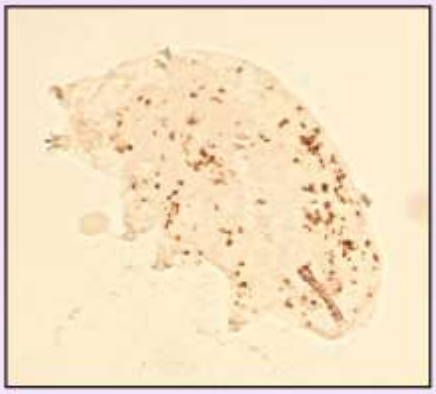

lichen into a labeled paper bag and allowed to dry thoroughly. Samples were prepared for processing by placing approximately one gram of dry sample into 20 mL of water and then soaking for 24 hours. Three, one- mL drops of water were placed in individual, black-backed dishes. These subsamples were observed using stereomicroscopes, and tardigrades extracted with an Irwin Loop were placed in double-stain before mounting to labeled slides in PVA medium, topping with a coverslip. The Coverslips were later sealed using clear nail polish to preserve the specimen. Tardigrades mounted to slides were later preliminarily identified to genus using light microscopy of morphological features. Target samples were then re-sorted for specimens to commit to DNA analysis and SEM imaging. Molecular analysis involved extracting single tardigrade DNA with Quick Extract (Lucigen), PCR amplification of COI and 28SrRNA genes, and both forward and reverse Sanger sequencing gene amplicons. Sequences obtained were compared to others in Genbank using NCBI BLASTn search tool to verify genus and species where possible.

Presently, 673 tardigrade specimens have been identified from Belize representing 18 species. Four species are in the Echiniscidae family of class Heterotardigrada. For class Eutardigrada, the numbers of species identified in four families were three Mlinesiidae, four Doryphoribiidae, five Macrobiotiidae, and two Hypsibiidae. This research project is presently still in progress, and samples and data are still being processed. It is believed the number of Tardigrade species from Belize will continue to climb as the remaining samples are processed. The results will be compared to prior studies of Central, South, and North America to support or offer new insights to current understanding for tardigrade biogeography across the Americas.

Acknowledgements- This work was supported by Lamar University, 2022 David J. Beck Fellowship awarded to A.M.F.

OFFICE OF UNDERGRADUATE RESEARCH
LAMAR UNIVERSITY

10th Annual Texas STEM Conference – November 5th, 2022

Beck Fellow Speaker

Medical Research

Zaid Mohammed

Beck Mentors: Dr. Ian Lian[1] and Dr. Ryan Russell[2]
[1]Department of Biology, Lamar University
[2]Department of Cellular and Molecular Medicine, University of Ottawa, Ottawa, Ontario

Talk in Archer Auditorium – Plenary Session from 1:15 to 1:30 p.m.

The Role of Autophagy Receptors in Cancer#

#Research done in the Department of Cellular and Molecular Medicine, University of Ottawa, Ottawa, Ontario
Supervisor Professor Zhihao Guo

Autophagy is a self-digesting mechanism where damaged cellular components are sequestered by an autophagosome and fused with lysosomes for degradation. It serves as a natural recycling system as the nutrients gained from breaking down the old parts can be utilized to build new organelles. This is beneficial to a normally functioning cell as it removes cellular waste and maintains efficiency. However, research into the role of autophagy in cancer cells has shown that it could increase tumorigenesis. The autophagy pathway provides an alternative way for tumor cells to obtain nutrients in stressful conditions such as chemotherapy treatment. Thus, it is heavily linked to drug resistance in cancer cells. The pathway is regulated by a series of proteins, of which the Ulk complex is an upstream component, and inhibition of Ulk has been shown to shut down the pathway. However, not much is known about the specific roles that the other proteins in the pathway play in cancer cells. We are looking for any receptors which, if inhibited, have a similar effect as the Ulk complex inhibition in fighting drug resistance and tumorigenesis, but still allow the pathway to function and perform its normal activities. This would be most advantageous, as shutting down the entire process can lead to adverse complications. This project utilizes a drug resistant MB49 cell line that has been infected with Nluc and OVA virus, and we will inhibit 84 autophagy receptors to observe the effects that each of them have on tumorigenesis and drug resistance.

Special Guest

OFFICE OF UNDERGRADUATE RESEARCH
LAMAR UNIVERSITY

10th Annual Texas STEM Conference – November 5th, 2022
Invited Speaker at the Focus Session
Modern Trends in Bioengineering and Medical Research

Kayla Meyers

Department of Biomedical Engineering, College of Engineering,
University of Texas at Arlington, Arlington, Texas

Talk in Archer Auditorium – Plenary Session from 1:30 to 2:15 p.m.

Melanoma Chemotherapy Treatment using Modified Cellulose-Based Injectable Hydrogels Combined with Temozolomide

Melanoma, the rarest form of skin cancer, is responsible for about 75% of all skin cancer deaths. A local delivery method of an injectable modified cellulose nanofiber hydrogel, DNCNF PAA 10%, loaded with the chemotherapy drug temozolomide, TMZ, was studied to investigate the most effective and safest therapy window on duke melanoma 6 (DM6) and human dermal fibroblast cells (HDF-α).

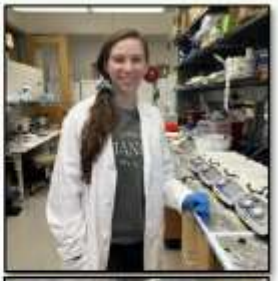

Loaded hydrogel concentrations of 25μM-1000μM were tested against the controls of no hydrogel, hydrogel alone, and free-drug TMZ. The treatments were administered inside PDMS microcurrent device for 72 hours, removed, cells stained, and quantified. For the long-term study, treatment was administered for 72 hours, treatment removed, and cells recovered for 72 hours. The data was quantified using a fluorescent live/dead cell assay and cells counted using ImageJ, Excel, and R/ANOVA with a significance of $p \leq 0.05$.

There was a plateau from 25μM-100μM, similar to hydrogel alone and a cell death dosage effect seen after the 250μM TMZ hydrogel treatment as the concentrations increased. The 500μM TMZ hydrogel had ~7-14% DM6 viability with ~50% HDF-α viability. Dosages higher than the 500μM TMZ hydrogel treatment and free 500μM TMZ had nonspecific killing of both cell types. The long-term melanoma recovery study showed surviving melanoma have possible TMZ resistance.

The most effective and safest therapy window was DNCNF PAA 10% 500μM-750μM TMZ. Currently, the treatment therapy window found is being studied further involving co-culturing of both cell types. Future studies recommended are TMZ resistance studies and in vivo animal studies.

Special Guest

OFFICE OF UNDERGRADUATE RESEARCH
LAMAR UNIVERSITY

10th Annual Texas STEM Conference – November 5th, 2022
Invited Speaker at the Focus Session
Modern Trends in Bioengineering and Medical Research

Alexus Locke

Clinical Research Coordinator on the Pediatric Emergency Medicine (PEM) Research Team at Children's Healthcare of Atlanta, GA

Talk in Archer Auditorium – Plenary Session from 1:30 to 2:15 p.m.

Unraveling the Role of Tumor Extracellular Vesicles in Angiogenesis to Inform the Design of Biomimetic Electronic Devices*

#Research done at Cornell University, Robert Frederick Smith School of Chemical and Biomolecular Engineering.

Extracellular vesicles (EVs) are lipid-bilayer particles secreted by various types of cells, including tumor cells. EVs are enriched with a discrete set of bioactive cargoes they can transfer to cells in both adjacent and distant sites to orchestrate multiple key pathophysiological events such as angiogenesis and cancer progression. Although several studies have emerged to probe and characterize these particles, the mechanisms involved in how EVs mediate their cargo transfers are still poorly understood. Accordingly, the development of model systems that may be able to recapitulate and expound upon these mechanisms have become attractive targets. Individually, supported lipid bilayers (SLBs) and organic electrochemical transistors (OECTs) have emerged as novel methods to study and monitor cellular functions. When combined, they have the potential to represent a versatile electronic biosensor capable of monitoring the properties and behavior of mammalian cell surfaces. Here, this hybrid SLB-OECT system is intended to analyze tumor EV (TEV) processes like binding, fusion, and potentially cargo transfer processes on model cell membranes in real-time. In this work, the interactions between TEVs and epithelial cells were studied to assess their ability to induce angiogenesis. The analyses revealed enhanced proangiogenic activity via Vascular Endothelial Growth Factor (VEGF) upregulation amongst cells infected with TEVs. In an effort to evade the effects of TEV exposure, they were treated with heparin to prevent the binding and uptake of TEVs by recipient epithelial cells. Cells exposed to heparin-coated TEVs showed minimal VEGF upregulation similar to the VEGF expression observed of untreated cells indicating successful TEV blocking. These results represent important feedback anticipated to aid in optimizing the design of the aforementioned model SLB-OECT device for the in-depth, mechanistic analysis of TEV-mediated processes.

Special Guest

OFFICE OF UNDERGRADUATE RESEARCH
LAMAR UNIVERSITY

10th Annual Texas STEM Conference – November 5th, 2022

Invited speaker at the focus session

Modern Trends in Bioengineering and Medical Research

Ben Morales, Ph.D. candidate

Louisiana State University, Baton Rouge, LA

Talk in Archer Auditorium between 1:30 p.m. to 2:15 p.m.

Biomechanics Research from Lamar to LSU

Julio Benjamin Morales, M.A., C.S.C.S. is a first-year Ph. D. student in Kinesiology at Louisiana State University. Ben has experience training and monitoring athletes through his past internships in strength and conditioning and as a track athlete at Lamar University. Ben was very fortunate to complete two research studies with Dr. Shannon Jordan and Dr. Julio Morales during his time at Lamar. Both studies were facilitated through the Office of Undergraduate Research consisting of the Summer Undergraduate Research Grant and the Office of Undergraduate Research Grant. These studies comprised of further understanding human performance and human performance testing aiding in his research skill development for his graduate studies at Indiana State University.

During his time at Indiana State University, he worked in the analysis of the Men's Basketball team monitoring data and worked as a graduate assistant in the Biomechanics Laboratory at Indiana State University assisting in teaching the undergraduate Biomechanics Laboratories. Through this experience, he has developed further skills in vertical jump assessment, gait analysis, motion analysis, and strength and conditioning to further examine human performance. In his thesis, he studied the relationship between vertical stiffness and reactive strength index-modified in the counter-movement vertical jump.

His current research interests are comprised of examining human performance testing using motor control and biomechanical assessment techniques.

Special Guest

OFFICE OF UNDERGRADUATE RESEARCH
LAMAR UNIVERSITY

10th Annual Texas STEM Conference – November 5th, 2022
Invited Speaker at the Focus Session
Modern Trends in Material Science and Engineering

Dr. Okafor Ekene Gabriel

Supervisor: Dr. David Ryan Huitink
Department of Mechanical Engineering, University of Arkansas, Fayetteville, USA

Talk in Archer Auditorium – Plenary Session from 2:25 to 4:00 p.m.

Laminated Transcient Liquid Phase Preform and Bond Fabrication and Characterization for High Temperature Power Electronic Application

Transient liquid phase (TLP) bonding is a diffusion bonding process for joining metals using low sintering temperature. Although, TLP is applicable to power electronics systems intended for high temperature application, the brittle inter-metallic compounds formed at its inter-phase has low resistance to thermomechanical stresses experienced during the operational life of the device. Laminated TLP (L-TLP) bonding which uses a preform with ductile core layer has potential to mitigate the thermally induced stress. L-TLP performance depends on the quality of the preform as well as formed bond. However, little emphasis has been dedicated to the preform and bond fabrication and characterization. Fabrication process variation and scratch test were used to evaluated the preform quality. In addition, scanning electron microscope (SEM), confocal scanning acoustics microscope (CSAM), energy dispersive x-ray (EDX) and shear test were used to evaluate the bond quality. From the results, Alumimun core layer subjected to alcohol cleaning as well as concentrated nitric acid and zincate treatment, show superior adhesion strength. In addition, relationship between aluminum core layer surface roughness and adhesion strength was observed. The bond shear force was found to be stable as well as higher than MIL-STD 883 acceptable threshold of 2.5kg for a die greater than 4.4mm^2 up to 250°C for 38 and 76um thick aluminum core layer L-TLP bond. Numerical simulation using ANSYS show, that for a fixed inter-metallic compound (IMC) thickness, change in core layer thickness didn't affect IMC layer inflection point, as the sample cools from peak process temperature to room temperature.

Special Guest

OFFICE OF UNDERGRADUATE RESEARCH
LAMAR UNIVERSITY

10th Annual Texas STEM Conference – November 5th, 2022

Invited Speaker at the Focus Session

Modern Trends in Material Science and Engineering

Nurul Azam, Ph.D. candidate

Auburn University, Auburn, AL

Talk in Archer Auditorium – Plenary Session from 2:25 to 4:00 p.m.

Laser-based Bottom-Up Synthesis of Monolayer 2D Crystals with Tunable Vacancy Concentrations

The type and concentration of defects in two-dimensional (2D) materials can significantly modify their properties. For example, deliberately creating chalcogen vacancies in a controlled manner can effectively modulate their physical, chemical, and electronic properties with a broad range of applications including energy, sensing, photonics, and spintronics. Here, we introduce a novel single-step bottom-up synthesis method to grow monolayer crystals (e.g., $MoSe_2$) with tunable vacancy concentrations. Instead of using the multicomponent precursor such as Se and MoO_3 used in conventional CVD to produce $MoSe_2$ crystal, here stoichiometric $MoSe_2$ powder is used to grow monolayer $MoSe_{2-x}$ crystals by controlled laser vaporization of the powder. A CO_2 laser (λ = 10.6 μm) is employed in the vaporization process along with a tube furnace to facilitate the growth environment to form monolayer crystals[1,2]. Experiments show that by regulating the net energy supplied to the powder via varying the laser power and laser irradiation time, the vapor dynamics can be customized so that the monolayer crystals with different vacancy concentrations can be uniformly grown on the substrate. The vacancy concentrations are estimated using optical spectroscopy and atomic imaging techniques at each experiment stage, indicating that monolayer $MoSe_{2-x}$ crystals with vacancies ranging from ~1-20% are successfully formed. Photoluminescence spectroscopy (PL), PL mapping, Raman mapping, atomic force microscopy (AFM), and time-correlated single-photon counting (TCSPC) are among the techniques utilized to evaluate the inherent quality of the vacancies in these samples.

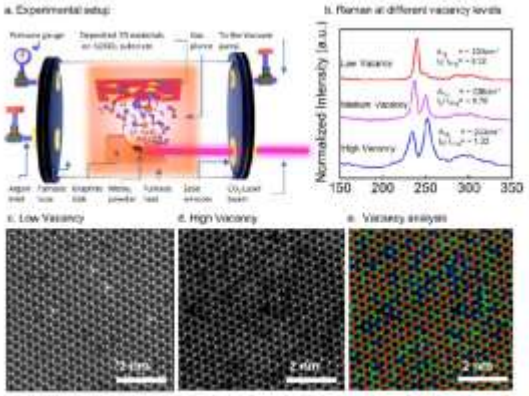

Figure 1 The experimental setup of laser-based synthesis of 2D materials (a). Raman profile shows the different range of vacancy tuning depending on the laser energy density (b), and corresponding STEM images show atomistical confirmation of low (c) and high vacancy concentrations (d), respectively. The vacancy concentration has been analyzed by a python-based algorithm (e) where the Se_2 (red), Se (blue), and Mo (green) sites are quantified to develop the vacancy concentration statics.

Special Guest

OFFICE OF UNDERGRADUATE RESEARCH
LAMAR UNIVERSITY

10th Annual Texas STEM Conference – November 5th, 2022
Invited Speaker at the Focus Session
Modern Trends in Material Science and Engineering

Dylan Palmer, Ph.D. candidate

Colorado School of Mines, Denver, CO

Talk in Archer Auditorium – Plenary Session from 2:25 to 4:00 p.m.

Thermal Fatigue of Secondary Cooling Support Rolls during Continuous Casting

In this work, the failure of a secondary cooling support roll in a continuous casting machine was analyzed using the finite element method. The heat transfer of continuous casting rolls was analyzed using a computational model in ANSYS Fluent. The effects of roll rotation and material non-linearity were incorporated into this model. Owing to the high Peclet number of this heat transfer problem, the cyclical temperature variation in the roll was found to be limited to small boundary region near the rolls exterior surface. The ANSYS Fluent model also provided insight into the important process parameters which drive support roll damage in casting, such as, the severity of roll quenching caused by the secondary cooling sprays. Additionally, the effects of different roll materials (base and cladding) were studied. Transient simulations were also conducted in order to estimate the thermal response of the rolls during different caster events, such as start-ups and slowdowns, which are common in industry. A thermal stress model of the roll assembly was implemented in ANSYS Mechanical to evaluate the material deformation during steady state operation. A stress life model was used to evaluate the service life of a support roll in the plant. The results of this model roughly matched the actual life of the part.

Special Guest

OFFICE OF UNDERGRADUATE RESEARCH
LAMAR UNIVERSITY

10th Annual Texas STEM Conference – November 5th, 2022
Invited Speaker at the Focus Session
Modern Trends in Material Science and Engineering

Daniel Quispe, Ph.D. candidate

Northwestern University, Chicago, IL

Talk in Archer Auditorium – Plenary Session from 2:25 to 4:00 p.m.

Magnetic Smart Materials

Magnetic smart materials (MSMs) offer an alternative to the typical piezo-electric actuators currently being used to control X-ray optics on beamlines. MSMs combined with an overcoating of a magnetic hard material means a deformable mirror whose non-reflecting side is coated with an MSM plus magnetic hard overcoat can work in a power-off mode. The process works by using an electromagnet (EM) to impose a magnetic field in the bilayer of MSM and magnetic hard overcoat. Once the EM is off, the mirror settles into a new shape within minutes. This new shape can then remain intact for days. Because the EM is not fixed to the mirror, the exact placement of the magnetic field can be adjusted by relocating the position of the EM itself. This feature allows for fine-scale adjustments and avoids the "dead pixel" replacement problem common with piezo patches attached to the mirror.

Special Guest

OFFICE OF UNDERGRADUATE RESEARCH
LAMAR UNIVERSITY

10th Annual Texas STEM Conference – November 5th, 2022
Invited Speaker at the Focus Session

Modern Trends in Material Science and Engineering

Tyler Nelson, Ph.D. candidate

Rice University, Houston, TX

Talk in Archer Auditorium – Plenary Session from 2:25 to 4:00 p.m.

Construction and Validation of a Multimodal 3D Single-Molecule Super-Resolution Microscope for Whole Cell Imaging

Single-molecule localization microscopy is a super-resolution technique which enables the investigation of structures and molecules in cells at a resolution surpassing the diffraction limit of light. The appropriate method with which to illuminate a sample varies according to the nature of the sample and the goals of the study, however, there is typically a tradeoff between simplicity of use and optimal performance when selecting an illumination method. Most commercial microscopes offer epi-illumination, where the entire sample is illuminated simultaneously. However, this creates high background fluorescence and increased risk of photodamage and photobleaching of the sample. Another commonly available illumination option is total internal reflection fluorescence (TIRF), where only a thin slice of the sample right at the coverslip is illuminated. This mode results in excellent contrast, but it is not compatible with whole-cell imaging. An alternative whole-cell compatible approach is light sheet illumination, where the sample is optically sectioned by a thin sheet of light introduced in a direction orthogonal to the detection axis.

In this work, we demonstrate a flexible microscopy platform using primarily commercially available parts which combines homogeneous flat-field epi- and TIRF illumination with the whole-cell sectioning capability of a light sheet. Our microscope will allow very fast switching between the illumination modes, all at several different laser wavelengths. In combination with a point spread function engineering system, our system will conveniently enable 3D super-resolution imaging and molecular counting in whole cells with an illumination mode that is optimized for the sample and region of interest.

Special Guest

OFFICE OF UNDERGRADUATE RESEARCH
LAMAR UNIVERSITY

10th Annual Texas STEM Conference – November 5th, 2022
Invited Speaker at the Focus Session
Modern Trends in Material Science and Engineering

David Quispe, Ph.D. candidate

Arizona State University, Tempe, AZ

Talk in Archer Auditorium – Plenary Session from 2:25 to 4:00 p.m.

Solar Cells Efficiency with Perovskite Materials

Transparent materials with tunable work functions are attractive to serve as carrier selective contacts in solar cells so that there is minimal current loss. Using sputtered NiOx as an example, we discuss the materials properties framework necessary to achieve a highly selective contact for perovskite-based solar cells. We characterize the work function and bandgap of NiOx as we vary the oxygen partial pressure during its deposition. Applying NiOx as a hole-selective contact in perovskite solar cells, we are able to achieve up to 14% solar cell efficiency



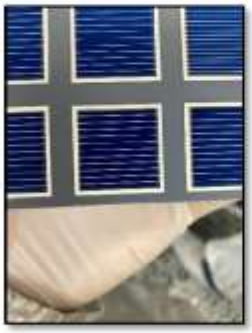
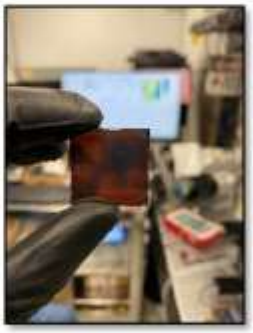

Special Guest

OFFICE OF UNDERGRADUATE RESEARCH
LAMAR UNIVERSITY

10th Annual Texas STEM Conference – November 5th, 2022

Invited Speaker

Rebekah Schilberg

University of Texas, Austin, TX

Talk in Archer Auditorium – Breakout Session 1 from 4:30 to 5:30 p.m.

The Ergonomic Design Process of the UT Austin Formula SAE

This report seeks to explain the ergonomic design process executed by the University of Texas at Austin Formula SAE (FSAE) team. FSAE is an organization where teams from across the globe compete with student designed and manufactured formula-style vehicles. Within the breakdown of UT Austin's team, the ergonomic subsystem is responsible for all parts of the car the driver interacts with, as well as the braking system. With our 2023 driver lineup, there is a height discrepancy greater than 12 inches between our shortest and tallest drivers, causing even more challenging design constraints than the FSAE rules require. As such, we must implement extreme adjustability in all aspects of the ergonomic subsystem, namely the driver positioning and pedal box. This report will also review the remaining aspects of our subsystem: steering wheel/column, anthropometrics, seat manufacturing, driver safety features, and dashboard, as well as their interactions with the other systems responsible for designing a functional car. Ergo is also in charge of selecting all the braking components. We must design a system to achieve full wheel lock at max speeds in second gear using dynamic analysis of the car. Since the 2023 season is the first chance since COVID that ergonomics has had a strong design team behind it, this year promises lots of discovery and growth in our ability to create a comfortable environment for any driver.

SURF 2022 STEM Fellows

1
Melissa Tan | Civil Engineering |
Mentor: **Dr. Thinesh Selvaratnam**
Research in Bioremediation and Resource Recovery
Project: "*Removal of Heavy Metals from Municipal Landfill Leachate using Galdieria sulphuraria*"

2
David Matherne | Biology |
Mentors: **Dr. Evgeny Romashets and Dr. Cristian Bahrim**
Research in Space Physics
Project: "*Heliospheric Storms"*

3
Kiley Mazdra | Mechanical Engineering |
Mentors: **Dr. Evgeny Romashets and Dr. Cristian Bahrim**
Research in Solar Physics
Project: "*The Physics of Active Longitudes and Their Impact on Earth Through the Interplanetary Coronal Ejection They Produce"*

4
Ian Sisson | Chemistry |
Mentor: **Dr. Paul Bernazzani**
Research in Sustainable Materials
Project: "*Developing Cellulose Based Nanocomposite as a Potential Substitute for High Strength Plastics"*

5
Jacob William Smith | Mechanical Engineering |
Mentor: **Dr. Sushil Doranga**
Research in Mechanical Vibrations
Project: "*Evaluation of Pin Fretting in the Electronic Connectors Using the Vibration Shake"*

6
Lily Yoder | Psychology |
Mentor: **Dr. Edythe Kirk**
Research in Human Behavior
Project: "*The Effects of Positive Mood and Stereotype Threat on Memory Recall"*

7
Rafael Gutierrez | Mechanical Engineering |
Mentor: **Dr. Rafael de la Madrid**
Research in Tribology
Project: "*Dynamical Wetting and Dewetting in Non-Uniform Solid"*

Melissa Tan

Major in Civil and Environmental Engineering

Mentor: Dr. Thinesh Selvaratnam

Research in Environmental Engineering

Department of Civil and Environmental Engineering

Removal of Heavy Metals from Municipal Landfill Leachate using *Galdieria sulphuraria*

Introduction

Rapid urbanization combined with population growth led to the increase of municipal solid waste (MSW) and industrial solid waste generation worldwide. Municipal landfills continue to be the most common method for the ultimate MSW disposal due to the easiness of the procedure [1]. After being disposed of in the landfills, the MSW degrades over time and releases gaseous products and a liquid waste known as leachate. Landfill leachate (LL) is high-strength wastewater containing dissolved organic matter, inorganic macro components, heavy metal, and xenobiotic organic components. The primary toxic pollutants in the LL are heavy metals. The main sources of the heavy metals present in the leachate are household hazardous substances (batteries, paints, inks, and dyes), industrial wastes, mine wastes, and incinerator ashes [2, 3]. Commonly found heavy metals in LL include lead, copper, cadmium, chromium, manganese, nickel, zinc, and iron [4, 5]. The presence of heavy metals in high concentrations can pose a greater risk to groundwater, surface water, and adjacent ecosystems [6]. Bioaccumulation of these heavy metals, even at very low concentrations, can pose significant health issues. Therefore, efficient removal of these heavy metals from the environment holds a greater significance to maintaining public safety and ecological stability.

Furthermore, some of these heavy metals are vital to the sustainability of certain industries and hold a prominent place in geopolitical issues. Therefore, these heavy metals' environmental safety, recovery, and recycling can improve the overall economics and pave the pathway for a sustainable future. Most of the current treatment options for LL heavy metals are operated using physicochemical and electrochemical processes. These treatment options include adsorption, ion exchange, precipitation, and electrocoagulation [7-9]. However, these

methods often have several disadvantages, such as generating toxic sludge, expensive equipment requirements, incomplete metal removal, and high reagent requirement. Therefore, it is paramount to develop sustainable, cost-effective heavy metal removal technologies focusing on the near and long-term contaminant and regulatory issues. This study evaluates the heavy metal removal and recovery potential from LL using a red algal extremophile found in acidic hot springs, ***Galdieria sulphuraria*** **(GS)**. This research also evaluates the metal uptake through the bioaccumulation pathway and the growth potential of GS using synthetic LL.

Materials

Galdieria sulphuraria (GS) is a thermophilic mixotrophic alga that thrives in low pH values and high temperatures. GS was grown in Cyanidum Media (CM) inside an incubator (Percival, IA, USA) with the conditions set at a temperature of 40 ºC with 24 hours of continuous illumination (4000 lux). The CO_2 levels of the incubator were maintained at ~2.5%. Table 1 shows the CM recipe that was used throughout this study.

Table 1. Cyanidium Media Recipe

Component	**Concentration**
$(NH_4)SO_4$	1.32 g L^{-1}
KH_2PO_4	0.27 g L^{-1}
NaCl	0.12 g L^{-1}
$MgSO_4 \cdot 7H_2O$	0.25 g L^{-1}
$CaCl_2 \cdot H_2O$	0.07 g L^{-1}
$FeCl_3$	0.29 g L^{-1}
Nitch's Trace Element Solution	0.50 mL L^{-1}
10 N H_2SO_4	pH 2.5

The synthetic LL recipe developed by Soda et al., 2016 [4], was used in this study with minor modifications by supplements target heavy metals. The targeted metals were Cd, Cu, Ni, Zn, Mn, Pb, and Fe. The concentration of the corresponding components was calculated to get a concentration of 10 ppm. Table 2 shows the metal concentration that was used in this study.

Table 2. Metal Concentration Recipe

Component	**Concentration**
$CdCl_2 \cdot H_2O$	16.28 mg L^{-1}
$CuCl_2 \cdot 2H_2O$	26.84 mg L^{-1}
$NiCl_2 \cdot 6H_2O$	40.46 mg L^{-1}
$ZnSO_4 \cdot 7H_2O$	43.96 mg L^{-1}
$MnCl_2 \cdot 4H_2O$	36.02 mg L^{-1}
$PbCl_2$	13.42 mg L^{-1}
$FeCl_3 \cdot 6H_2O$	48.40 mg L^{-1}

Two experiments were conducted using four cases with different media compositions. The different compositions are listed in Table 3. Each case had an initial pH of ~2.7 and initial algal biomass of ~0.5 g L^{-1}. Each case had 5 replicates of 125 mL Erlenmeyer flasks with a working volume of 50 mL. Since GS is mixotrophic, it can receive nutrients from different sources. The growth can be sped up by providing an additional source of carbon in addition to CO_2. In this experiment, 25 mM of glucose was added to Cases 2 and 4 as an additional carbon source.

Table 3. Four Media Compositions

Case	**Composition**
1	Cyanidium Media
2	Cyanidium Media + Glucose
3	Cyanidium Media + Metal Concentration
4	Cyanidium Media + Metal Concentration + Glucose

Methods

Both experiments were identical except for the time in which they were conducted. Experiment 1 was conducted over 7 days, and Experiment 2 was conducted over 9 days. Each experiment had 20 flasks that were placed on a platform shaker (Innova 2000-New Brunswick Platform Shaker, Eppendorf, Enfield, CT, USA) at a continuous speed of 120 rpm and placed inside an incubator with the same conditions that the cultures were grown in. The experimental setup is shown in Figure 1.

Each day, the algal biomass was measured by measuring the optical density (OD) value at 750 nm from each flask using a spectrophotometer (HACH, Colorado, USA). A higher OD value would indicate that the algal biomass had increased. Cases 2 and 4, with the addition of glucose, would be expected to significantly increase algal biomass compared to Cases 1 and 3 without glucose.

The nutrient and metal analyses were done on the initial and final days of the experiments. For the nutrient analyses, the ammoniacal nitrogen, phosphorus, and chemical oxygen demand (COD) were determined using the same spectrophotometer that was used to measure the OD values. The metal analyses were determined using inductively coupled plasma optical emission spectrometry iCAP 7000 (ICP-OES) (Thermo Fisher Scientific, Waltham, MA, USA) as can be seen in Figure 2.

Figure 1. Experimental Setup

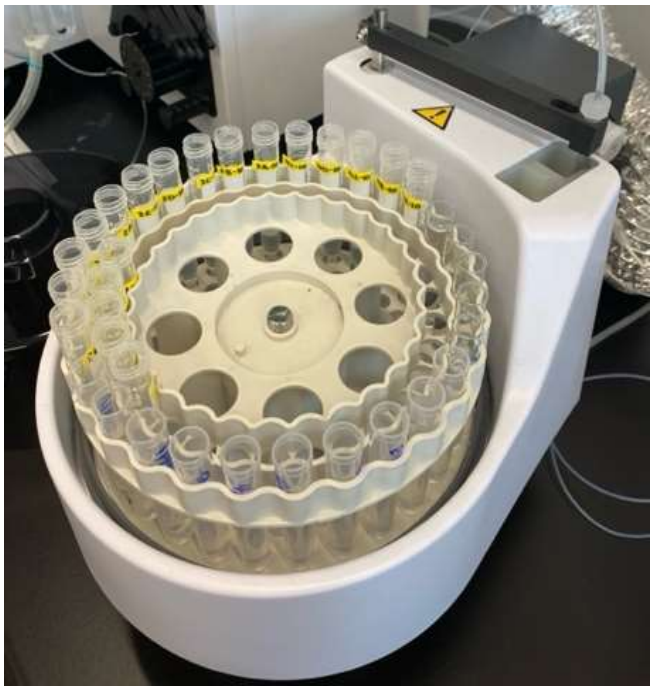

Figure 2. Inductively Coupled Plasma for Metal Analyses

Data & Results

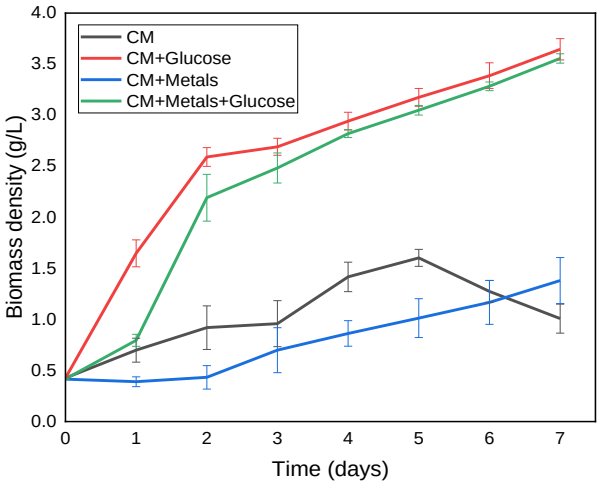

Figure 3a. Algal Biomass Density For Experiment 1

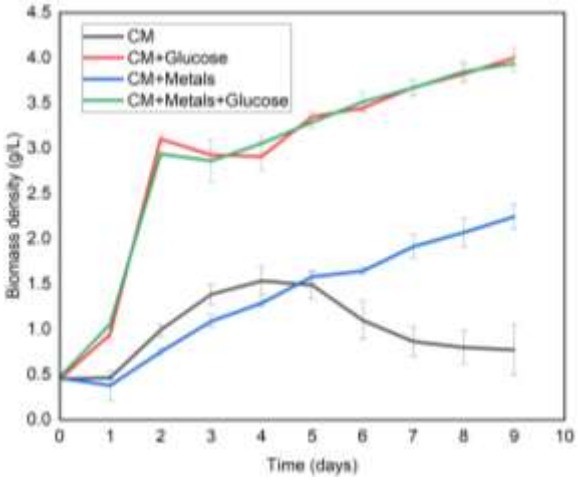

Figure 3b. Algal Biomass Density For Experiment 2

Figures 3a and 3b show the algal biomass density throughout 7 and 9 days, respectively. The algal biomass was determined by measuring the OD values at 750 nm. Each data point after Day 0 represents the average of 5 replicates. Cases 2, 3, and 4 showed an increase in algal biomass throughout both experiments. On the other hand, Case 1 showed an increase in algal biomass density up until Day 5 and Day 4, respectively, when it began to decrease. As was expected, the algal biomass density in Cases 2 and 4 with the addition of glucose showed a significant increase compared to Cases 1 and 3. Another observation that was made was that the algal biomass in Cases 3 and 4 with the added metal concentration had a slight delay in growth on Day 1 before increasing. This suggests that the metals present may be a limiting growth factor for the microalgae.

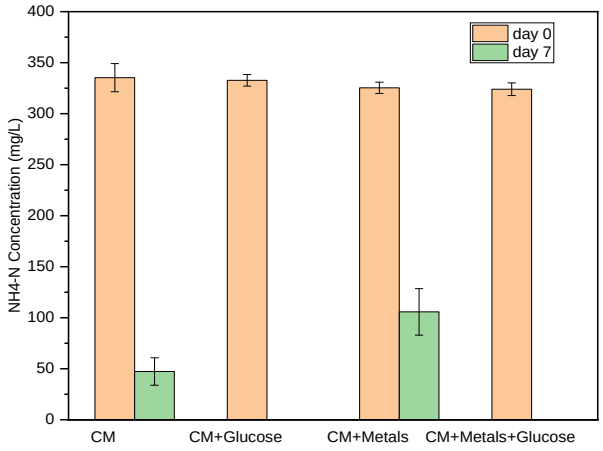

Figure 4a. Ammoniacal Nitrogen Removal For Experiment 1

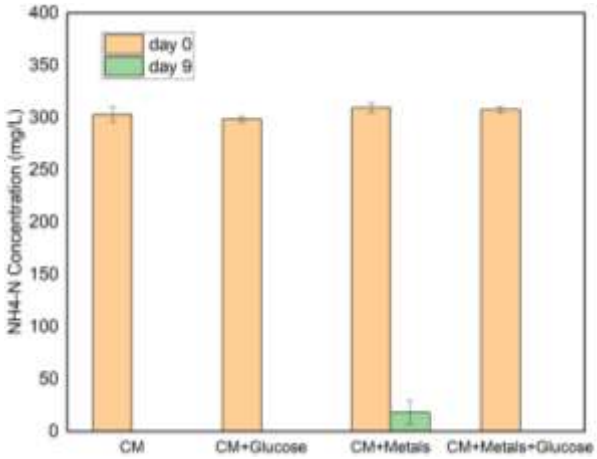

Figure 4b. Ammoniacal Nitrogen Removal For Experiment 2

Figures 4a and 4b show the ammoniacal nitrogen removal for all cases. Each bar represents the average of quintuplicates. The tests were done only on both experiments' initial and final days. The ammoniacal nitrogen decreased in all cases. In Cases 2 and 4 with the addition of glucose, the ammoniacal nitrogen removal was around 100%. Overall, the ammoniacal nitrogen removal was higher in Experiment 2, which was conducted over a longer period of time.

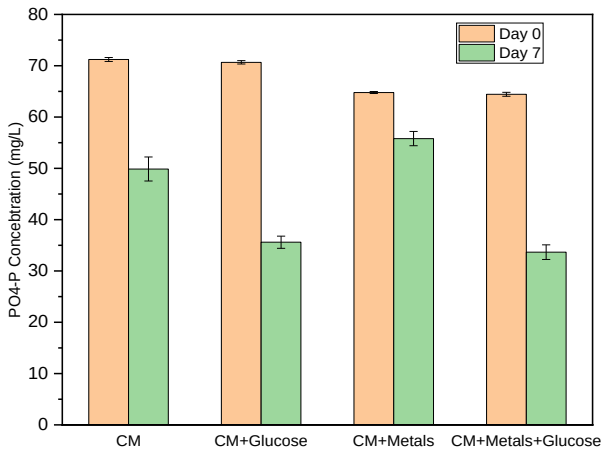

Figure 5a. Phosphorous Removal For Experiment 1

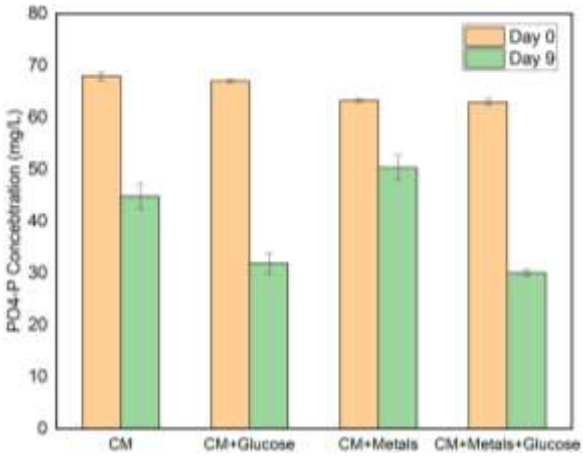

Figure 5b. Phosphorous Removal For Experiment 2

Similarly, the phosphorus tests were done on the initial and final days, as seen in Figures 5a and 5b. In Cases 2 and 4 with the addition of glucose, the phosphorus removal was around 50%, which was greater than that in Cases 1 and 3 without glucose.

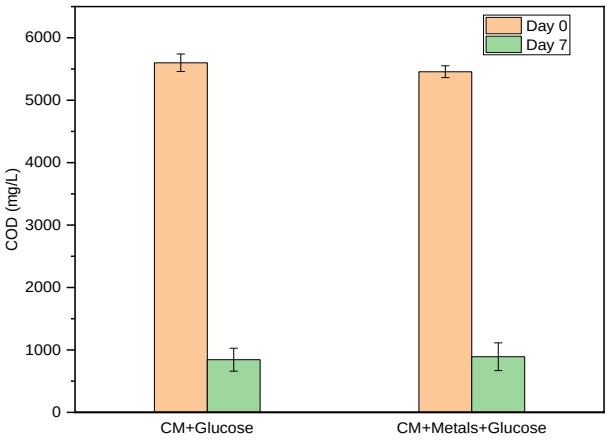

Figure 6a. Chemical Oxygen Demand Removal For Experiment 1

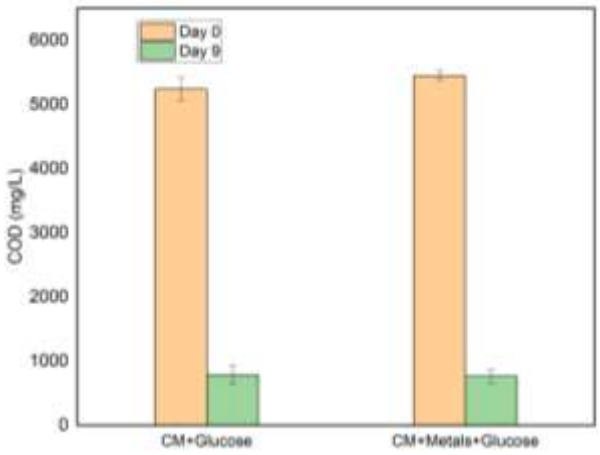

Figure 6b. Chemical Oxygen Demand Removal For Experiment 2

Figures 6a and 6b show the COD removal for Cases 2 and 4 with the addition of glucose. Again, the tests were done on the initial and final days. As the algal biomass density increased, the COD decreased. In all cases, the COD removal was around 80%.

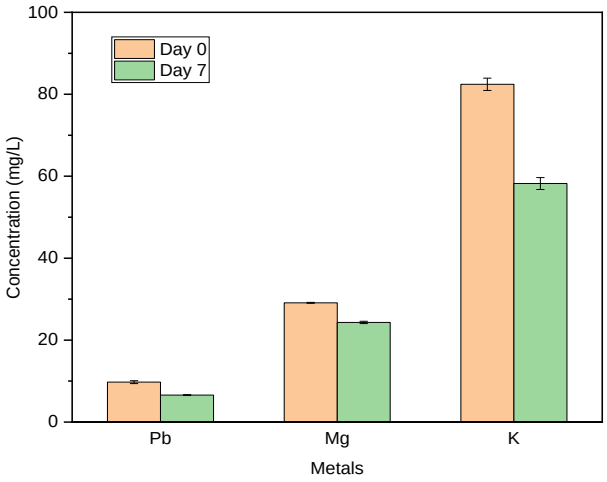

Figure 7a. Metal Removal For Experiment 1

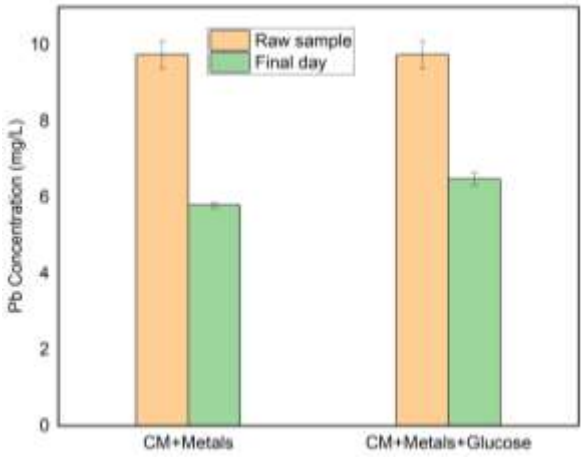

Figure 7b. Lead Removal For Experiment 2

Figure 7a shows the metal removal of lead, magnesium, and potassium, and Figure 7b only shows the metal removal of lead. In Experiment 1, the metal removal of Pb, Mg, and K ranged from ~10% to ~25%. In Experiment 2, the metal removal of Pb was around 40%. There was no significant heavy metal removal that was observed in all other metals that were used in Cases 3 and 4.

Conclusions

From the results that were obtained, we can conclude that glucose addition (heterotrophic / mixotrophic growth mode) is beneficial to the growth of microalgae. In both experiments, Cases 2 and 4 with the addition of glucose, showed higher nutrient removal efficiency with ammoniacal nitrogen removal at around 100%, phosphorus removal at around 50%, and COD removal at around 80%. The microalgae seemed to have very little metal removal for all metals with the exception of lead, magnesium, and potassium. More experimentation is needed to make further conclusions.

Future Directions

Similar experiments will be conducted with different factors, such as initial metal ion concentrations, initial biomass concentrations, and pH levels. Based off of these results, we have also been conducting experiments with lead.

Published Paper

Here is a paper publication that I am a co-author of containing more details about a similar project that can be accessed here:

Selvaratnam, T.; Pan, S.; Rahman, A.; Tan, M.; Kharel, H.L.; Agrawal, S.; Nawaz, T. Bioremediation of Raw Landfill Leachate Using Galdieria sulphuraria: An Algal-Based System for Landfill Leachate Treatment. Water 2022, 14, 2389. https://doi.org/10.3390/w14152389

References

[1] T. Eggen, M. Moeder, A. Arukwe, Municipal landfill leachates: A significant source for new and emerging pollutants, Science of The Total Environment, 408 (2010) 5147-5157.

[2] S. Mohan, R. Gandhimathi, Removal of heavy metal ions from municipal solid waste leachate using coal fly ash as an adsorbent, Journal of Hazardous Materials, 169 (2009) 351-359.

[3] A. Suna Erses, T.T. Onay, In situ heavy metal attenuation in landfills under methanogenic conditions, Journal of Hazardous Materials, 99 (2003) 159-175.

[4] D. A, M. Oka, Y. Fujii, S. Soda, T. Ishigaki, T. Machimura, M. Ike, Removal of heavy metals from synthetic landfill leachate in lab-scale vertical flow constructed wetlands, Science of The Total Environment, 584-585 (2017) 742-750.

[5] W.D.M. Souza, W.S. Rodrigues, M.M.S. Lima Filho, J.J.F. Alves, TMBF Oliveira, Heavy metals uptake on Malpighia emarginata DC seed fiber microparticles: Physicochemical characterization, modeling and application in landfill leachate, Waste Management, 78 (2018) 356-365.

[6] H.A. Aziz, M.S. Yusoff, M.N. Adlan, N.H. Adnan, S. Alias, Physico-chemical removal of iron from semi-aerobic landfill leachate by limestone filter, Waste Management, 24 (2004) 353-358.

[7] A.R. Kaveeshwar, S.K. Ponnusamy, E.D. Revellame, DD. Gang, M.E. Zappi, R. Subramaniam, Pecan shell based activated carbon for removal of iron(II) from fracking wastewater: Adsorption kinetics, isotherm and thermodynamic studies, Process Safety and Environmental Protection, 114 (2018) 107-122.

[8] K. Nithya, A. Sathish, P.S. Kumar, T. Ramachandran, Fast kinetics and high adsorption capacity of green extract capped superparamagnetic iron oxide nanoparticles for the adsorption of Ni(II) ions, Journal of Industrial and Engineering Chemistry, 59 (2017) 230-241.

[9] C.F. Carolin, P.S. Kumar, A. Saravanan, G.J. Joshiba, M. Naushad, Efficient techniques for the removal of toxic heavy metals from aquatic environment: A review, Journal of Environmental Chemical Engineering, 5 (2017) 2782- 2799.

[10] Selvaratnam, T.; Pan, S.; Rahman, A.; Tan, M.; Kharel, H.L.; Agrawal, S.; Nawaz, T. Bioremediation of Raw Landfill Leachate Using Galdieria sulphuraria: An Algal-Based System for Landfill Leachate Treatment. Water 2022, 14, 2389. https://doi.org/10.3390/w14152389

David Matherne

Major in Biology

Mentors: Dr. Evgeny Romashets and Dr. Cristian Bahrim

Research in Geo-space Sciences

Department of Physics

Heliospheric Storms

Goal: This research helped us understand possible mechanisms that produce magnetic disturbances in Heliosphere (an area centered on Sun and limited by the Earth's orbit), with relation to the creation of geo-effective structures (such as geo-magnetic disturbances). Until recently, it has been assumed that such disturbances came from the solar corona, only, such as through large magnetic clouds. There are indications that they can be formed closer to the Earth's orbit during the interaction between the Interplanetary Coronal Mass Ejections (ICMEs) and the Heliospheric Current Sheet (HCS), which is a helical shaped 3D surface. These phenomena are called Heliospheric Storms. The topic of Heliospheric Storms is novel research in scientific literature. In this project, we examined ICMEs listed by Marubashi *et al.* (2015) and determined parameters associated with Heliospheric Storms, such as maxima in the current density of streamers and the induced magnetic fields' magnitudes.

Significance of the research project: Study of geomagnetic storms is very important. They can produce disruption in the electric power distribution as it happened during the March 1989 storm, when blackout was produced over a large part of Quebec or can cause damage to low altitude artificial satellites. It is possible to prevent losses from the storms if a warning signal is timely and reliably sent. But too many false alarms or too many missed storms can jeopardize the forecast service reliability and the users will not properly protect their equipment. And with today's technology and programs scientists are closer than ever to uncovering information about the solar corona never seen before.

Research hypothesis: We enhanced a reliable algorithm that can be used by geo-magnetic storm forecasters. It is important to find a unique algorithm for separating situations leading to the formation of geo-effective

disturbances and spreading out the news in a timely manner. As practice proved it, monitoring of solar sources, flares and disappearing filaments is not enough for achieving reliable predictions of geo-magnetic disturbances. We believe that IMCEs creating intense current streamers along HCS can be equally important in space weather predictions.

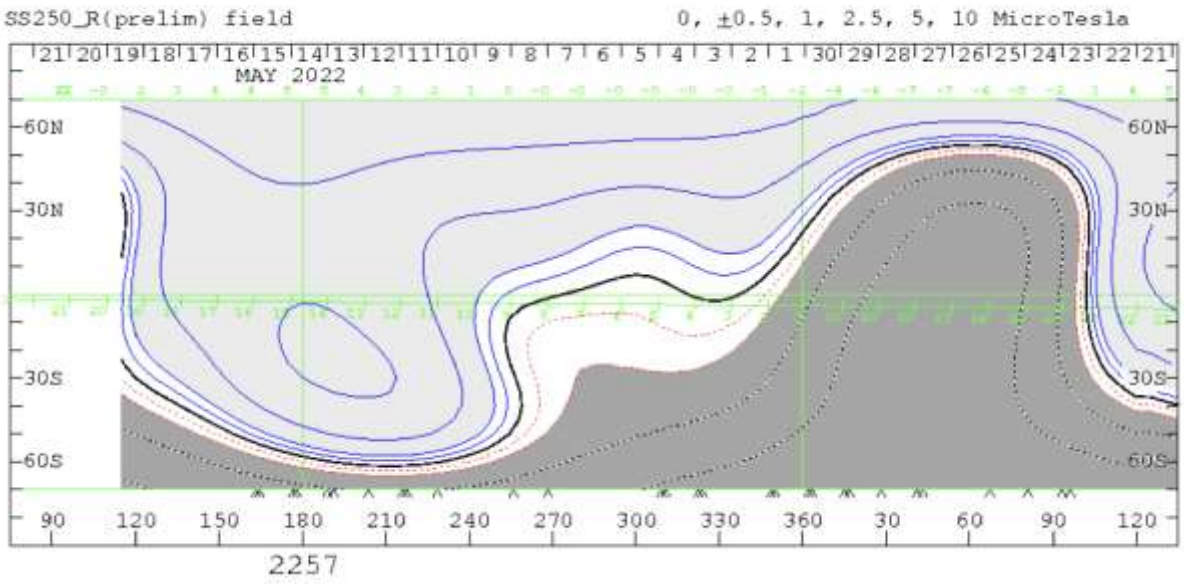

Figure 1. *Coronal field map produced by Wilcox Solar Observatory (WSO) of Stanford University. Radial component (Br) of the magnetic field at source surface, defined as 2.5 solar radii (where 1 solar radius is 700,000 km). Solid blue lines are contour lines of positive values for Br, while Dotted red lines are contour lines of negative values for Br.*

Background and Technical Details: It has been shown by Ivanov and Romashets (1998) that an interaction between ICMEs and HCS causes an increase in the intensity of current streamers along HCS, and hence, an increase in the magnitude of the magnetic field in the vicinity of the streamers. The phenomenon is known as *Heliospheric Storm*. Literature shows that maximum geomagnetic effect is achieved if the solar source of the ICME is located 30 degrees to the west of the projection of the Earth onto the Sun, and if HCS is greatly curved near the Earth's orbit. The situation can be demonstrated by the sketch in Figure 2 from Ivanov and Romashets (1999)

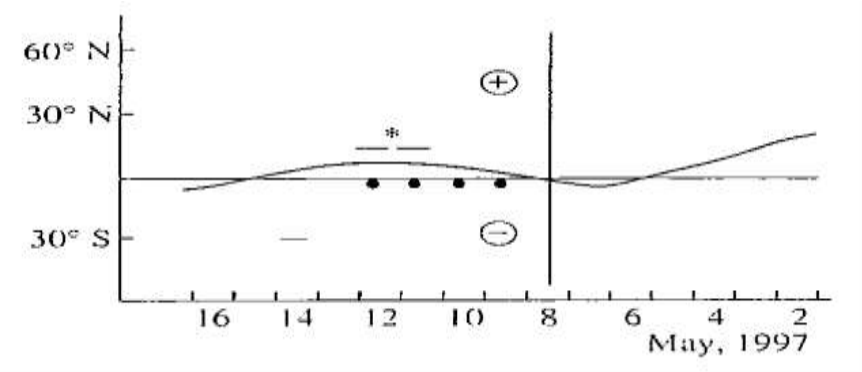

Figure 2. *Schematic representation of the HCS in angular position and over two-week span during May of 1997 (days are indicated on the horizontal axis), with position of the Earth shown in dots, the angular location of a solar flare (* symbol), and 3 disappearing filaments (- symbols), as projected onto the solar surface. The plus (+) symbol represents the field associated with the IMF spiral away from Sun and minus (-) symbol represents the field associated to IMF toward the Sun.*

According to Romashets *et al.* (2007), the heliospheric current sheets (HCS) is a 3D surface separating positive and negative sectors (see Figure 2) of interplanetary magnetic field (IMF) and is reproduced as a 3D surface in Figure 3. The interaction between ICMEs and HCS causes an increase in the intensity of current streamers, which can be imagined as particle streams flowing along the curvature of the HCS (Greater the curvature, more intense the current streamer gets).

Figure 3. *Three-dimensional view of Heliospheric Current Sheet (HCS) (Romashets et al., 2007).*

The potential scenario of a Heliospheric Storm was described by Ivanov and Romashets (1999) and is shown in Figure 4. In this figure we show the interaction between the HCS and ICME (labelled CME in the source article by Ivanov and Romashets (1999)).

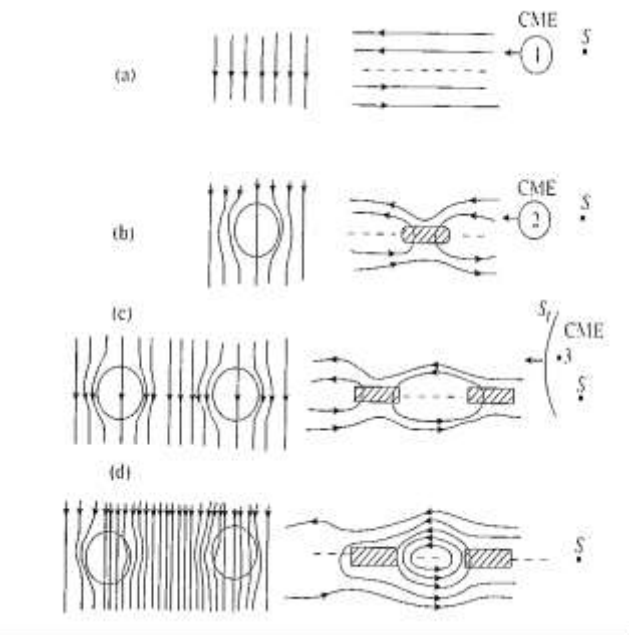

Figure 4. *The vertical full lines are IMF. The left column is a top view, and the right column is a side view. The HCS zero line is the middle-dashed line. In (a) we show a Heliosphere before HCS interacts with an ICME 1 (circle); In (b) we show the interaction of the HCS with a second ICME 2; In (c) we show the interaction between HCS with another ICME 3; In (d) we show the complexity of the interaction zone with the ICMEs positions, the IMF configuration in the heliomeridian plane, and the current configuration in the HCS plane.*

Main steps in my research:

STEP 1 – Selected from a list of strong geomagnetic storms for analysis. The list by Marubashi *et al.* (2015) contains the largest list of specific heliospheric situations leading to geostorms.

In the year 1999, we have identified three days with Ap index average larger than 20

on April 17 when Ap = 46.8

on June 27 when Ap = 25.4 and

on June 28 when Ap = 26.

All three events are in list of flux-ropes reported by Marubashi *et al.* (2015).

STEP 2 - These strong geomagnetic disturbances were produced by solar sources. From solar summary reports, I determined the position and coordinates of each potential solar source.

On April 17, I found the solar event at N16 E00 1:45 on April 13 1999

On June 27 and 28, I found the solar event at N29 W13 on 12:04 June 24 1999

Other possible candidates were solar events that happened on 13-14 April 1999 are listed below

5950 1999 4 13 0331 //// 0524 COM 3 DSF -13 -29 010

5890 1999 4 13 B1135 U1136 A1150 RAM 3 FLA 23 46 SF 8508

5900 1999 4 13 1257 1300 1310 RAM 3 FLA 23 46 SF 8508

5920 1999 4 13 1747 1751 1817 COM 3 FLA -19 -10 1F 8515

5940 1999 4 13 + 1836 1838 1841 COM 3 FLA -19 -11 SF

5940 1999 4 13 + 1836 1838 1841 COM 3 FLA -19 -11 SF

5980 1999 4 14 0806 0808 0812 COM 3 FLA -28 25 SF DS 8512

6000 1999 4 14 B1827 U1827 1926 COM 3 FLA -19 4 SF 8515

6000 1999 4 14 B1827 U1827 1926 COM 3 FLA -19 4 SF 8515

A comprehensive map of solar events which have happened in April 1999 are on the map in Figure 5.

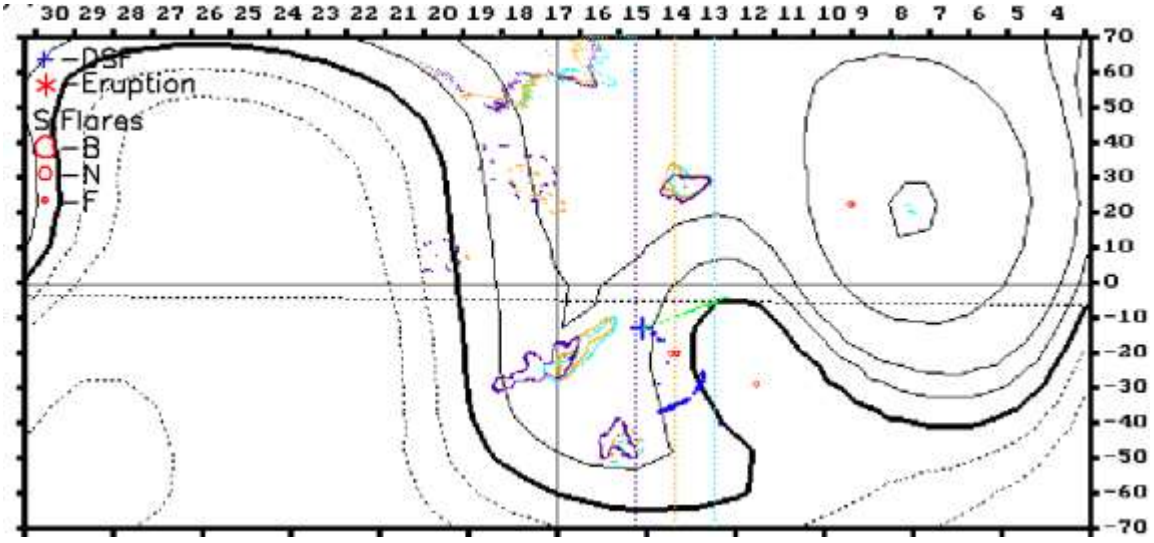

Figure 5: *Solar map of April 1999, with candidates for solar sources.*

The conditions in the vicinity of Earth's orbit and two geomagnetic indices are shown in the graph below.

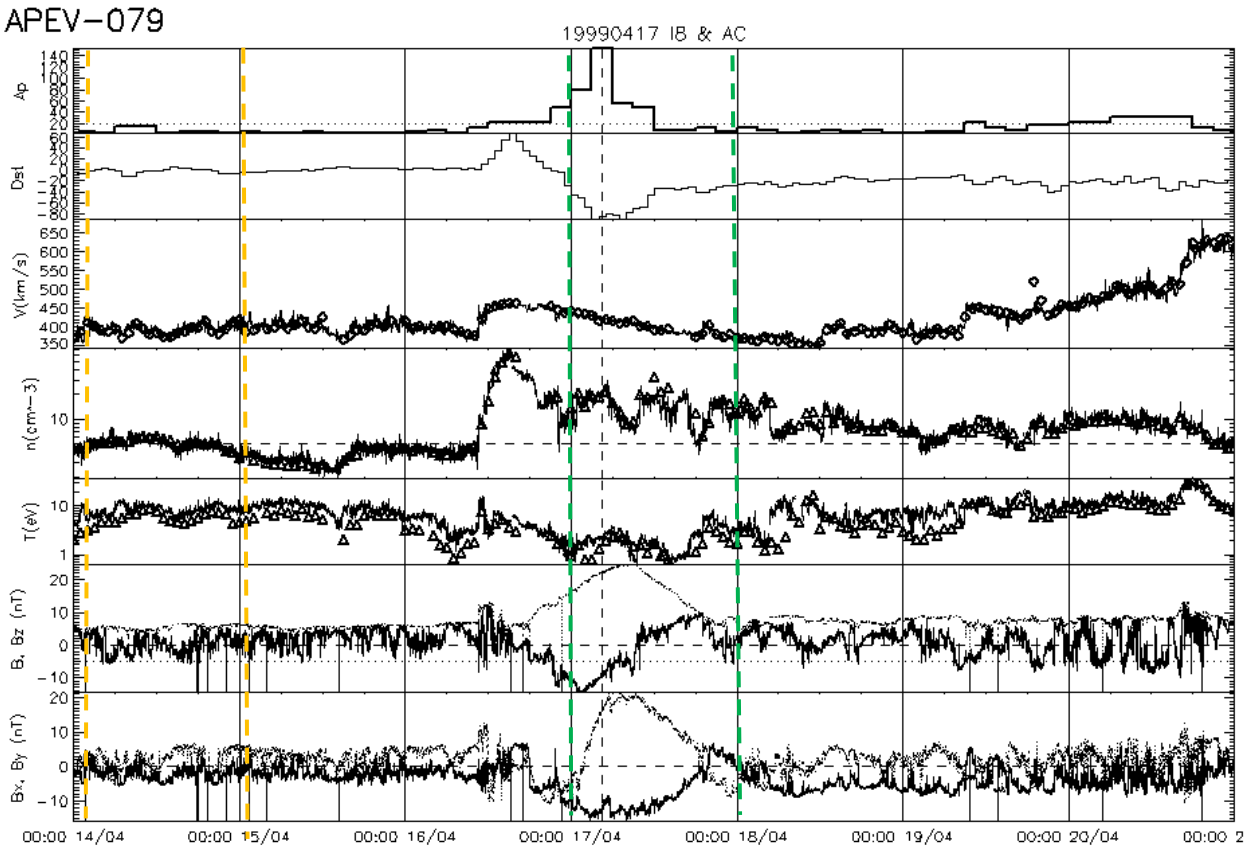

Figure 6: *The maps from the Space Weather Prediction Center (SWPC). They tell us the variation of the Ap, Dst, velocity, density, temperature, magnetic field components Bx, By, and Bz for the geomagnetic storm on April 17th (with the temporal location between the vertical dashed green lines) and the solar wind preceding it (the vertical yellow dashed lines).*

In figure 6, Dst, in nT, is the disturbed time index, Ap, in nT, v is the speed of solar wind speed (between the yellow lines) and of the magnetic cloud (between green lines), n is proton number density, T is temperature, and B, Bx, By, Bz are the magnetic field magnitude and components.

STEP 3 – From Figure 6, I determined parameters of near Earth interplanetary magnetic fields prior and during the storms as well as the speed of propagation of the interplanetary disturbances from near-Earth in-situ measurements, from WIND and ACE spacecrafts data.

- Number density in the solar wind before arrival of the magnetic cloud to the Earth's orbit,

  $n_2 = 7 * 10^{-7}\ m^{-3}$,

* Number density inside the magnetic cloud $n_1 = 10^{-7}\ m^{-3}$,

* Solar wind speed was v_2=380 km/s, and
* Speed of the magnetic cloud v_1=440 km/s.
* Interplanetary magnetic field was 5 x10^{-9} T.

This was done by interpreting values from Marubashi's list (seen in Figure 6) by adjusting the values in our dynamic model by slight amounts until the graph presented a pattern that makes sense for the magnetic cloud's velocity. The graphs shown below, in Figure 7, demonstrate what happens when density is just 5*10^{-8} m^{-3} off.

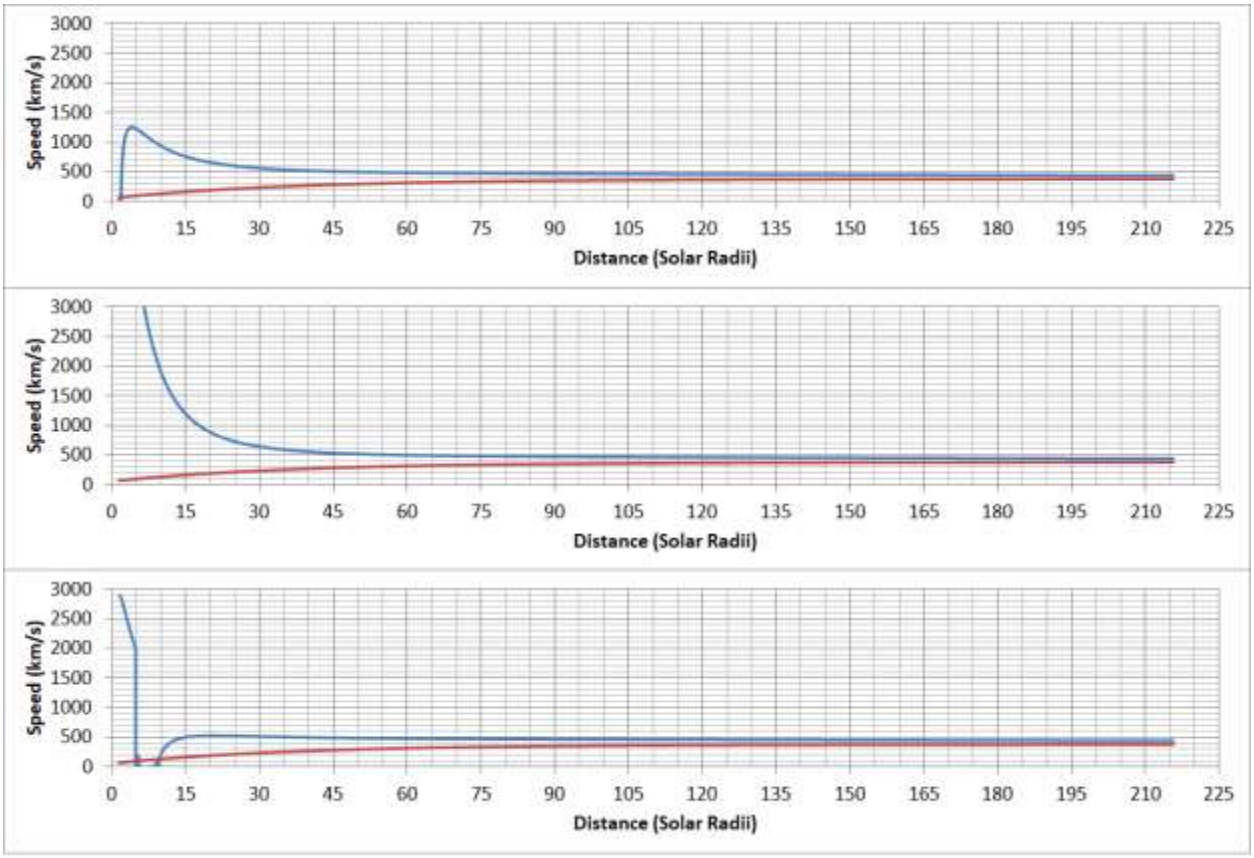

Figure 7: The graphs here show density of the magnetic cloud where n1=10*10^{-7} m^{-3}, 10.5*10^{-7} m^{-3}, and 9.5*10^{-7} m^{-3}, respectively. A typical event shows the bell curve seen on the first graph of Figure 7. The similarity factors are 15.7%, 19.5%, and 44.1% respectively.

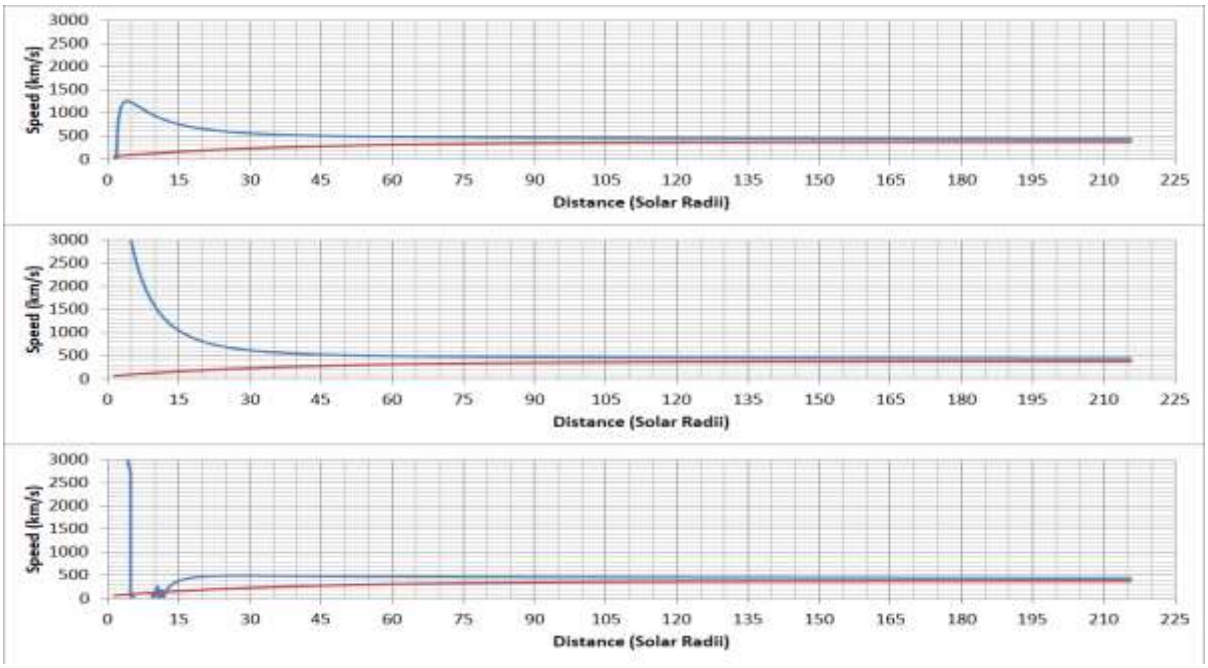

Figure 8: The graphs here show density of the solar wind where n2=, $7.5*10^{-6}$ m^{-3}, $7*10^{-6}$ m^{-3}, and , $6.5*10^{-6}$ m^{-3}, respectively. A typical event shows the bell curve seen on the second graph of Figure 7. The similarity factors are 24.4%, 15.7%, and 10% respectively.

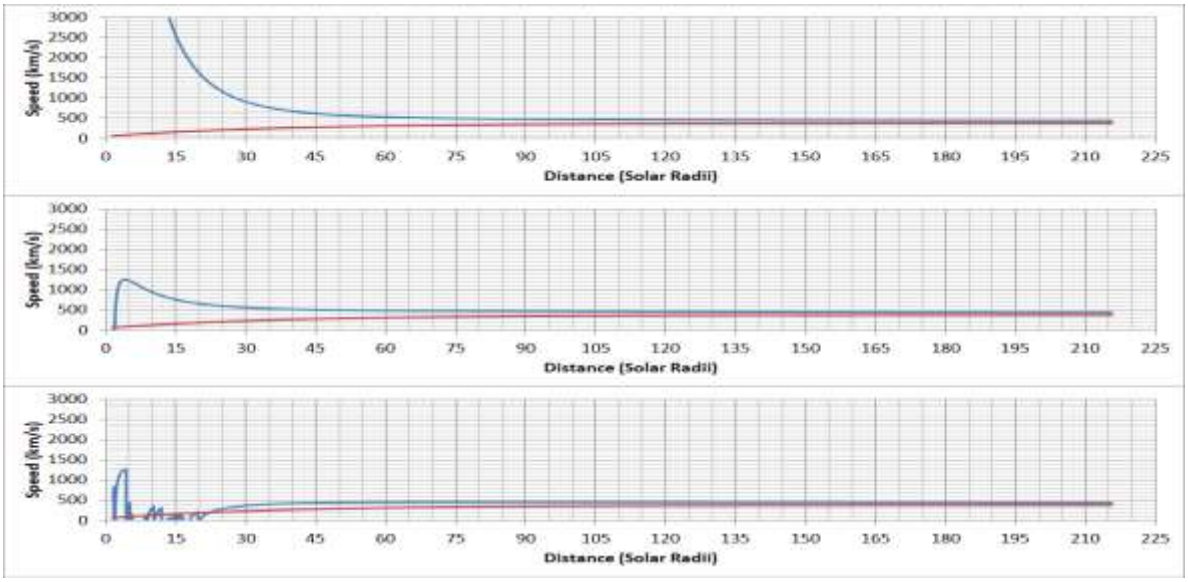

Figure 9: The graphs here show drag coefficient where Cd=, 2.61, 2.66, and 2.56 respectively. A typical event shows the bell curve seen on the second graph of Figure 7. The similarity factors are 15.7%, 19.6%, and 9.6% respectively. This value wasn't interpreted from Marubashi's list and is a newly discovered value.

In most situations, when approaching the true value, the graph becomes more shaped like a bell curve, but if the value is exceeded its actual value the graph becomes unstable like seen on graph 3 of Figure 7. In Figures 8, 9, and 10 the same methods are used in order to find the exact value of each parameter. In cases where the S-factors end up being lower, it's usual at the compromise of the graph's bell curve.

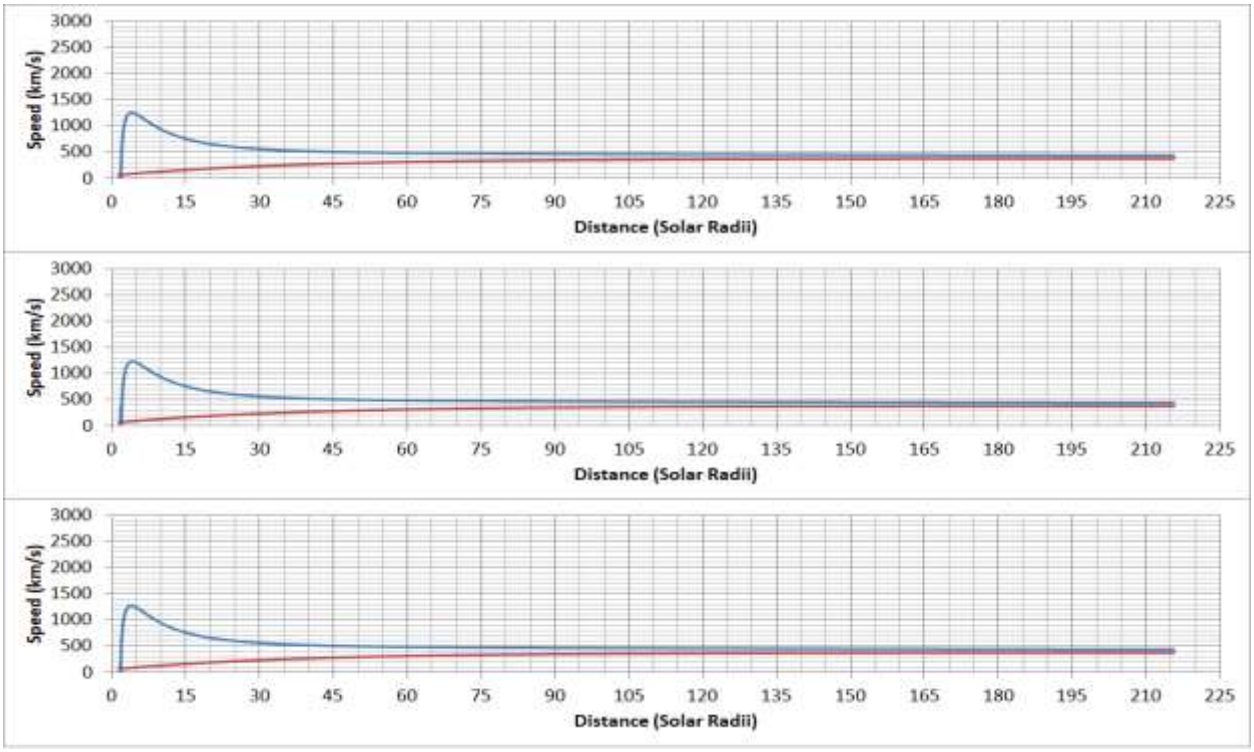

Figure 10: The graphs here show temperature of the solar wind where T2=, $1.5*10^4$eV, $1.299*10^4$eV, and $1*10^4$eV respectively. A typical event shows the bell curve seen on the second graph of Figure 7. The similarity factors are 16.7%, 15.7%, and 16.4% respectively. This value seems to be an exception from the trend of graphs. The graphs don't change at all even with changing the parameter by large amounts.

STEP 4 – Geometrical parameters of the toroidal magnetic cloud were extracted from Marubashi *et al.*'s interpretations of ICMEs near the Earth's orbit. Thus, the major radius R_0 and the minor radius r_0 of the toroid near the Earth are 6 $x10^{10}$m and 8.25 $x10^9$ m, respectively.

STEP 5 – Ran the numerical model in order to find velocity profile of the magnetic cloud.

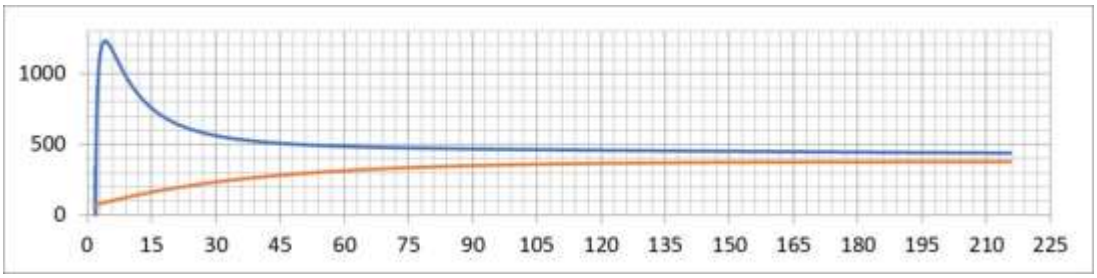

Figure 11: *This graph is provided under a numerical model made by Dr. Romashets showing the similarity of our experimental event and an actual event. We were able to ultimately decrease the S-factor to 15.7%.*

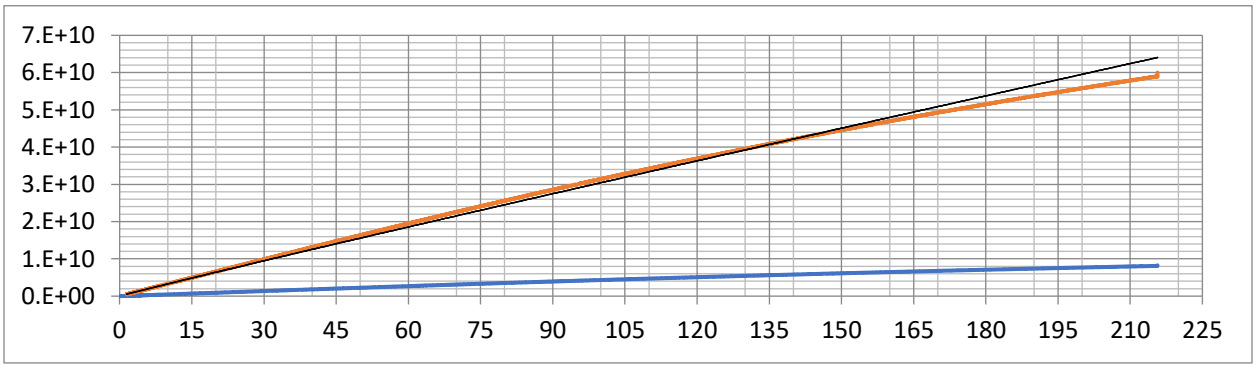

Figure 8: *Minor radius, blue, and major radius, red, of the toroidal magnetic cloud.*

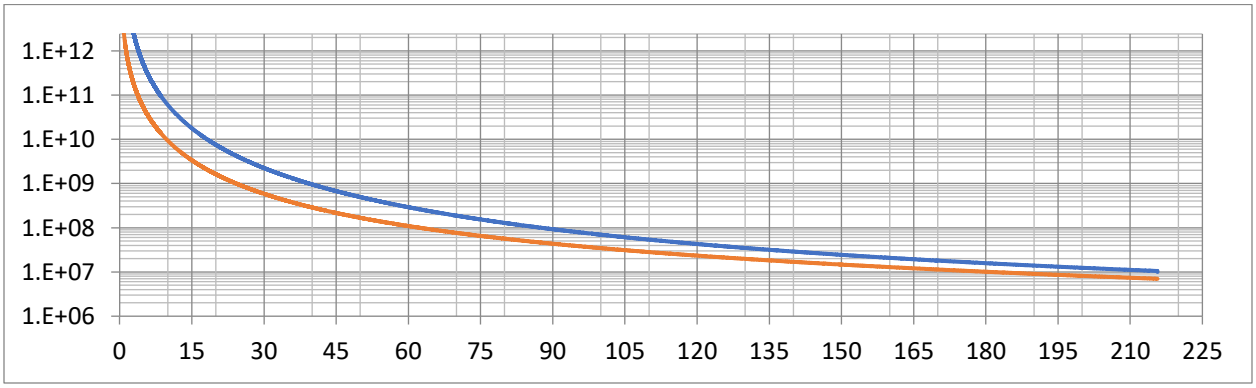

Figure 12: *Number density inside the magnetic cloud, blue, and in the solar wind, red line.*

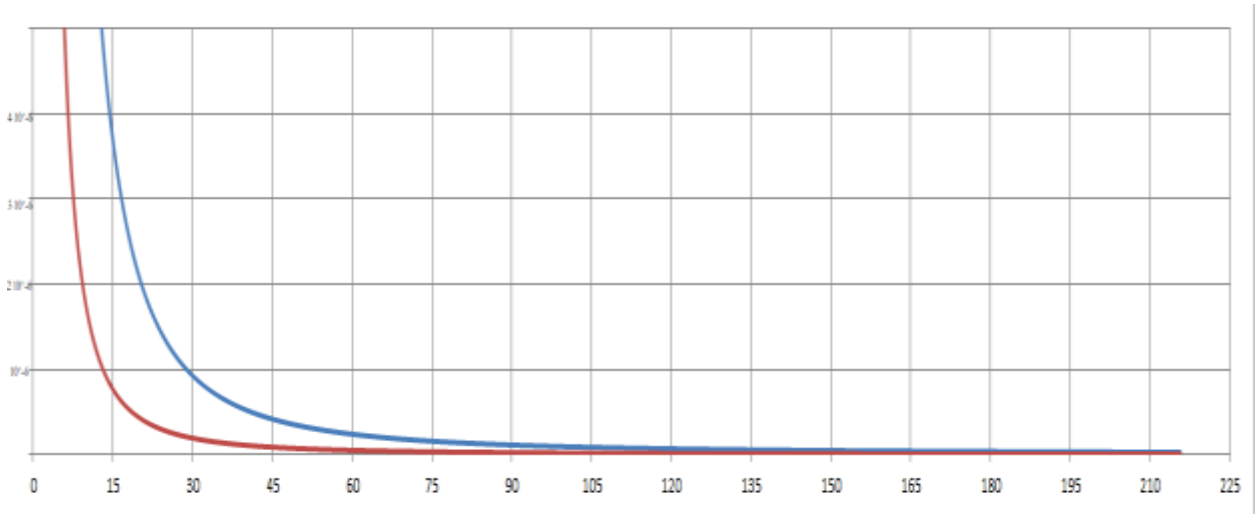

Figure 13: *Magnetic field in the magnetic cloud, blue, and in the solar wind, red line.*

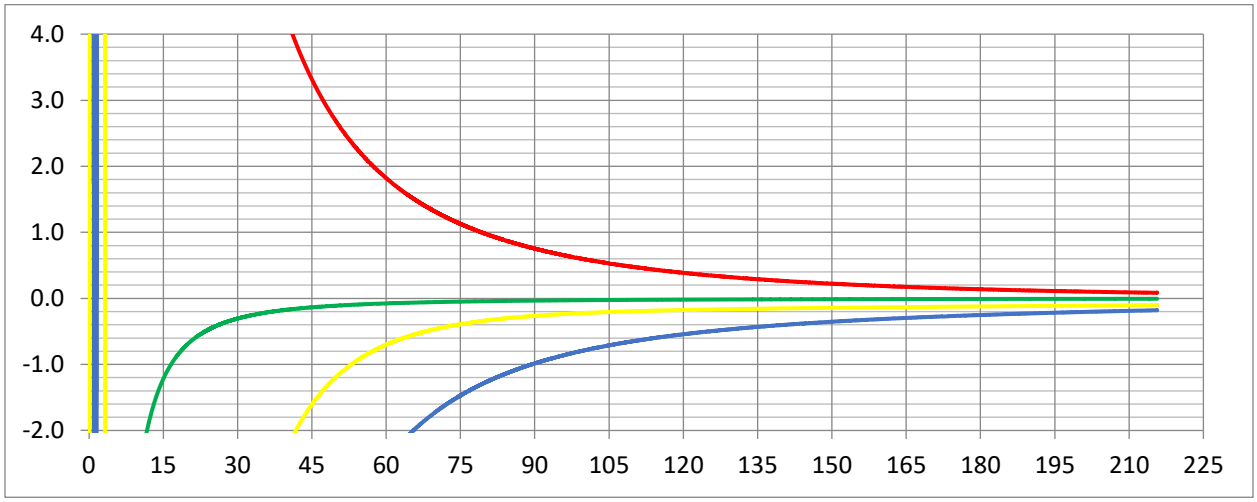

Figure 14: *Acceleration of the magnetic cloud due to gravity, diamagnetic force, drag force, and total acceleration.* The red line indicates diamagnetic acceleration. The green line indicates gravitational acceleration. The yellow line indicates the total of all listed accelerations. The blue line indicates acceleration caused by the drag force.

Results and Conclusion:

My research determined the optimum parameters for the geomagnetic event from April 17th, 1999 using a dynamics numerical model and looking for a minimum value of the S-factor, which measures the percent difference between the experimental travel time of the center-of-mass of the IMC and the value calculated with our dynamics model. The change

in the AP index allowed as to isolate the geomagnetic disturbance. Using the experimental parameters from Marubashi *et al.*'s list, we adjusted the drag coefficient, which is responsible for the main dynamics force that pushes a magnetic cloud from the source surface to the Earth's orbit. We discovered that for a drag coefficient of 2.6116 gives the minimum value of 15.7% for the S-factor. The event we analyzed in this research project will be used as benchmark for future projects that require an analysis of Heliospheric storms. Our model predicts that IMCs with large initial speeds, greater than 1,000 km/s at a few AU near the Sun's corona, and which end up with large speeds near the Earth's orbit, can reach the Earth's orbit faster, in about 3 days.

References

1. K. G. Ivanov and E. P. Romashets, *Heliospheric Storm of the First Interval of the International Solar-Terrestrial Project: Sun-Wind-Geotail* **Geomagnetism and Aeronomy**, 38(1), 1-6, 1998.
2. K. G. Ivanov and E. P. Romashets, *Filament-streamer Interplanetary disturbances*, **Geomagnetism and Aeronomy**, 39(2), 135-143, 1999.
3. E. P. Romashets, M. Vandas, and S. Poedts, *Modeling of the three-dimensional motion of toroidal magnetic clouds in the inner heliosphere*, **Astronomy and Astrrophysics**, 466, 357–365, 2007.
4. K. Marubashi, S. Akiyama, S. Yashiru, N. Gopalswamy, K.-S. Cho, and Y.-D. Park, *Geometrical Relationship Between interplanetary flux ropes and their solar sources*, **Solar Physics**, 290, 1371-1397, 2015.
5. K. G. Ivanov, A.F. Kharshiladze, and E.P. Romashets, *Mutual position of energetic flare, heliospheric layer, and Earth, contributing to the appearance of a strong geomagnetic storm*, **Geomagnetism and Aeronomy**, 32(6), 775-778, 1992.
6. Hoeksema, J.T., and Scherrer,P.H. *Harmonic Analysis of the Solar and Heliospheric Magnetic Fields*. **Bull. Amer. Astron**. Soc. 16, 452, 1984.

Kiley Mazdra

Major in Mechanical Engineering

Mentors: Dr. Evgeny Romashets and Dr. Cristian Bahrim

Research in Geo-space Science

Department of Physics

The Physics of Active Longitudes and Their Impact on Earth through the Interplanetary Coronal Mass Ejection They Produce

1. Background information

1.1. The goal of the project

This project includes our study over the relation between the number of sunspots created by solar activities, the change in the Ap-index of Earth's geomagnetic field and possible geomagnetic storms. It was found by Vitinsky *et al.* (1986) that longitudinal zones with active sunspot formation produce most of the strongest solar flares and other solar activities. The predominance of such solar sources in certain longitudinal zones can favor the generation of various near-Earth disturbances, including a recurrent series of geomagnetic extra storms as demonstrated by Ivanov *et al.* (in 2002 and 2005). This research is novel in the field of solar physics and space science, and has enlarged my knowledge in these fields.

This research helps us to understand the role of active longitudes (ALs) in solar corona. The anomaly in the longitudinal distribution of active regions themselves is often referred to as active longitude (AL). To reveal the connection between the AL and CME spatial occurrences, here we investigate the morphological properties of active regions. The term active longitudes was introduced by Vitinsky *et al.* (1986). It is defined as a range of latitudes 270-300 degrees, where most of solar events occur according to their statistical analysis. It is known that most of the 1995-2005 events were associated with ALs, including a superstorm in October 2003, as reported by Ivanov *et al.* (2005). Until now, the corresponding data on 2005-2022 events were not analyzed from this perspective, but we assumed they follow similar trends as the ones from 1995-2005.

Not all solar flares from active regions (ARs) close to active longitudes (ALs) can cause geo-effective disturbances. On the other hand, it turns out that geo-effective structures that triggered strong geomagnetic storm originated in AL solar sources. We wanted to find a criterion which will provide a hint when ALs are either on

or off in this sense. Together with more specific indicators, the level of solar activity measured in terms of Wulf (sunspot) number could be another candidate. One possible indicator for distinguishing if AL solar sources can or cannot lead to geomagnetic storms is the total area covered by open solar field lines in the vicinity of ALs. The complexity of interplanetary magnetic field (IMF) sector structure is another possible indicator.

1.2 My research hypothesis

It is well-known that solar sources, such as flares and disappearing filaments, causing inter-planetary disturbances which can produce geomagnetic storms upon their arrival to the Earth's orbit have originated from ARs located near ALs in solar corona. But not all such flares and disappearing filaments can lead to geomagnetic storms. The hypothesis was that it is possible to find a criterion which can tell when an active longitude region is on or off, so we can relate a solar source to a possible geomagnetic storm.

1.3 Literature review

Studies about the solar activity are very important for understanding the underlying physics and identifying various processes taking place in solar corona. Open magnetic field regions (ORs) located in the vicinity of ALs are involved into large scale counterclockwise circulation of magneto plasma of the convection zone. Rossby waves are usually observed in the vicinity of this zone. According to Tikhomolov and Mordvinov (1996), the Rossby waves can arise in the active transition layer (ATL) at the bottom of the convection zone and can produce various large scale, long duration deviations from a regular differential rotation. This can lead to global hydrodynamic instability. The configuration of ORs near ALs changes from one Carrington Rotation (CR) to another. All these processes can be better understood when we will have results of a full statistical analysis of ALs.

Ap Index is the earliest occurring maximum 24-hour value obtained by computing an 8-point running average of successive 3-hour Ap indices during a geomagnetic storm event and is uniquely associated with the storm event. I measure the Ap Index for the 24 hours and see if it is a geomagnetic storm. In Table 1 we list all solar sources from Oct 20-30, 2003 (Ivanov *et al.*, 2005) which could be associated to the super-storm on October 29, 2003, together with the AR, the date they occurred and the time (UT), the class of the solar flare, the angular latitude (Θ), relative longitude (Φ), and Carrington longitude (L) all in degrees:

Table 1. Solar flares from Oct 20-30, 2003 reported by Ivanov *et al.* (2005).

AR	Date	UT	Class	Θ, deg	Φ. deg	*L*, deg
484	Oct. 20	0648	2n	04N	46E	350
484	Oct. 21	0334	sf	06N	37E	346
484	Oct. 22	1507	sn	05N	22E	348
484	Oct. 22	1559	sn	03N	17E	353
484	Oct. 23	0236	sn	03N	15E	341
486	Oct. 23	0835	lb	2IS	88E	268
484	Oct. 24	2138	In	05N	09W	352
486	Oct. 25	0415	2n	15S	43E	286
486	Oct. 26	0617	3b	15S	44E	272
484	Oct. 26	2126	2n	OIN	38W	354
484	Oct. 27	0746	2f	OON	45W	348
484	Oct. 27	1721	ln	02N	38W	341
484	Oct. 27	1949	In	07N	50W	353
484	Oct. 27	2149	sn	08N	09E	294
484	Oct. 28	0054	If	03N	55W	345
488	Oct. 28	0353	If	08N	06E	284
486	Oct. 28	1001	4b	16S	08E	282
486	Oct. 29	0029	lf	18S	08E	268
486	Oct. 29	0048	If	16S	JOE	266
486	Oct. 29	0437	sn	17S	06E	270
486	Oct. 29	2037	2b	15S	02W	278

From this table one can see that all the solar flares prior to October 29, 2003 super-storm were in the vicinity of the active longitude's interval (270-350) degrees. The relative distribution of all solar flares in the interval September to December 2003 was reported by Ivanov *et al.* 2005, and we reproduce it in Figure 1. One can see that the solar magnetic field structure is very complicated, and many aspects should be considered to reconstruct the interactions between each element. Still, the maps shown in Figure 1 are much simpler than the one generated by the Carrington Rotation (CR) 1968 shown in Figure 2 (which is still considered as being the standard).

On Figure 2, each small area which contains magnetic field lines going outside of the source surface, is a sphere of radius 2.5 solar radii (measured from Sun's center of mass). Each such area is labeled with a small circle. This label is not present if the area contains only closed magnetic field lines. One can see that only 10-15% of solar photosphere contribute to interplanetary magnetic field. Other observation here is that open field lines are more spread out in latitudinal direction closer to AL's interval (300-350) than in the region to the east of it (240-270), where open fields are concentrated in +/-10 degrees zone from the equator.

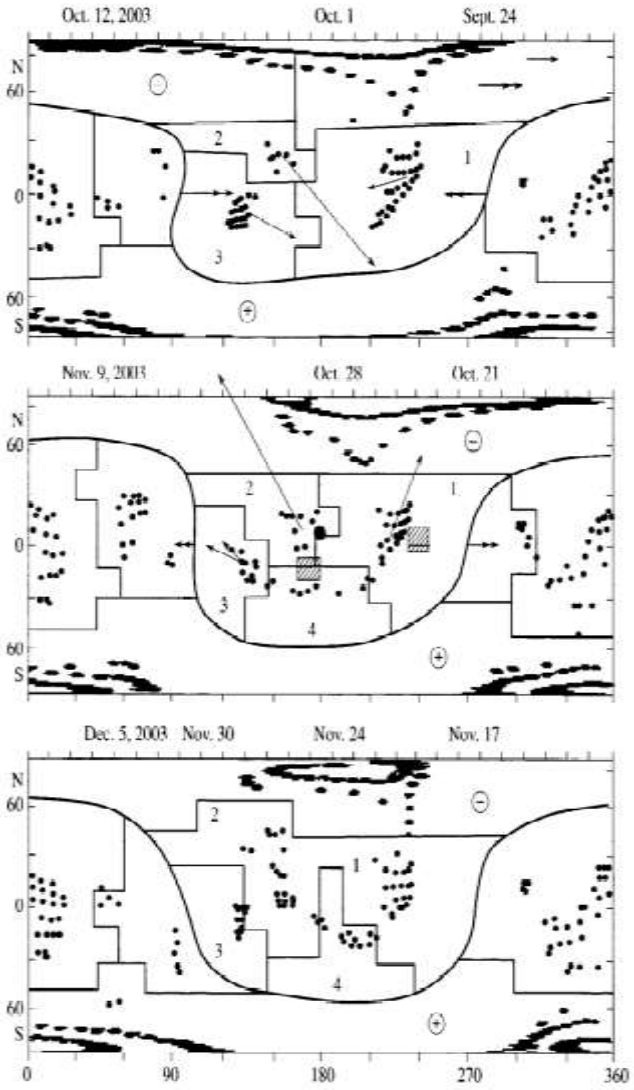

Figure 1. *The subsector structure of open solar magnetic field lines during three successive rotations centered on October 1, October 28, and November 24, 2003. Thick and thin curves show the sector and subsector boundaries, respectively, of the coronal magnetic field on the source surface (defined at 2.5 solar radii from Sun's center).Filled dots indicate the photospheric sources of the open field lines. Arrows mark the shift rates of the centers of photospheric sources between a given and the next rotation. Rectangles and dots show the ARs and Earth's helio-projection, respectively. This plot was reported by* Ivanov *et al.* (2005).

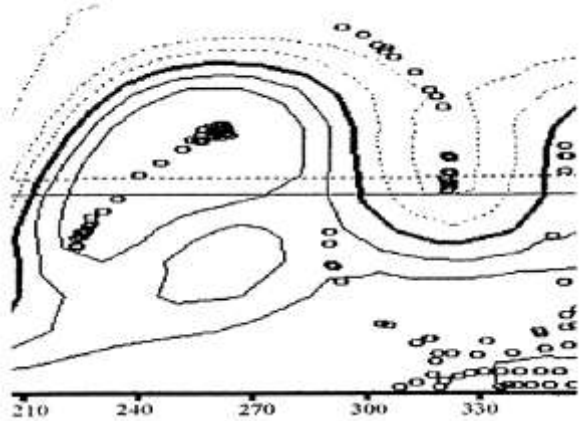

Figure 2. *Open solar fields in the vicinity of one of the main active longitudes during CR 1968 (source* Ivanov *et al.*,2005).

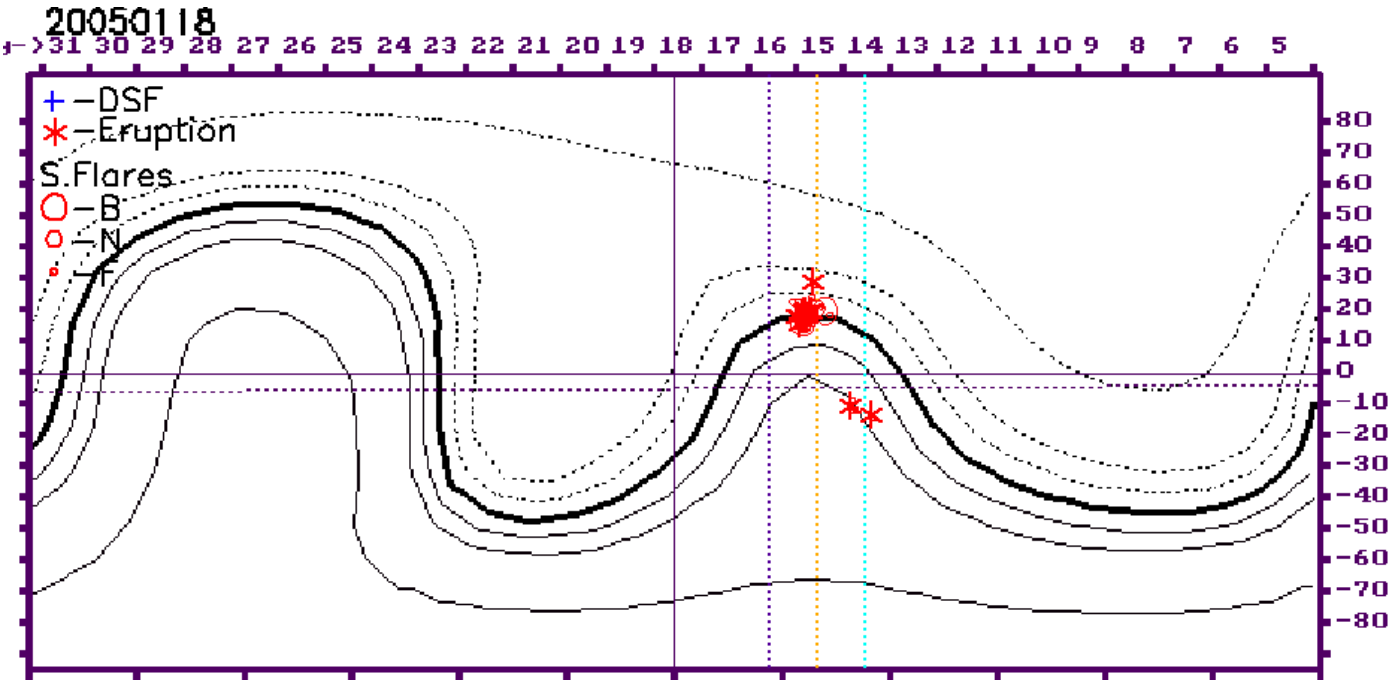

Figure 3. *Solar sources of January 18, 2005, geomagnetic storm were located in the longitudes range of 190-200 degrees, CR 2025, very far from active longitudes at 270-300 degrees, determined with the maps used in Ivanov et al. (2005).*

2. Results of the project and Discussions.

In this research project I followed the steps:

1) First, I have identified the geomagnetic storms with Ap > 50 nT during year 2005.

2) Next, I have identified the potential solar sources of 2005 geomagnetic storms.

3) I determined the position of solar sources relative to active longitudes using Figure 3 below.

4) Next, I plotted the number of sunspots (Wulf numbers) and compared with the Ap-index for the whole year 2005, Figures 4 and 5 below.

5) My analysis indicates that all solar sources of 2005 geo-magnetic storms are far from ALs.

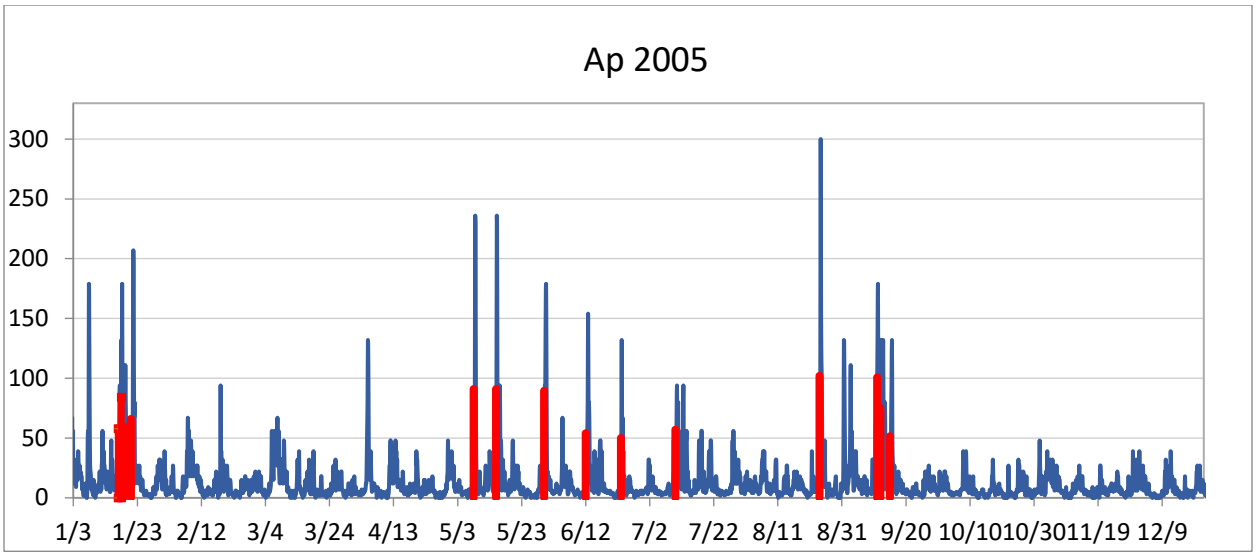

Figure 4. *Ap three hours averaged in 2005. Daily averaged with Ap > 50 nT are shown by red bars*

The Ap index is measured every three hours, eight times a day. In figure 4, the blue bar represents the daily average. The red bars represent daily average of Ap indexes with values > 50 nT. Originally, we were looking for days with the Ap indexes above 20. But Ap 20 is just a small disturbance in the geomagnetic field. Because there were so many days with the Ap index above 20, we have narrowed our results down a bit by focusing on the days with daily averages above 50.

The blue bars in Figure 4 represents three-hour average values of Ap, while the red bars indicate daily average Ap in the days when this daily value was more than 50 nT. One can see many spikes of three-hour average Ap, above 100 nT, and sometimes even above 150 nT, which have not led to daily average above 50 nT.

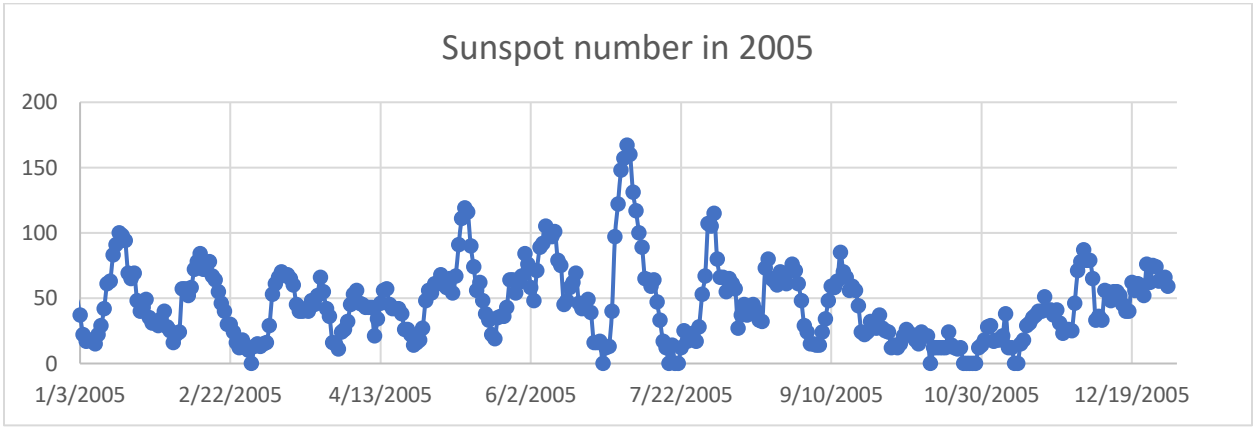

Figure 5. Sunspot number during the year 2005. The maximum value was reached on July 4.
The daily sunspot (labeled by some authors - number R) is computed using a formula-derived by Rudolph

Wolf in 1848: R= 10g+s, (Wolf, 1952), where R is the sunspot number; g is the number of active regions or groups with sunspots on the solar disk; s is the total number of individual spots in all active regions or the groups. For example, if there is only one sunspot, the sunspot number R is 10·1+1=11. If there are two sunspots in two different locations, then R is 10·2+2=22. If there are four active regions with one sunspot in each one, then R=4·10+4=44. Because data on sunspots is available for many centuries, Wolf calculated R for many solar cycles before 1848. Nowadays, Royal Observatory of Belgium continues this service and provides the sunspot numbers on regular basis.

For me, it was interesting to see that the maximum of R=167 on July 6, 2005 actually was followed by the daily average of Ap = 57 nT on July 11, five days later. On the other hand, the strongest Ap daily values of 102 nT and 101 nT were reached in August and September, while preceded by much smaller values of R than that of July 6, 80 and 85. Sometimes, a spike of R number is followed by the spike of Ap index, sometimes – not.

3. Conclusions.

I found that all solar sources of interplanetary disturbances leading to strongest geo-magnetic storms in 2005 were far from active longitudes. This can be explained by the decrease of sunspot number volatility. One can see in Figure 5 that closer to the end of 2005 the sunspot number graph becomes smoother, with smaller variations compared to the beginning of the year. We can assume that active longitudes are more geo-effective in the rise of an eleven-year solar cycle but becomes less geo-effective on declining phase of this solar cycle. More statistical analysis is needed.

References

1. Vitinsky Yu.I., Kopecky M. and Kuklin G.V., Statistics of Sunspot Formation Activity, Nauka, (1986).

2. K. G. Ivanov, V. Bothmer, A. F. Kharshiladze, E.P. Romashets, and I. S. Veselovsky, Dynamics of open solar magnetic fields, active longitudes, and near-Earth disturbances, ESA SP-506, 141-144 (2002).

3. K. G. Ivanov, A.F. Kharshiladze, and E.P. Romashets, Solar-Terrestrial storms of October 2003. 1. Solar sources and Near-Earth interplanetary disturbances, Geomagnetism and Aeronomy, 45(1), 5-22 (2005).

4. E. Tikhomolov and V. I. Mordvinov, Rossby vortices in the layer between convection zone and radiative interior, Solar Physics, 172(1).

5. Wolf, R. (1852). "Sonnenflecken-Beobachtungen in der ersten Hälfte des Jahres 1852; Entdeckung des Zusammenhanges zwischen den Declinationsvariationen der Magnetnadel und den Sonnenflecken" [Sunspot observations in the first half of the year 1852; discovery of a relation between the variations of the declination of the magnetic needle and sunspots]. Mittheilungen der Naturforschenden Gesellschaft in Bern (in German). 245: 179–184.

Ian Sisson

Major in Chemistry

Mentor: Dr. Paul Bernazzani

Research in Chemistry

Department of Chemistry and Biochemistry

Iron-Cellulose Bioplastic Nanocomposite Research

Abstract

Research was conducted into the efficacy of using ferromagnetic cations bound within a cellulose-based biopolymer to increase the crystallinity of the resulting material by using a magnetic field to orient the cations and therefore the cellulose nanofibers. Analysis using Fourier Transform Infrared (FTIR) spectroscopy, differential scanning calorimetry (DSC), and polarized light microscopy was carried out on the product to study structural changes and differences in thermal properties.

Introduction

Plastics are a necessary and useful part of the modern world with a high degree of ubiquity in many industries. This ubiquity has made them an equally ubiquitous pollutant, which is an ever compounding problem as they break down into smaller and smaller microplastics and nanoplastics due to their nonbiodegradability. These microplastics have entered streams, rivers, oceans, fish, and eventually the majority of humans on the planet. Furthermore, these materials are inherently limited and finite by simply being non-renewable petroleum products.

Therefore, any alternative to plastics with similar utility and greater biodegradability and renewability will ultimately be of great benefit to the environment and human society. This has resulted in a great deal of interest in cellulose biopolymers, as cellulose is biodegradable, biocompatible, renewable, and is the most abundant biomass on the planet.

Cellulose is capable of taking on many forms, however, the creation of a useful plastic-like material often occurs through a crosslinking reaction, which involves binding multiple cellulose nanofibers (CNF's) together with an intermediate. Epichlorohydrin (ECH) was used as a crosslinking agent to bind the CNF's together, making them

more rigid. Unit cells and effectively crystals form as these CNF's are packed together as the crosslinker causes them to rigidify. The orientation of the fibers has a known effect on the crystallinity and strength of the material, which can be gained by drawing and stretching the material as it dries (1). Increasing the strength of the material by increasing the crystallinity is the goal of this research.

Cellulose itself is a polymer chain of glucose molecules, which has many hydroxide and ether functional groups. These functional groups will react with or be attracted to positively charged cations, and it is the goal of this research to use this attraction to orient the CNF's to a higher degree by orienting ferromagnetic cations such as Fe^{2+} with a magnetic field, resulting in an overall increase of the crystallinity and physical properties of the cellulose biofilm.

Methodology

Powdered cellulose was rapidly dissolved in a pre-cooled 0°C aqueous solution of 7% NaOH and 12% urea to create a viscous 6.00 wt % solution while maintaining temperature control to facilitate complete dissolution of the cellulose. 250 µl of ECH and 20 mg of iron oxide nanoparticles (Fe_3O_4 and Fe_2O_3) were added while stirring.

Several groups of films were made, consisting of B group which contained 4 Fe_3O_4 films, R group which contained 2 Fe_2O_3 films, and C group which consisted of one control film lacking any nanoparticles. Each group was subjected to differing magnetic conditions and contained one control film that was not exposed to any magnetism. The strength of the magnets used for B group was 15 kg, 50 kg, 150 kg for B1, B2, and B3 respectively. R group used a 40 kg magnet for film R1.

The solution was placed in an ultrasonic desiccator filled with ice water to ensure temperature control for 10 minutes to get rid of any bubbles and properly disperse the nanoparticles

Equal amounts of the solution were weighed in identical proportioned petri dishes to ensure uniformity, then left to cross link for 20 hours The crosslinking reaction was then stopped by the addition of 50% ethanol for 4 hours, resulting in the formation of hydrogels. The hydrogels were then soaked in water for 10 minutes to ensure any excess solution has been washed off.

These gels were left to dry for 12 hours so they could be more easily handled, then were hung up to dry and weighted for 1-3 days. This method decreased drying time and the force applied by the weight gave more structure to the CNF's (1)

Each film underwent structural, thermal, and microscopic analysis using FTIR, DSC, and a polarized light microscope.

Results and Discussion

Structural analysis of the films through FTIR, shown in Figures 1, 2, and 3, can be used to monitor the progress of the crosslinking reaction to a degree. For each crosslink, 2 hydroxide groups are replaced by 2 ethers and 1 hydroxide. The alcohol stretch at 3000-3600 cm^{-1} and the ether peak at 1050-1185 cm^{-1} can be used to roughly determine the extent of the reaction as the O-H stretch decreases and the C-O stretch increases. However, O-H stretch tends to increase in the samples as the biofilms age due to an unknown mechanism, so the changes from 1050-1185 cm^{-1} are the most informative.

Among the B group, shown in Figure 1, B2 had the highest absorbance, indicating it had the best crosslinking of the group. The R group, as shown in Figure 2, was mostly quite similar, with R1 having a slightly higher peak, and the control, C1, showing an overall different structure without the presence of nanoparticles. When the highest performing films (B2, R1, and C1) are directly compared in Figure 3, B2 has the overall highest amount of crosslinking according to this metric.

Crystal formation can be directly monitored using a polarized light microscope, as these crystals all have differing sizes, orientations, and refractive indexes. Through a process called birefringence, polarized light has its wavelength increased into the visible spectrum by going through multiple different refractive indexes. The color of the light can indicate the overall change in wavelength, which informs the sizes of crystals formed. Blue light indicating small crystal structures, red light indicating larger crystal structures, etc.

The B group, seen in Figure 4, shows an increasing amount of crystal formation as magnetic strength increases. There is very little crystallinity at 15 kg, but at 50 kg the coloration becomes more apparent and contains several different colors, including blue, green, and purple. This indicates a variety of sizes of crystals in the structure. In contrast, B3 crystals are primarily blue, indicating formation of primarily small crystals.

The R group, pictured in Figure 5, shows a stark contrast between the two films. R2 has no apparent crystal formation, while R1, shows substantial crystal structures refracting many different wavelengths of light, indicating the presence of many sizes and orientations of crystals.

The presence of all these crystal structures and the fact that they appear to correlate positively with the strength of the magnetic field supports the initial hypothesis that the magnetic field in conjunction with the iron oxide nanoparticles can be used to increase crystallinity and preferentially orienting the cellulose nanofibers.

Thermal analysis using DSC was carried out to better quantify the crystallinity of the structures. Due to the complexity of the multiple reactions and transitions occurring as the sample is heated, it was determined that

endothermic reactions were primarily of interest as the degradation of the crystal structures would require input of energy, which occurs from approximately 10-250°C. This region was integrated to find the overall enthalpy of these reactions, informing on how well organized the crystalline structures are.

Figure 6 shows the raw DSC results of the B group and their enthalpy values compared to the magnetic force used. B1 shows a slight improvement over the control, B4, with 6768.48 and 6562.09 W/g respectively. B2 on the other hand shows a 14% increase over the control with 7516.63 W/g, and then B3 drops below the control with 6550.09 W/g. This further supports the hypothesis that crystallinity can be increased with magnetization, but it also implies that there is some maximum, either between 15 and 50 kg or between 50 and 100 kg that further testing and more data points can determine.

The R group, depicted in Figure 7, showed a more substantial enthalpy increase of 29% over the control with R1, having 7277.7 W/g and R2 having 5618.9 W/g. This is a very encouraging sign for the efficacy of the Fe_2O_3 nanoparticles ability to increase crystallinity over the Fe_3O_4 nanoparticles, despite the overall enthalpy between R1 and B2 being similar. More tests are needed to find the point at which a theoretical maximum of crystallinity is achieved.

While these results have been encouraging for their support of the initial hypothesis, none of these films had greater enthalpy values than C1, the cellulose control film at 8036.06 W/g. While these nanoparticles can bring structural stability, their presence also has an initial negative impact that further research must overcome.

Conclusion

The results at every point support the hypothesis that magnetic cations in a magnetic field can be used to orient cellulose nanofibers increasing crystallinity. More testing is required to definitively determine the optimal type of nanoparticle. However, the presence of these nanoparticles can be disruptive to the nanofiber matrix, so any gains made must overcome these deficiencies. It is possible that once more data points are taken and the process is refined that a material with properties superior to cellulose alone can be made, which will be the ongoing goal of any further research.

References

1) Unique Stress Whitening and High-Toughness Double-Cross-Linked Cellulose Films Pingdong Wei, Junchao Huang, Ying Lu, Yi Zhong, Yongfeng Men, Lina Zhang, and Jie Cai *ACS Sustainable Chemistry & Engineering* **2019** *7* (1), 1707-1717
DOI: 10.1021/acssuschemeng.8b05485

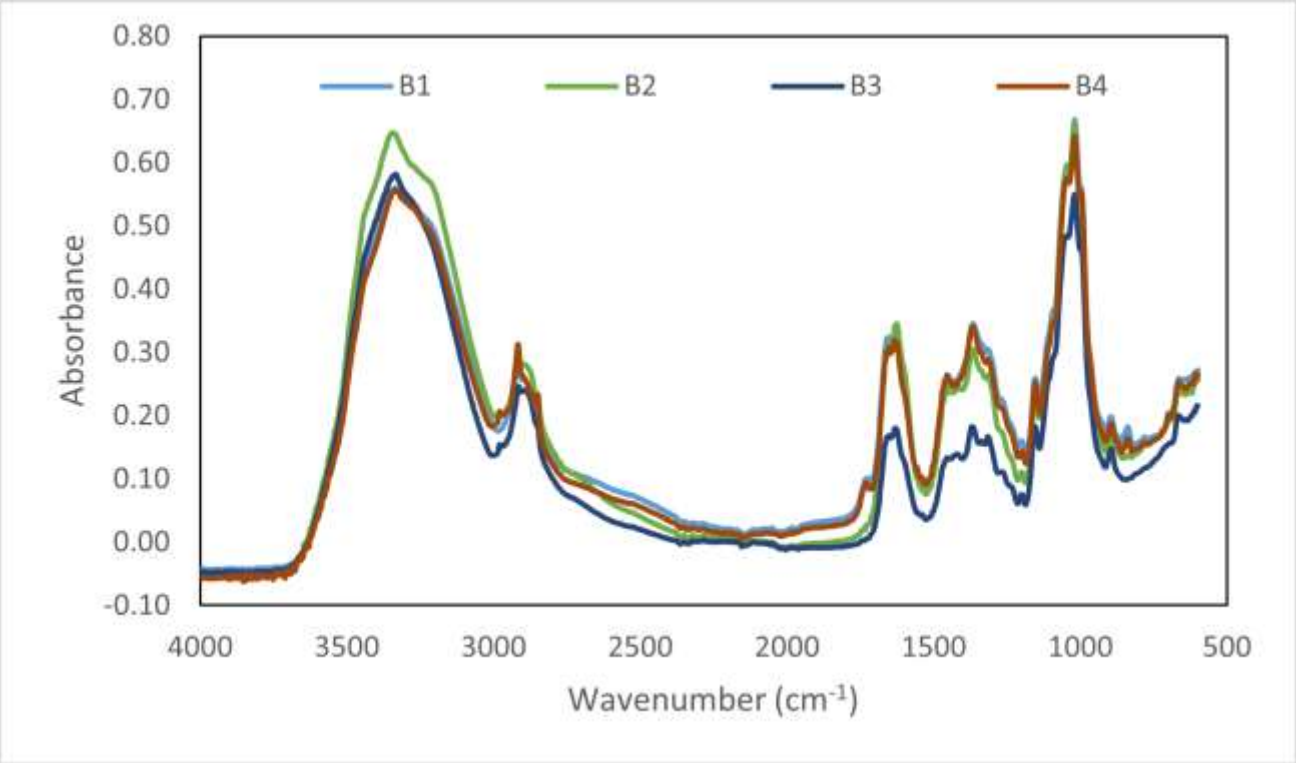

Figure 1: FTIR analysis of group B.

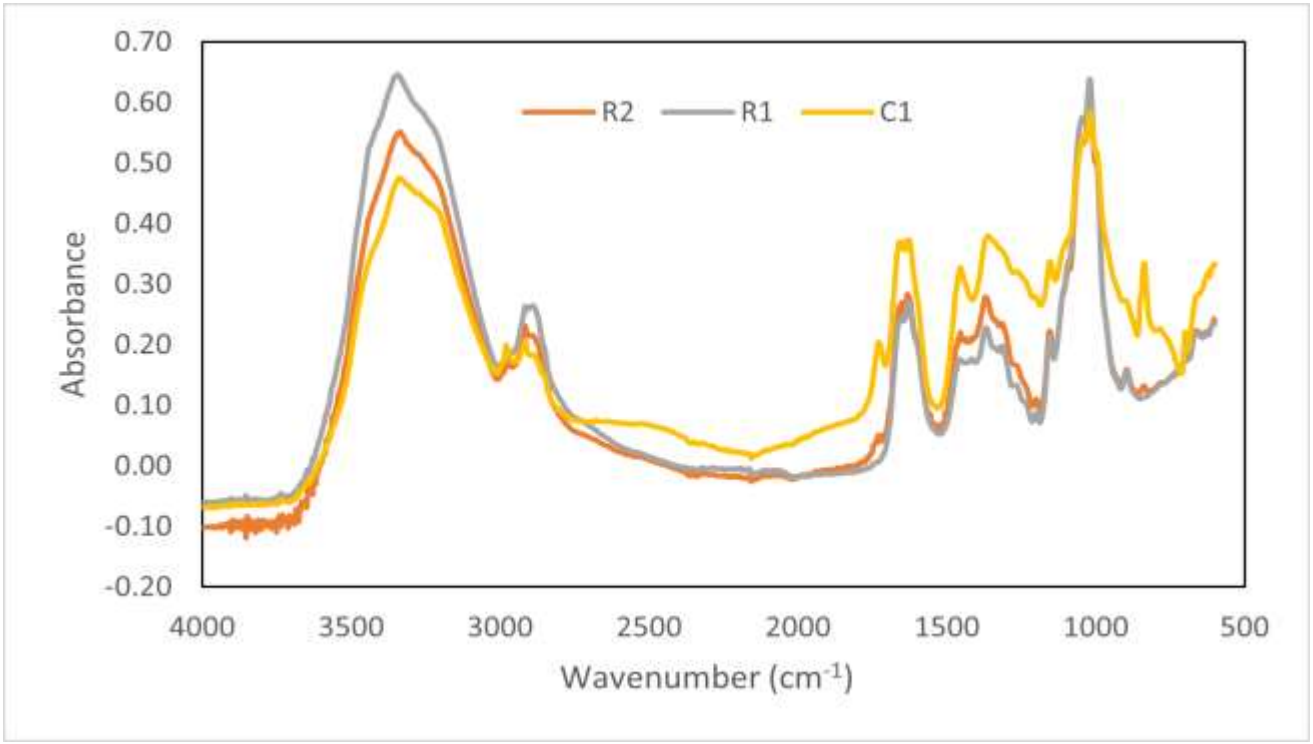

Figure 2: FTIR analysis of group R

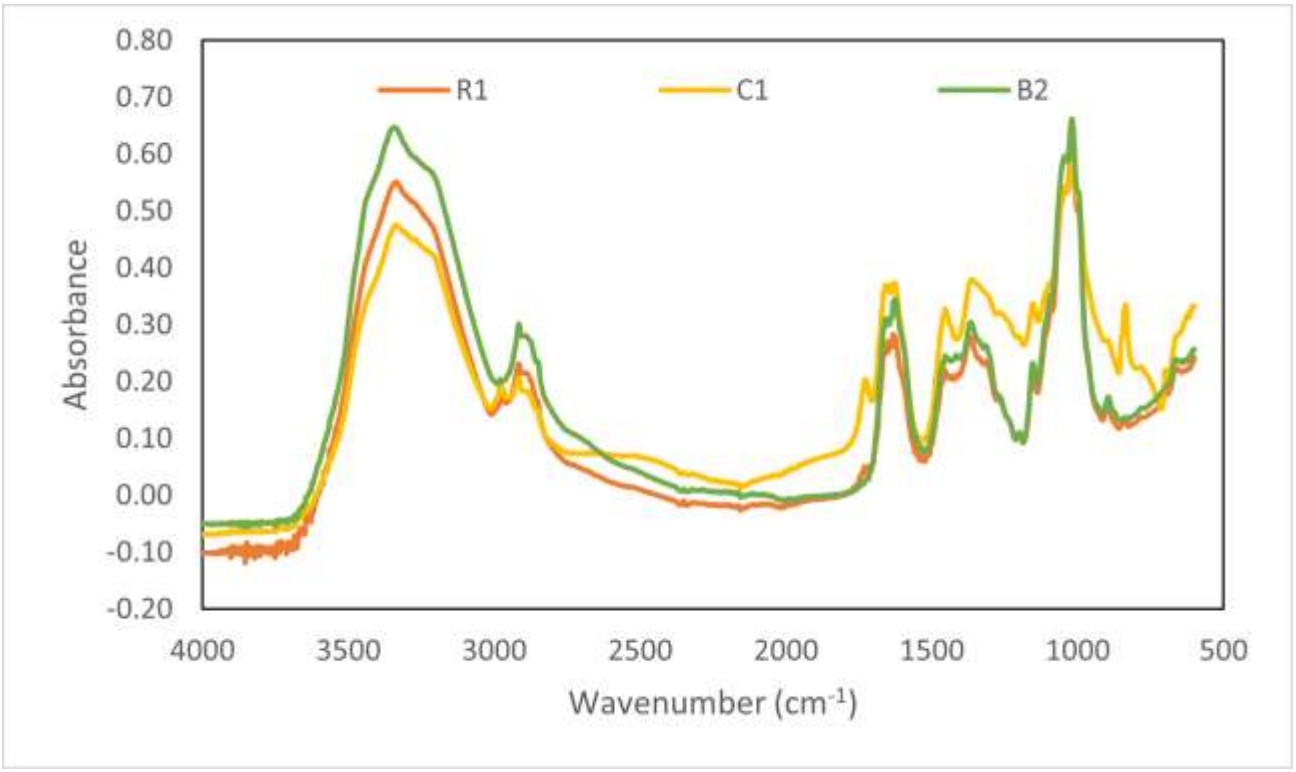

Figure 3: Comparison of FTIR results from groups B and R with the control group C

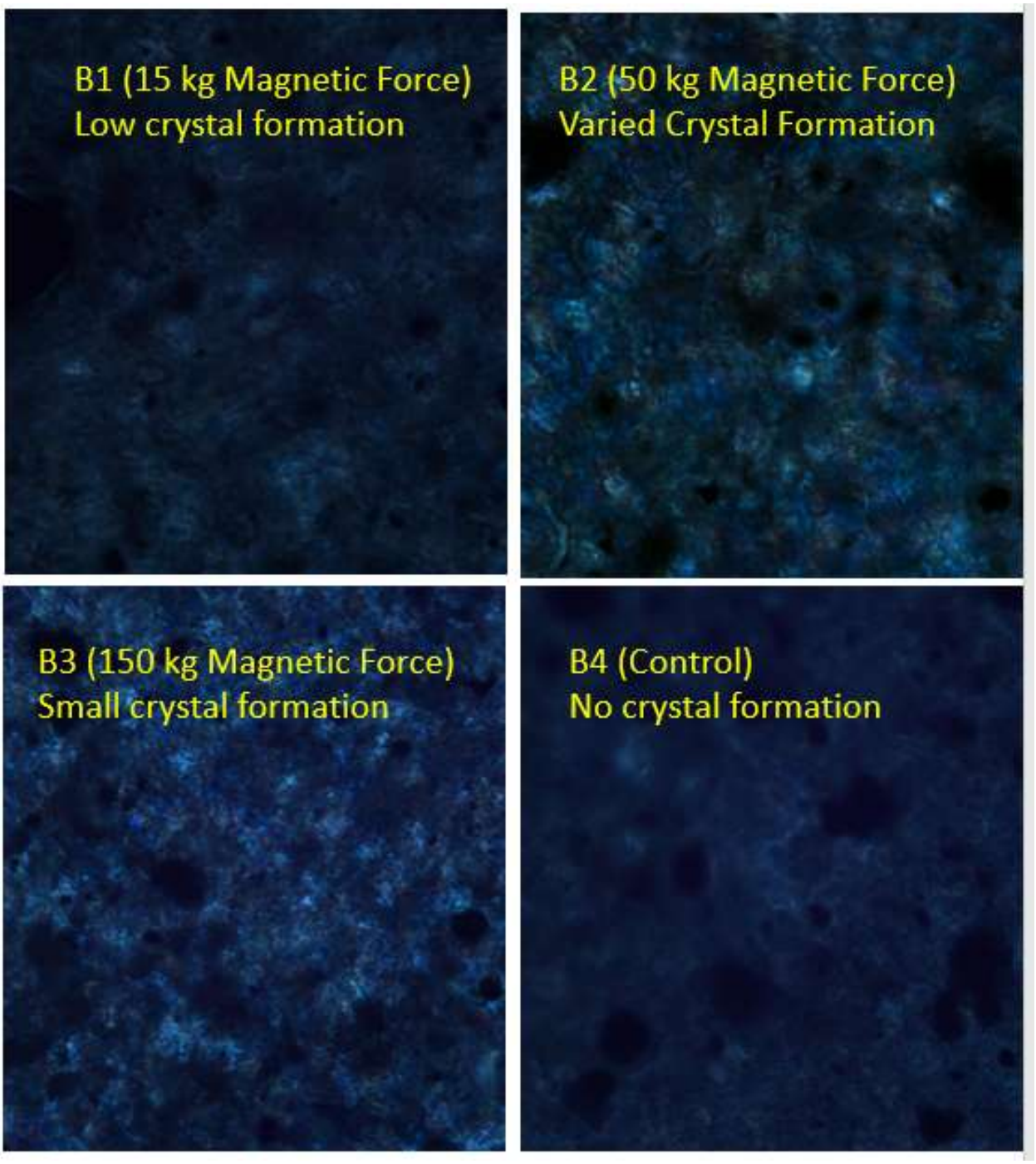

Figure 4: Polarized Light Microscope images of the B group with various levels of crystal formation

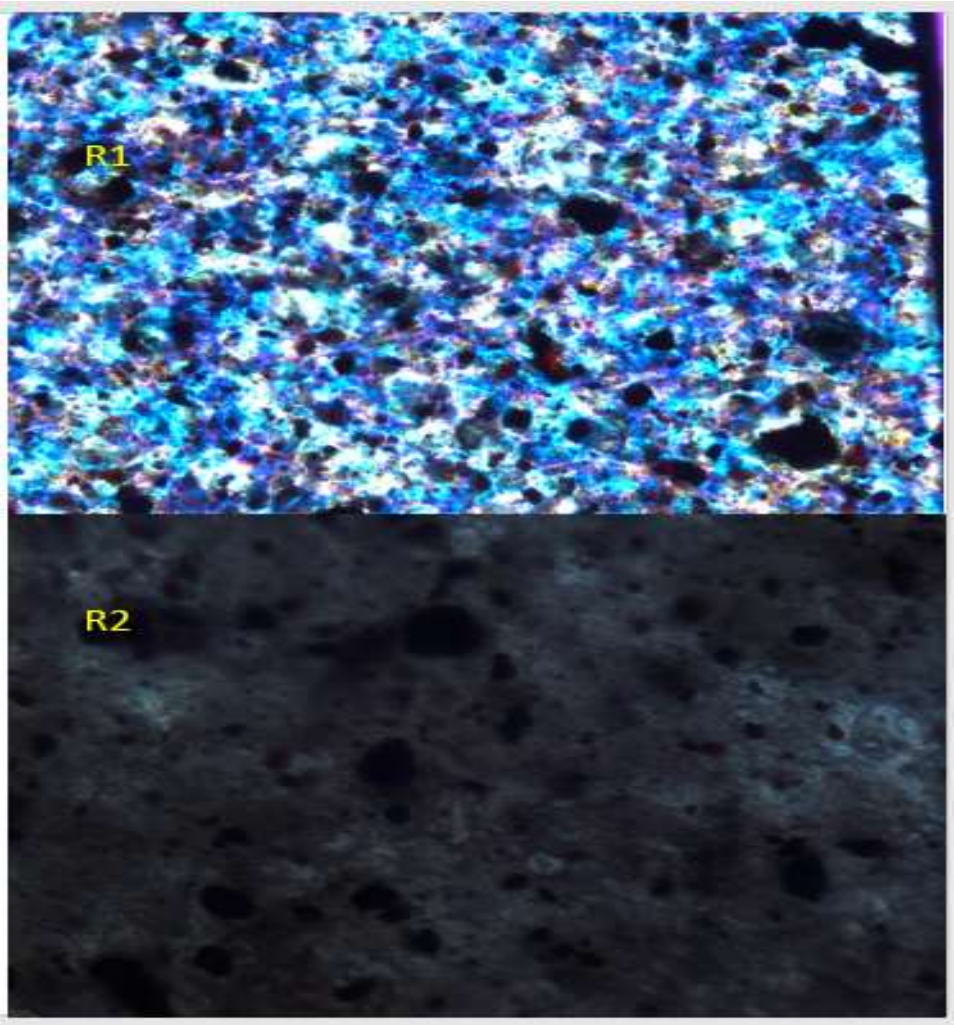

Figure 5: Polarized light microscope images of the R group

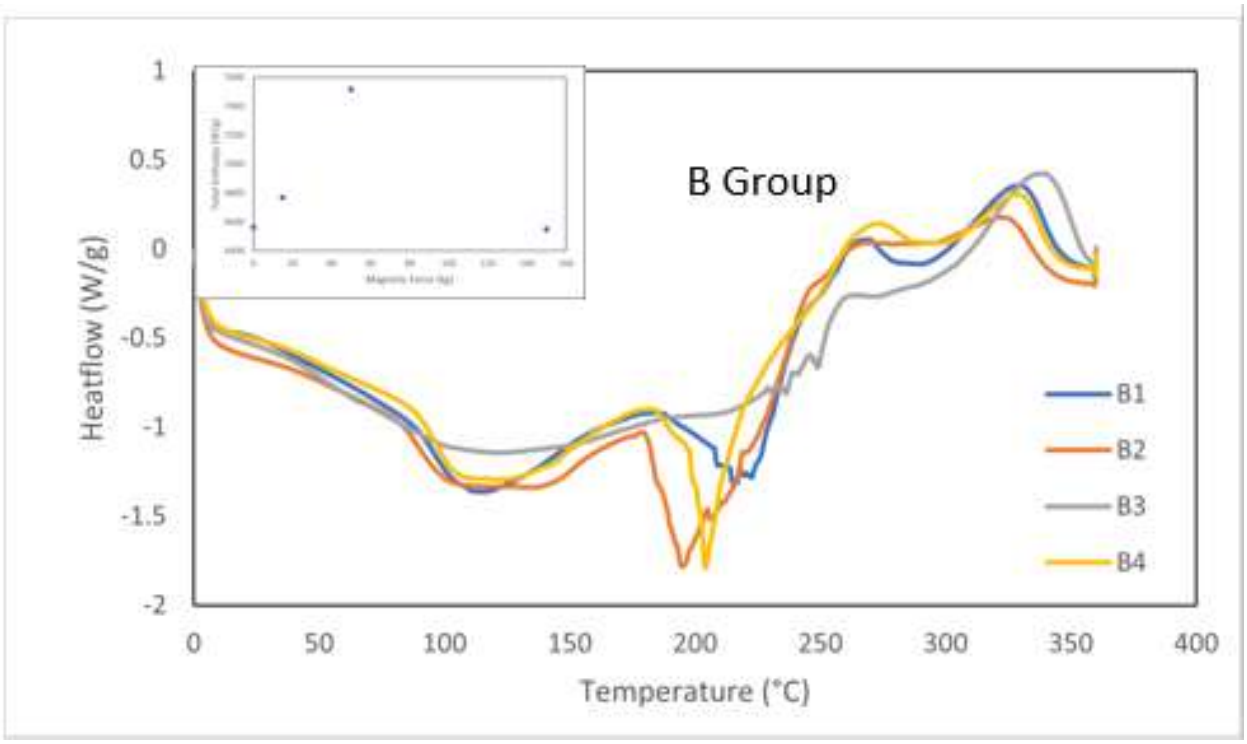

Figure 6: DSC analysis of the B group and integrated enthalpy values from 10-250°C compared with magnetic force

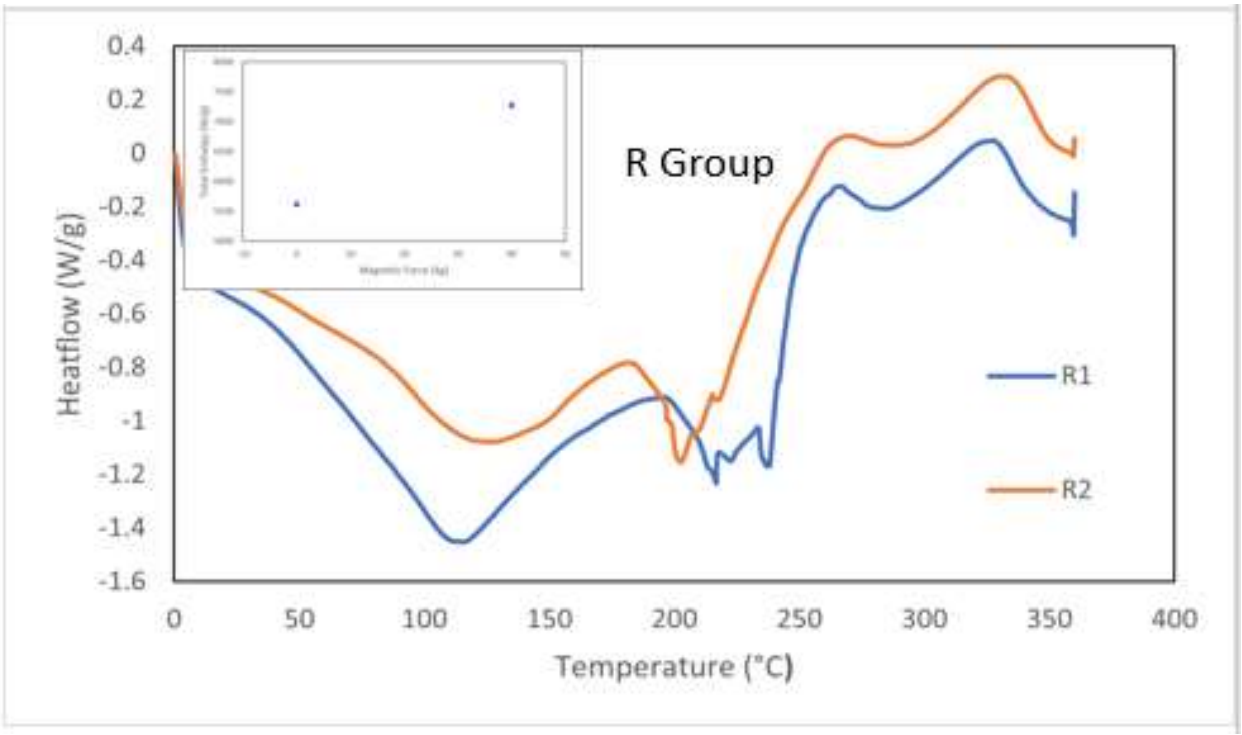

Figure 7: DSC analysis of the R group and integrated enthalpy values from 10-250°C compared with magnetic force

Jacob Smith

Major in Mechanical Engineering

Mentor: Dr. Sushil Doranga

Research in Mechanical Engineering

Department of Mechanical Engineering

Evaluation of Pin Fretting in the Electronic Connectors Using the Vibration Shaker

Abstract

Electronic Connectors used in printed circuit board assemblies (PCBAs) are important in everyday life as they allow transmission of signal at high speed consistently. These connectors used in PCBAs are used in industries like transportation, agriculture and home networking. However, due to the harsh vibration environments, the overall reliability of the connectors is always questionable. This project aimed at quantifying the failure of the connectors, especially the pin fretting problem due to different vibrations signal. The goal of this research is to understand the relationship between frequency and amplitude of vibrations with respect to the change in the resistance of the mating connectors.

Introduction

Backplane connectors are specifically effective and have high data transfer rates. Furthermore, they are physically compact, so they do better in small confined spaces that require an almost instantaneous computing action– such as brake systems in cars. The same theory is applied to connector's used in locomotive, telecommunications and aerospace industries. These connectors are assembled to the programmable PCB using the press fit technique. During, vibrations, because of the dynamics of the PCBs, there exist a relative motion between the mating connectors. The magnitude of the relative motion will in turn define the fretting rate of the connectors. In this project, I used the sample backplane connectors from Molex Inc., and designed the PCBs to fit the connectors. The designed PCBs are fabricated and a suitable fixture is designed to perform the vibrations testing. Beside this, the concept of pin fretting is demonstrated by using the finite element approach. In order to demonstrate the pin fretting concept, the overall experimental assembly is modeled using the SolidWorks

simulation and the modal frequencies, mode participation factors and sliding motion between the mating connector are explored.

Simulation

This project relied heavily on the use of software and running simulations. I used SolidWorks for two important reasons: designing the base for the bracket [Figure 1] for my set-up and finding theoretical natural frequencies, sliding motion between the mating connector and the mode participation factor.

PCB connectors are small and without having the luxury of time to prototype different positions for mounting, a lot of work went into designing the frame housing, and to then be able to reassemble it after the completion of the 3D printing process.

Using the frequency analysis tool in SolidWorks I was able to obtain three frequencies that would in theory be modes with high resonance at three different locations that I hope to prove once the experiment is underway [Figures 2, 3, and 4.]

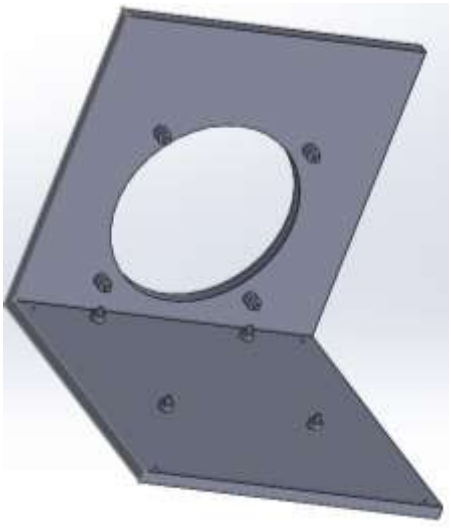

Figure 1: 3D printed base

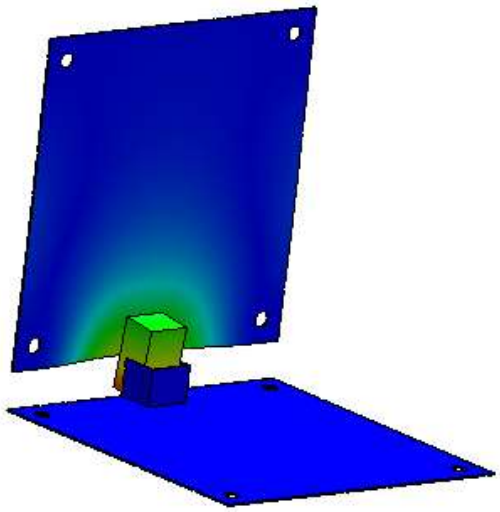

Figure 2: First mode position

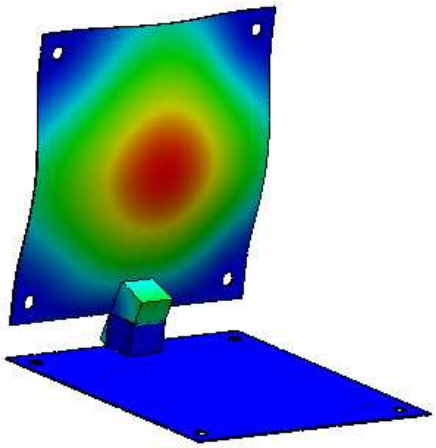

Figure 3: Second mode position

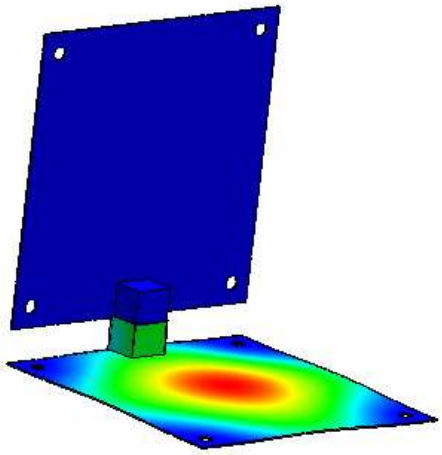

Figure 4: Third mode position

Manufacturing

Manufacturing all the pieces for the testing was incredibly challenging. Lamar University's 3D printers are not the largest so in attempting to print any piece that was larger than a six-inch cube was impossible. Initial iterations of the frame were dependent on it being printed out as a solid in one whole turn, so having to design a way that it could be pieced back together [figure 5.]

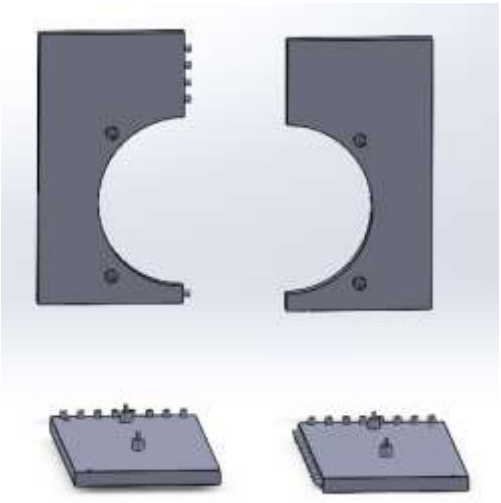

Figure 5: Unassembled 3D printed base

Mentioning again the PCBs that were required, they had to be manufactured by a third-party vendor to fit not just our requirements, but also Molex's. What Molex's connector required was that the mating pitch had to

be exact, and the through holes had to be designed for whether the connector would be soldered or simply press fitted into the board. As for my experiment the only requisites were that the pitch concentration was to be near the edges to allow for an easier setup and that the corner holes be large enough to fit the Shaker's stand to be able to screw it into a rigid connection,

Experiment

The setup for the experiment is to fix the housing of the frame to the laboratory's table in which the Shaker is located in. Depending on which mode I am trying to validate either the shaker or the PCBA could be relocated for ease. Attached to the board in which the primary mode was being tested, the resonance and amplitude probes would be attached, and the 4 wire Kelvin clips would be attached to the board-mating pins of the assembled connectors, which would theoretically give us the resistance values between the pins of the male and female parts.

While the digital multimeter (DMM) was attached (via the Kelvin clips,) I would then use one of the simulated frequencies to then apply that vibration to the entire PCBA. Once the assembly was run out of its life cycle, I can then investigate establishing correlations between frequency and amplitude.

Results

Unfortunately, my most important part has not arrived as of present, however I am still able to run a sample run using a single board and single connector prototype to establish a more accurate, experimentally derived, natural frequency [Figure 6, 7, and 8.]

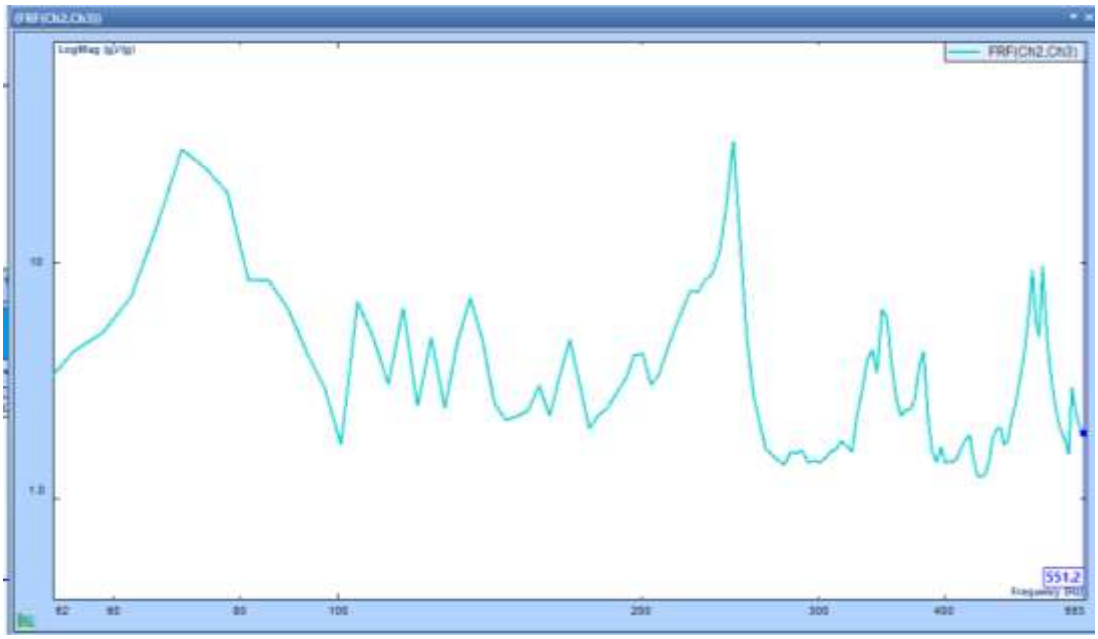

Figure 6:Sine Sweep Test of prototype from 20-1000Hz

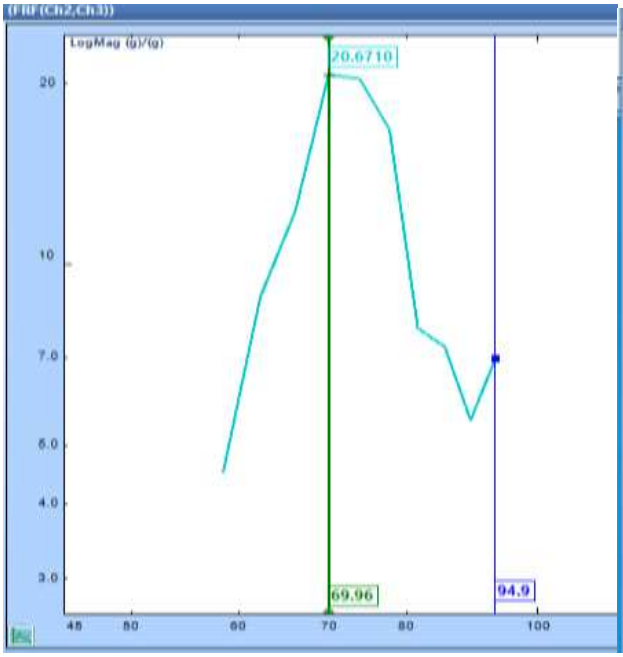

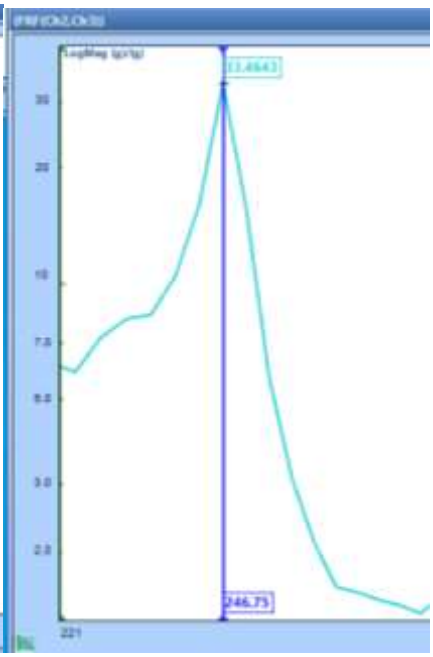

Figure 7: 1st natural frequency of prototype *Figure 8: 2nd natural frequency of prototype*

Conclusions and Future Works

As stated above, it is simply too early to start making conclusions as there is technically no data that has been accumulated that I can use in support of the original problem statement. But I am cautiously optimistic.

Moving forwards with this research, once it has been completed, would be to analyze how this data can improve existing models of performance. This would take the form of actual research and development and either then attempt to redesign either a new housing for the pins, or looking into better metal plating for the connector pins.

References

(2022). Retrieved 18 August 2022, from https://www.allaboutcircuits.com/textbook/direct-current/chpt-8/kelvin-resistance-measurement/.

Imechanica.org. (2022). Retrieved 18 August 2022, from https://imechanica.org/files/Zhai%20Hanaor%20Gan%20-%20stress%20dependent%20ECR%20at%20fractal%20rough%20surfaces_0.pdf.

Kim, M., & Rho, J. (2022). CDPDS: Coupled dipole method-based photonic dispersion solver. Retrieved 18 August 2022, from.

Reddit.com. (2022). Retrieved 18 August 2022, from https://www.reddit.com/r/ElectricalEngineering/comments/ufn5ya/measuring_resistance_through_backplane_connectors/.

Telaar, N. (2022). Frequency, Amplitude, Vibrations: How is Resonance Created? | RINGFEDER®. Blog.ringfeder.com. Retrieved 18 August 2022, from https://blog.ringfeder.com/frequency-amplitude-vibrations-how-is-resonance-created.

Telecom Infrastructure. Molex.com. (2022). Retrieved 18 August 2022, from https://www.molex.com/molex/industry/wireless_infrastructure.

What is Fatigue Strength? - Matmatch. Matmatch.com. (2022). Retrieved 18 August 2022, from https://matmatch.com/learn/property/fatigue-strength.

Lily Yoder

Major in Psychology

Mentor: Dr. Edythe Kirk

Research in Psychology

Department of Psychology

The Effects of Positive Mood and Stereotype Threat on Memory Recall

Psychology is a relatively new science that has proven to be fast paced, making discoveries that alter our knowledge of the human psyche daily. It is no surprise that researchers have studied how mood affects memory processing (Terry, 2017). For example, it is generally agreed that a positive mood causes us to switch to a "heuristic processing mode," which involves short-cut thinking and utilizes fewer cognitive resources, whereas a negative mood can lead to utilization of more "cognitive resources and more effort" (Zhang et al., 2018). Essentially, when individuals are in a negative mood, they are more likely to assign more meaning (otherwise known as semantics) to what they are processing, and therefore the information will be encoded more effectively (Zhang et al., 2018).

This leads to the question of whether mood affects the number of *false memories* an individual will have. Human memory is subject to many errors, and the phenomenon of false memory refers to when people "recall or recognize things that did not actually happen" (Dang et al., 2020). If positive mood leads to less accurate memory storage, does this mean that memories encoded while an individual is in a positive mood are likely to be less accurate? A study by Zhang et al. examined how mood and age affected false memory recall by priming participants with a video (positive, negative, or neutral) and then administering the Deese–Roediger–McDermott Paradigm (DRM), which is an assessment commonly used to assess memory recall. Their results indicated that positive mood did not increase false memory recall, but they attributed this finding to inconsistent arousal levels. There was no significant difference in false recall between children and adults when the children were in a positive mood, but children did have less false recall when in a negative mood recalling negative information. This difference makes sense considering that negative mood predisposes one to more concrete semantic processing.

The DRM paradigm has been used as a measure of false memory in many studies, comparing false memories across age, such as in a study by Dang et al. (2020), which used the DRM paradigm to assess age

differences in false memory recall. The DRM paradigm involves a researcher reading a list of related words to a participant, and then the participant must recall as many words as they can remember. There is always one word that is related but not actually said by the researcher, and if the participant falsely recalls hearing this word (the critical lure), it is used as a measurement of false memory. Falzarano and Siedlecki (2019) examined the validity of false memory constructs, such as the DRM itself, and found that false memory assessments are only loosely correlated to one another and are likely measuring different aspects of false memory.

My study used the framework of the Zhang et al. study by using videos for priming and using a DRM paradigm test to assess false recall but added the element of stereotype threat. Research has shown that when participants subscribe to harmful stereotypes (such as "girls are bad at math"), their performance on a related task will tend to be worse than if they do not subscribe to the stereotype (whether consciously or unconsciously). This is known as *stereotype threat.*

Stereotype threat and mood has been studied quite a bit, such as in a study Bodenhausen et al. (1994). Bodenhausen et al. found that participants in a happy mood were more likely to make quick, stereotypic judgments than participants in an unpleasant mood. However, little to no research has been done to see how mood and stereotype threat interact to affect memory. Since positive mood allows individuals to more readily accept harmful stereotypes, would they also be more willing to accept harmful stereotypes about themselves? If positive mood leads to short cut thinking, will the addition of stereotype threat lead to worse memory recall?

Under the SURF grant, I designed and conducted an experiment to examine the effects of both stereotype threat and positive mood on memory recall. I primed participants by showing them either a positive mood video or neutral mood video. All participants watched their assigned video for five minutes. Then, they read an instruction sheet that either had just the instructions (control) or false data for stereotype threat appropriate to their gender. Finally, participants completed four memory recall tasks using the DRM paradigm assessment. Each level of treatment and the methodology used is explained in more detail in the next section.

Hypothesis: I hypothesized that stereotype threat combined with positive mood would lead to higher levels of false memory recall on neutral word lists than when positive mood or stereotype threat alone are tested.

Methodology:

Participants: Participants (N = 14) were randomly assigned to one of the four conditions below. The same four DRM word lists were used for each participant, despite their mood or stereotype threat conditions.

Visual Representation of the Factorial Model and the groups in this study

Stereotype Threat	Neutral Mood	Positive Mood
Absent	**Group A** Neutral video Stereotype threat absent Neutral DRM paradigm test	**Group B** Positive video Stereotype threat absent Neutral DRM paradigm test
Present	**Group C** Neutral video Stereotype threat present Neutral DRM paradigm test	**Group D** Positive video Stereotype threat present Neutral DRM paradigm test

Priming Conditions:

Those in the positive mood group watched a video of baby animals for five minutes, and those in the neutral mood group watched a video used for studying, with chill lofi music and shrimp swimming around (relaxing, but not very emotionally stimulating).

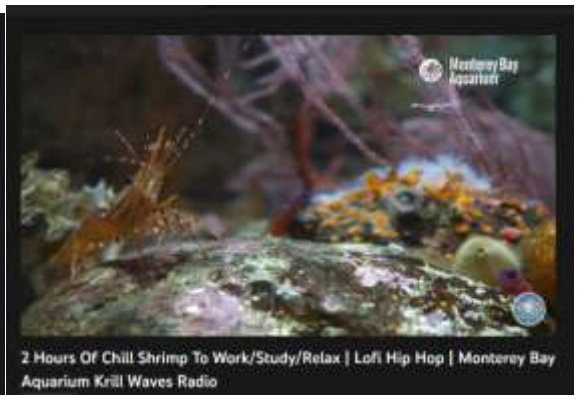

Stereotype Threat Conditions

After watching the assigned video, participants received an instruction sheet further explaining the study. Those in the control group for stereotype threat received an instruction sheet with no false data.

THE MEMORY STUDY

You are participating in a study on human memory. The researcher will read a list of words to you, most if not all these words will be related to one another. After the researcher has completely read the list, she will instruct you to write down the words that you can remember. You can record the words you remember in any order; order is not a measure of this study. After you have recalled as many as you can remember, let the researcher know and the procedure will be repeated with a different word list.

Those in the stereotype condition received an instruction sheet with the procedure as well as false data from "prior trials." Men received data that women did significantly better at the task,

Data Used for Male Participants

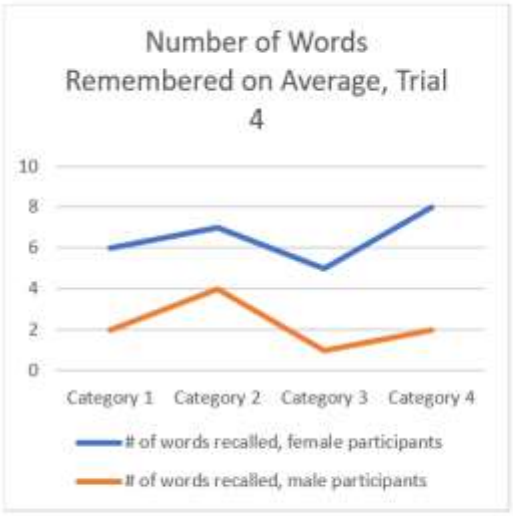

Data Used for Female Participants

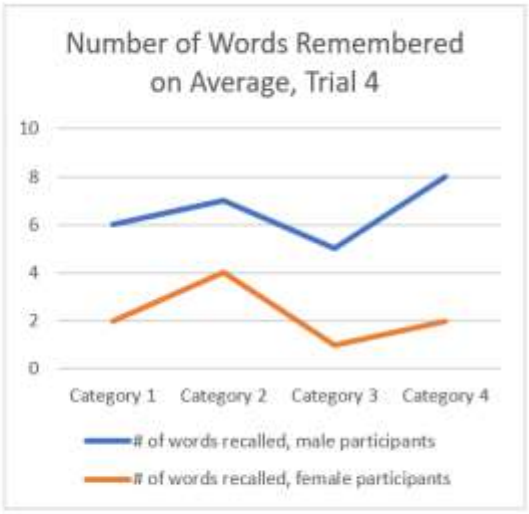

and women received data that men did statistically better at the task. This led these participants to believe that the study was assessing memory differences in men and women, when gender was not a part of the experiment. Above are charts that were used for the stereotype threat conditions.

DRM Memory Recall

After participants finished reading their instruction sheet, I began the memory recall task. I read a list of 15 related words, and after the list was complete participants wrote down as many words they could remember. This made it a *recall* task rather than a *recognition* task, where participants would have options to pick from. An example used is included below. After the memory test was complete, the participant was debriefed, and I recorded their data.

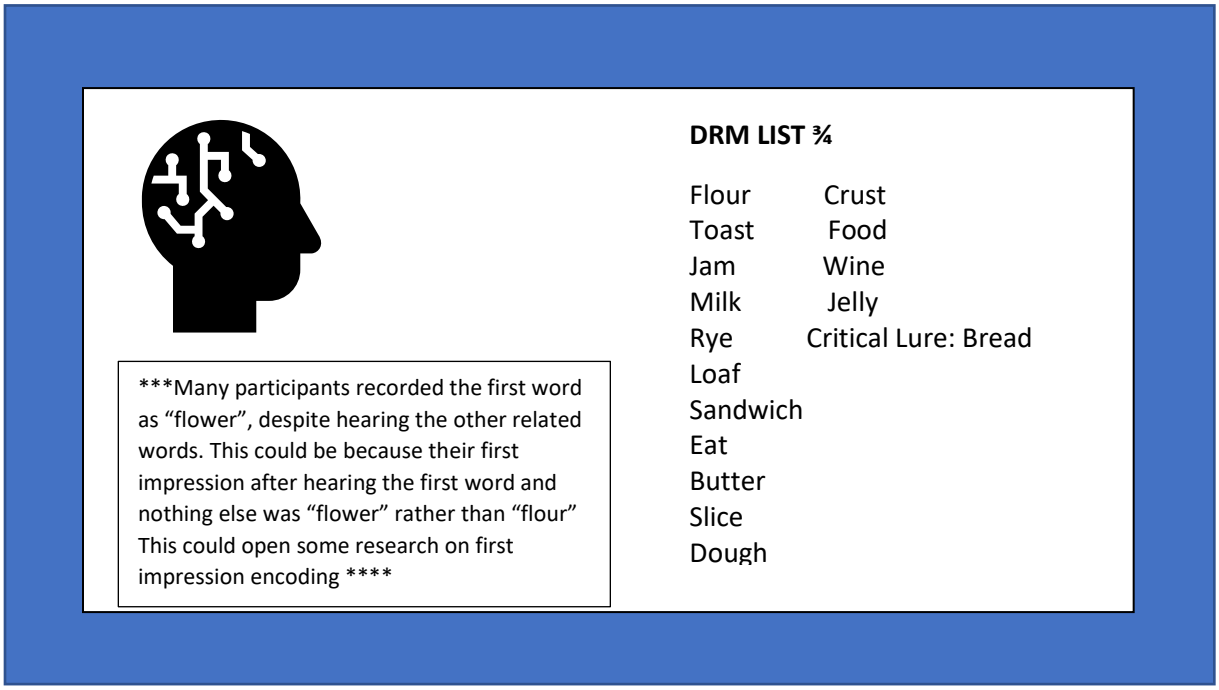

Results

Because the study was done in the summer, it was hard to find participants. This is a common problem in behavioral research. I hope to continue the research in the fall when there will be more students on campus. However, the data I did collect has been summarized in the following table.

Preliminary Results: Means for Each Condition and Measure

Stereotype Condition	Mood Condition	
	Positive	Neutral
ST	Total recall = 27.50 False recall = 1.25 Critical lures = 1.00	Total recall = 30.00 False recall = 0.33 Critical lures = 0.33
No ST	Total recall = 32.00 False recall = 0.75 Critical lures = 0.50	Total recall = 32.00 False recall = 0.67 Critical lures = 0.33

Conclusions and Limitations

Because the study was done in the summer, it was challenging to get participants. To avoid bias, I did not endorse the study on my social media and instead used flyers around campus. Because there was a relatively small participant pool, there is no conclusive evidence that stereotype threat and mood affect memory recall. However, preliminary results are promising. The group that received a stereotype threat and the positive video had the lowest mean total recall, the highest mean false recall, and the highest mean number of critical lures recalled. In addition to the small sample, another limitation is that mood was not measured after participants watched the video, so it is unknown if the videos stimulated a positive or neutral mood. However, the method of using a video to prime participants has been used in prior studies, so it is a valid measurement. I also was able to observe body language. Those who watched the positive video were more likely to smile, and those watching the neutral video were more likely to shift in their seat and check their watch, social cues indicating boredom. If I continue my project in the fall, I would like to add a way to measure their mood after watching the videos, as a manipulation check to try and minimize arousal level inconsistencies. After gathering more participants, I should be able to see a trend in mood and stereotype threat and how it affects memory. However, the framework of this study has proven to be solid and I am eager to see how it progresses.

References

Bodenhausen, G. V., Kramer, G. P., & Süsser, K. (1994). Happiness and stereotypic thinking in social judgment. *Journal of Personality and Social Psychology*, *66*(4), 621-632. http://doi.org/10.1037/0022-3514.66.4.621

Dang, X., Zhu, B., Chen, C., & Li, X. (2020). Age differences in false memories for visual scenes and the effect of prior recall. *Journal of Pacific Rim Psychology*, *14.* https://doi.org/10.1017/prp.2019.26

Falzarano, F., & Siedlecki, K. L. (2019). Investigating the relations among different measures of false memory. *Advances in Cognitive Psychology*, *15*(4), 290–300. https://doi.org/10.5709/acp-0276-0

Terry, W. S. (2017). *Learning and memory: Basic principles, processes, and procedures.* Routledge.

Zhang, W., Gross, J., & Hayne, H. (2018). If you're happy and you know it: Positive moods reduce age-related differences in false memory. *Child Development*, *89*(4), e332–e341. https://doi.org/10.1111/cdev.1289

Rafael Gutierrez

Major in Mechanical Engineering and Physics

Mentors: Dr. Rafael de la Madrid

Research in the Physics of Surfaces

Department of Physics

Dynamic Wetting and Dewetting in Non-Uniform Solids

Wetting and dewetting phenomena plays a vital role in many areas of science, engineering and technology including ink printing, microfluidics, and self-cleaning hydrophobic surfaces [1-3]. The focus of this research is to characterize dynamical wetting of liquid drops on non-uniform surfaces by characterizing the lateral retention force, $f_{\parallel}$, and the sliding work of adhesion, w_s , of a drop that is moving (or about to move) on a non-uniform surface.

Lateral retention force. One approach to quantify dynamic wetting is by the lateral retention force, $f_{\parallel}$, on a drop that is about to move on a solid surface. When a solid object is resting on a solid surface and we try to slide the object along the surface, there appears a frictional force that opposes the motion. For example, in order to slide a crate across a floor, our push needs to overcome the frictional force between the crate and the floor before the crate begins to move. Similarly, when a liquid drop is in contact with a solid surface and we try to slide the drop along the surface, a lateral retention force appears (due to adhesion) that opposes the motion and that can be thought of as the liquid-solid analog of solid-solid friction. The most accepted form of such lateral retention force is [4-5]

$$f_{\parallel} = k\, w\, \gamma_{lv}(cos\theta_r - cos\theta_a) \qquad (1)$$

here k is a shape factor, w is the width of the drop perpendicular to the direction of the motion, γ_{lv} is the liquid-vapor surface tension, and θ_a (θ_r) is the advancing (receding) contact angle. Equation (1) is valid whenever the solid substrate is uniform, i.e., whenever the solid-liquid and solid-vapor surface tensions γ_{sl} and γ_{sv} are constant. However, when the solid substrate is not uniform, surface tensions are not constant, and Eq. (1) needs to be modified. The first future objective of this research is to experimentally measure the lateral retention force of a

drop that rests on a non-uniform surface. Such experimental value will be compared with a theoretical formula that the Faculty Mentor of this research (Dr. Rafael de la Madrid) is developing.

Sliding work of adhesion. Energy provides a description of a solid-liquid interaction that is complementary to force. In a recent paper [6], an expression for the energy needed to slide a drop on a solid substrate has been developed and tested experimentally. It was found that the work per unit area necessary to slide a drop on a surface is

$$w_s = \gamma_{lv}(\cos\theta_r - \cos\theta_a) \qquad (2)$$

Equation (2) is valid only for uniform surfaces. The second future objective of this research is to measure such work for a drop that is sliding on a non-uniform surface, and to compare the experimental values with a theoretical formula that the Faculty Mentor of this research is developing.

Experimental apparatus. Our experimental apparatus (see Figure 1) consists of a metallic frame with dimensions 90 cm×90 cm×120 cm inside of which the rotary unit is mounted. The four legs of the frame are bolted to the floor to reduce mechanical vibrations. The rotary unit consists of a servo motor, a shaft, and two pairs of aluminum rails that are attached perpendicularly to the shaft. The motor is connected to a power supply and a computer, whose software controls the motor. A metallic box is mounted on the aluminum rails (see Figure 2).

The box has two cameras placed on top and on the side, which provide top and side views of the drops. A remote-controlled LED is used to set a common starting time in the videos of the cameras. On the door of the metallic box, we mount the surface (in Figure 2, it is a PMMA sheet) such that, when a drop is placed on the sheet and the door is closed, the cameras have side and top views of the drop.

Illumination for the side camera is provided by the remote-controlled LED. Lighting for the top camera is provided by an LED panel and an optical gradient. To make the drops slide, we rotate the box with a constant angular acceleration (usually around 1 rpm/s). As the angular velocity of the drop increases, the centrifugal force increases. This eventually makes the advancing edge of the drop crawl forward, although the receding edge of the drop stays pinned to the surface. While the advancing edge crawls forward, the triple line deforms slightly from its initial circular shape. At some point, when the centrifugal force is large enough, the receding edge of the drop also starts moving. When that happens, the whole drop moves. Hence, we identify the onset of the motion of the drop with the instant at which the receding (i.e., trailing) edge of the drop starts moving. We then use the videos of the side camera and custom-made software to determine the instant when the receding edge of the drop starts moving. At such instant, we obtain the contact angles from the videos of the side-view camera using ImageJ [7].

The width and contact area of the solid-liquid interface are obtained from the videos of the top-view camera using ImageJ as well.

Data collection. Three types of drops were analyzed using the drop centrifuge. The drops were characterized by the respected width (vertical distance from top edge to bottom edge) and length (horizontal distance from left edge to right edge), and were classified as either radial, circular, or tangential. Radial (tangential) drops consisted of drops measuring with a larger length (width) with respect to width (length), and circular drops had similar length and width measurements. Each type of drop was analyzed three times per uniform PMMA sheet, there being a total of 30 PMMA sheets. The initial and final advancing and receding contact angles were collected using the initial and final frames collected through the side-view camera. The frames were then analyzed through ImageJ [7]. Similarly, the initial and final width and contact area of the solid-liquid interface were obtained via the initial and final frames collected from the top-view camera that were then analyzed within ImageJ.

Results. The results of the data collected are shown in Table 1 below.

	t(s)	w_i(mm)	A_i(mm^2)	$\theta_{a,i}$	$\theta_{r,i}$	w_f(mm)	A_f(mm^2)	$\theta_{a,f}$	$\theta_{r,f}$
Radial	46.494	6.682	52.644	51.187	51.268	6.850	49.783	72.523	43.998
Circular	49.482	7.711	48.367	63.977	63.960	7.688	50.850	73.379	45.148
Tangential	52.713	9.694	52.924	64.151	64.011	9.430	54.728	71.649	44.569

Table 1: Average Results

In Table 1: t in the time between the initial and final frame in seconds, w_i (w_f) is the average initial (final) width in millimeters, A_i (A_f) is the average initial (final) area in millimeters squared, $\theta_{a,i}$ ($\theta_{a,f}$) is the initial (final) average advancing angle, and $\theta_{r,i}$ ($\theta_{r,f}$) is the average initial (final) receding angle. Figures 3 and 4 are examples of the initial and final side-view frames and Figures 5 and 6 are the examples of the initial and final top-view frames.

Conclusion. The purpose of this research was to collect data of different drop types on uniform surfaces to prepare for the collection of drop types on non-uniform surfaces. The results gathered are shown to be promising as they follow the expectations of my Faculty Mentor and set a sturdy foundation to build upon. The study of drop-surface interaction has important applications (see Refs. [1-3]), from pesticides to hair sprays, to ink-jet printing, to microfluidics. The future step is data collection of drops on non-uniform surfaces, such as, hydrophobic and etched surfaces.

Figure 1: Drop Centrifuge

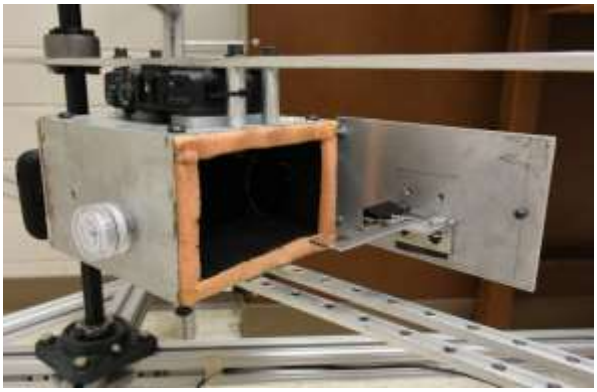

Figure 2: The Box

Figure 3: Circular initial side-view

Figure 4: Circular final side-view

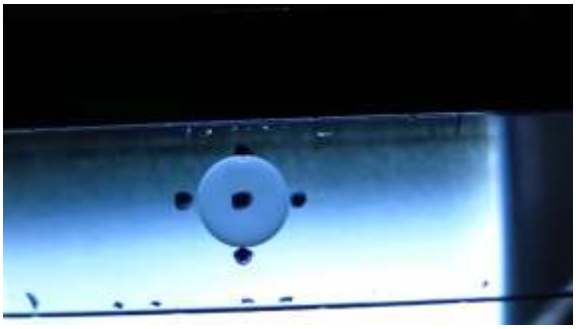

Figure 5: Circular initial top-view

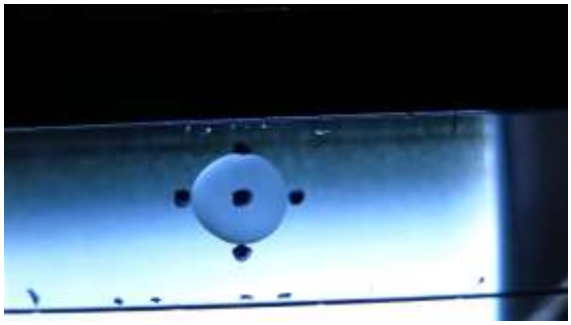

Figure 6: Circular final top-view

Bibliography

[1] de Gennes, P.G.; Brochard-Wyart, F.; Quere, D. *Capillarity and Wetting Phenomena*, Springer, New York, 2004.

[2] Erbil, H.Y. *Surface Chemistry of Solid and Liquid Interfaces*, Wiley-Blackwell, 2006.

[3] Bormashenko, E. A. *Wetting of Real Surfaces*, Walter de Gruyter, 2013.

[4] Furmidge, C. G. L. *Studies at Phase Interfaces I. The Sliding of Liquid Drops on Solid Surfaces and a Theory of Spray Retention*. J. Coll. Int. Sci.17, 309-324 (1962).

[5] Dussan, E. B.; Chow, R. T.-P. *On the Ability of Drops and Bubbles to Stick to Non-Horizontal Surfaces of Solids*. J. Fl. Mech.137, 1-29 (1983).

[6] de la Madrid, R.; Luong, H.; Zumwalt, J. *New insights into the capillary retention force and the work of adhesion.* Colloids and Surf. A: Physiochem. Engin. Aspects 637, 128195 (2022).

[7] https://imagej.nih.gov/ij/

Poster Session

OFFICE OF UNDERGRADUATE RESEARCH
LAMAR UNIVERSITY

Special Guest

OFFICE OF UNDERGRADUATE RESEARCH
LAMAR UNIVERSITY

10th Annual Texas STEM Conference – November 5th, 2022

Research done in the Medical Field

Poster Presentation

Ashley Driscoll

The University of Texas Medical Branch at Galveston, TX
The Menon Laboratory, Division of Basic & Translational Research,
Department of Obstetrics and Gynecology

Novel Bench-To-Bedside Tools for Modeling Intrauterine Organs During Pregnancy

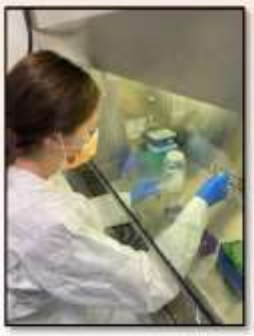

Drug testing during pregnancy is challenging as two patients, mother and fetus, must be evaluated. Current, *in-vitro*/*in-vivo* methods structurally nor functionally mimic the human feto-maternal interface (FMi) or the female genital-maternal uterine tract. To overcome these limitations, we have developed organ-on-chip (OOC) models that represent the structure, functions, and responses of intrauterine organs. Specifically, three devices have been established mimicking both FMi's, fetal membranes (FMi-OOC) and placenta (PLA-OOC), as well as the vaginal-cervix-decidua tract (VCD-OOC) to advance *in-vitro* testing. OOCs were fabricated in poly(dimethylsiloxane) (PDMS) using a two-step photolithography master mold, followed by soft lithography. The FMi-OOC contains four concentric circular chambers filled with cells and collagen matrix (decidua, chorion trophoblasts, amnion mesenchyme, and epithelium). The PLA-OOC is comprised of three rectangular chambers containing syncytiotrophoblasts, cytotrophoblasts, and umbilical cord endothelial cells. Both trophoblast layers formed natural 3D cell barriers to mimic placental barrier function. The VCD-OOC is composed of six culture chambers to mimic the lower female genital-uterine tract (vaginal epithelial cells, ectocervix, transformation zone, cervical stroma, endocervix, and decidua). Within each of these three devices, microchannels allow for individual treatment of chambers while promoting cell migration and communication between layers. Novel on-chip PDMS reservoir systems have been established for each OOC, allowing gravity-fed media to maintain long-term cell culture *in-vitro*. Each device has been developed and validated in animal models. These results describe platforms that can be used as novel tools to study physiological and pathological pregnancy conditions as well as to conduct preclinical trials and toxicology screening.

Special Guest

OFFICE OF UNDERGRADUATE RESEARCH
LAMAR UNIVERSITY

10th Annual Texas STEM Conference – November 5th, 2022

Research done in the Medical Field

Poster Presentation

Briana Ortiz

The University of Texas Medical Branch at Galveston, TX
The Menon Laboratory, Division of Basic & Translational Research,
Department of Obstetrics and Gynecology

Chlamydia infection induces TLR4-TAB1-mediated inflammation, but not cell death, in maternal decidua cells

During gestation, the maternal decidua is an essential layer of the maternal-feto interface, providing immune support and maintaining inflammatory homeostasis. Although Chlamydia Trachomatis (*Ct.*) infection during pregnancy is associated with reproductive tract cell death and inflammation, its effect on the decidua is not fully understood. To answer this question, this study examines how *Ct.* infection affects cell signaling, cell death, and inflammation in the decidua. Primary decidua cells (pDECs) from term, not-in-labor, fetal membranes were cultured using the following conditions: 1) control - standard cell culture conditions, 2) 100ng/mL of *Ct.* antigen to model chlamydia infection *in-vitro*, 3) 200ng/mL of *Ct.* antigen within 6 well plates. Toll-like receptor (TLR) 4, phosphorylated TGF-Beta Activated Kinase (PTAB1), TAB1, phosphorylated p38 mitogen-activated protein kinases (Pp38 MAPK), and p38 MAPK (western blot), apoptosis & necrosis (flow cytometry), and inflammation (ELISA) were determined in cells exposed to *Ct.* T-test was used to assess significance. *Ct.* significantly induced expression of TLR4 ($p=0.03$) and activation of TAB1 ($p=0.02$) when compared to controls; however, it did not induce p38 MAPK activation. pDECs also maintained their elongated morphology when introduced to *Ct.* infection and showed no signs of apoptosis and/or necrosis but did induce pro-inflammatory cytokine interleukin (IL)-6 (100ng/mL:$p=0.02$; 200ng/mL:$p=0.03$), in pDECs compared to controls. Prenatal *Ct.* infection can induce TLR4-TAB1 signaling and IL-6 inflammation without activating Pp38 MAPK and apoptosis & necrosis. This suggests that *Ct.* infection can affect cell signaling and inflammatory homeostasis within the decidua leading to dysfunction during pregnancy.

Posters

Posters to be set up after Friday 11/4 from 9:00 AM
or Saturday 11/5 before 8:15 AM

Poster session I : 8:20 – 8:50 AM (Chair Dr. He and Dr. Selvaratnam)
Poster session II : 12:30 – 1:00 PM (Chair Dr. Stefan Andrei and Dr. Berna Tokgoz)
Poster session III : 4:00 – 4:30 PM (Chairs Dr. Stefan Andrei and Dr. Ian Lian)

Poster 1

Undergraduate Level Research

Presenter: David Matherne

Mentors: Dr. Evgeny Romashets and Dr. Cristian Bahrim
Department of Physics, Lamar University

Interplanetary Magnetic Cloud of April 17, 1999

Poster 2

Undergraduate Level Research

Presenter: David Matherne

Mentor: Dr. Ashwini Kucknoor
Department of Biology, Lamar University

Characterization of drug resistance in cattle pathogen Tritrichomonas foetus

Poster 3

Undergraduate Level Research

Presenter: Ashley Driscoll

Mentor: Dr. Lauren Richardson
The University of Texas Medical Branch at Galveston, TX
The Menon Laboratory, Division of Basic & Translational Research,
Department of Obstetrics and Gynecology

Novel Bench-to-Bedside Tools for Modeling, Intrauterine Organs During Pregnancy

Poster 4

Undergraduate Level Research

Presenter: Briana Ortiz

Mentor: Dr. Lauren Richardson
The University of Texas Medical Branch at Galveston, TX
The Menon Laboratory, Division of Basic & Translational Research,
Department of Obstetrics and Gynecology

Chlamydia infection induces TLR4-TAB1-mediated inflammation, but not cell death, in maternal decidua cells

Poster 5

Undergraduate Level Research

Presenter: Ian Sisson
Mentor: Dr. Paul Bernazzani
Department of Chemistry and Biochemisty, Lamar University

Iron-Cellulose Nanocomposites: A Potential Replacement for High Strength Plastics

Poster 6

Undergraduate Level Research

Presenter: Jennifer Arredondo
Mentor: Dr. Robert Kelley Bradley
Department of Industrial Engineering, Lamar University

Silicone Nanocomposites Ferroelectrets

Poster 7

Undergraduate Level Research

Presenter: Kimberlie Travelstead
Co-authors: Brittney Brevell, Cody M. Cox,
Ashley N Kelahlyah, Juana Perez,
Jonathan Richards, Samana Shah
Mentors: Dr. Matthew Hoch[1] and Dr. Elizabeth Silvy[2]
[1]Department of Biology, Lamar University
[2]Department of Rangeland Wildlife and Fisheries Management,
600 John Kimbrough Blvd TAMU 2124 College Station TX 77843
Department of Biology

Determining baseline fish assemblage composition for pre-restoration efforts in North Pleasure Island, Sabine Lake, Texas

Poster 8

Undergraduate Level Research

Presenter: Landen Barrow[1,2]
Co-authors: Mubarak Adesina[1], Saba Huriya Syeda[2]
Mentor: Dr. Nicholas Brake
[1]Department of Civil Engineering, Lamar University
[2]Center for Resiliency, Lamar University

Reliability Assessment of a Flood Sensor Network

Poster 9

Undergraduate Level Research

Presenter: Lac Nguyen
Mentor: Dr. Robert Kelley Bradley
Department of Industrial Engineering, Lamar University

An Investigation of Environmentally Friendly Filler for Polymer Nanocomposites

Poster 10

Master Level Research

Presenter: Elizabeth Claire Alexander
Mentor: Dr. Maryam Vasefi
Department of Biology, Lamar University

CBD Mechanisms of Action at the Human 5-HT1A Receptor

Poster 11

Master Level Research

Presenter: Kalen Baker
Co-author: Rahagir Ridwan Anik
Mentor: Dr. Ping He
Department of Mechanical Engineering, Lamar University

Development of Gibbs Energy Model for Testing Hydrophobicity of Hierarchical Surface Structures

Poster 12

Master Level Research

Presenter: Aniket Kamthe
Co-authors: Matish Godambe and Mahesh Nutakki
Mentor: Dr. Robert Kelley Bradley
Department of Industrial and System Engineering, Lamar University

Smart Walking Stick for Vision-Impaired Users

Poster 13

Master Level Research

Presenter: Huiling Liu
Co-author: Solomon Fensico Eugine
Mentor: Dr. Stefan Andrei
Department of Computer Sciences, Lamar University

Portable Solar Panels: Energy Maximization & Business Model

Poster 14

Doctoral Level Research

Presenter: Rishi Bharadwaj[1]
Mentor: Dr. Cristian Bahrim[2]
[1]Phillip Drayer Department of Electrical Engineering, Lamar University
[1,2]Opto-Electronics Laboratory, Department of Physics, Lamar University

Influence of an Isotropic Energy Background in the Interaction between a TEM_{oo} Laser Beam and a Non-Conductive Surface

Poster 15

Doctoral Level Research

Presenter: Md Mahbubur Rahman
Mentor: Dr. Robert Kelley Bradley
Department of Industrial Engineering
Lamar University

Use of silicone micro-molds and UV-Curable Resin to Manufacture Single Wall Carbon Nanotube Carding Devices

Poster 16

Doctoral Level Research

Presenter: Daniel Quispe
Mentor: Dr. Mel Ulmer
Ulmer Research Group, Department of Physics and Astronomy.
Northwestern University, IL

A Concept for deployable Normal Incidence UV Mirror Based on Shape Memory Alloy Sheets

Poster 17

Doctoral Level Research

Presenter: Seyyed Saeed Vaezzadeh
Mentor: Dr. Robert Kelley Bradley
Department of Industrial and System Engineering, Lamar University
Center for Midstream Management and Science, Lamar University

Creep-Resistant Thermoplastic Composites for Load-Bearing Applications

Post deadline submissions

Poster 18

Undergraduate Level Research

Presenter: Tyler Stuck[1,2]
Mentor: Dr. Suazo and Dr. Oraby[2]
[1]Department of Mathematics, Lamar University
[2]The University of Texas Rio Grande Valley

Deep Learning and Solutions for Fractional ODEs

Poster 19

Undergraduate Level Research

Presenter: Tarin Hill
Co-author: Haley Snyder
Mentor: Dr. Ozge Gunaydin-Sen
Department of Chemistry and Biochemistry, Lamar University

Exploiting the hydrogen storage properties of ammonia borane with the addition of polyacrylic acid and calcium chloride: Thermal and kinetic studies

Poster Abstracts

Undergraduate / In-progress / Poster 1

Presenter: David Matherne

Mentor: Dr. Evgeny Romashets and Dr. Cristian Bahrim

Department of Physics

Lamar University

Research in Geo-Space Sciences

Interplanetary Magnetic Cloud of April 17, 1999

This project enhances our understanding of the relationship between solar activities and geo-magnetic storms. Strong inter-planetary disturbances travel through the inner heliosphere with speeds larger than that of the ambient solar wind. If such a disturbance has large negative Bz – field component, then it can trigger a geo-magnetic storm. The process of magnetic reconnection on the magnetopause begins if the magnetic fields on the opposite sides of it are antiparallel. A typical situation corresponds to a Bz value of 40 nT on the inner side and -40 nT on the outer side. In 2015, Marubashi and co-workers studied 50+ interplanetary magnetic clouds of toroidal shape using formulas generated by Romashets and Vandas published. In Marubashi et al.'s work the time of the launch and the arrival time of the cloud were determined correctly. The data offered by Marubashi et al. (2015) is used as initial lower boundary condition for our dynamic model.

NASA source "Solar Flare and Coronal Mass Ejection".
earthobservatory.nasa.gov/images/43191/solar-flare-and-coronal-mass-ejection

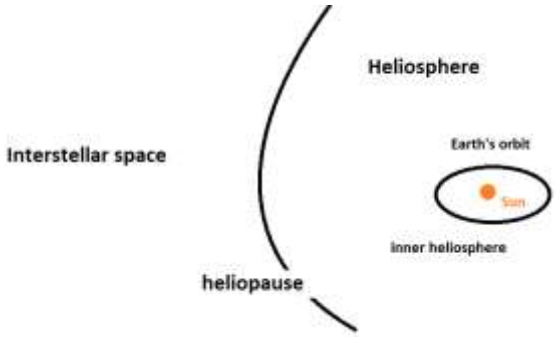

Undergraduate / In-progress / Poster 2

Presenter: David Matherne

Mentor: Dr. Ashwini Kucknoor

Department of Biology

Lamar University

Research in Microbiology

Characterization of Drug Resistance in Cattle Pathogen *Tritrichomonas foetus*

Bovine trichomoniasis is caused by the protozoan *Tritrichomonas foetus* and is a common disease in the beef industry, costing US cattle ranchers an estimated $650 million annually due to fetal abortion and infertility. Tinidazole and metronidazole have been used to treat trichomonad infections since 1960, but studies suggest emergence of resistant trichomonads worldwide. Using this, a hypothesis was made that certain genes in surviving generations of *Tritrichomonas foetus* allow for resistance to build up in this species. Research is still ongoing, but we're continuing to isolate and clone the DNA in order to discover the genes responsible for survivability.

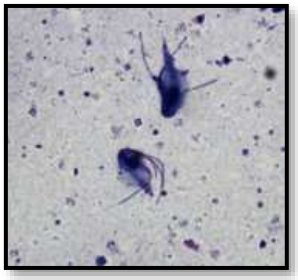

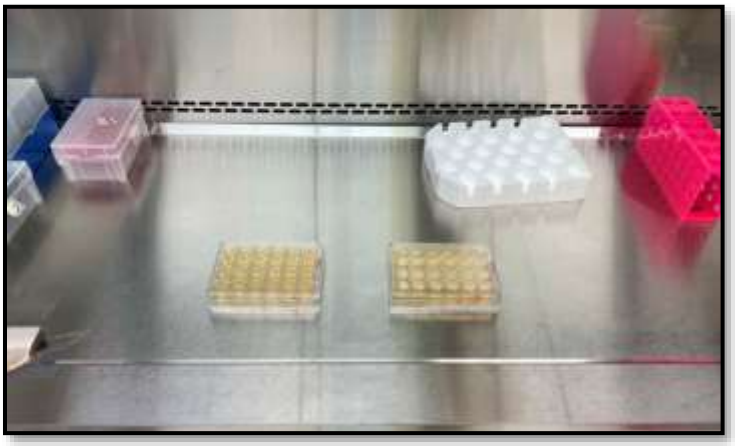

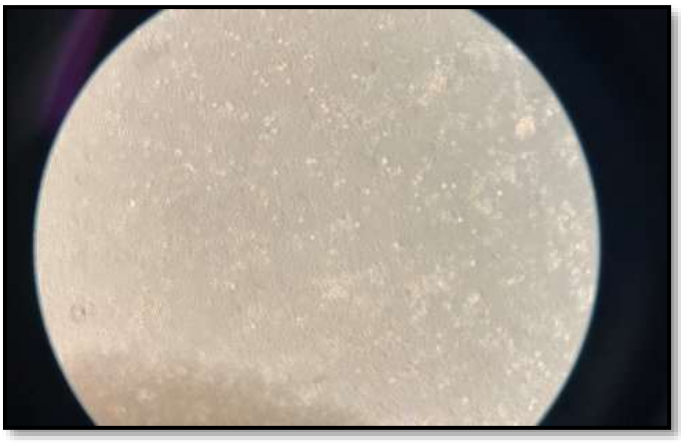

Tritrichimonas cells under a microscope at x100 magnification. The ones with highlighted circumferences are thriving, living cells, while the clumps are unhealthy or dead cells.

Undergraduate / In-progress / Poster 3

Presenter: Ashley Driscoll

Mentor: Dr. Lauren Richardson

The University of Texas Medical Branch at Galveston, TX

The Menon Laboratory, Division of Basic & Translational Research,

Department of Obstetrics and Gynecology

Research in Obstetrics and Gynecology

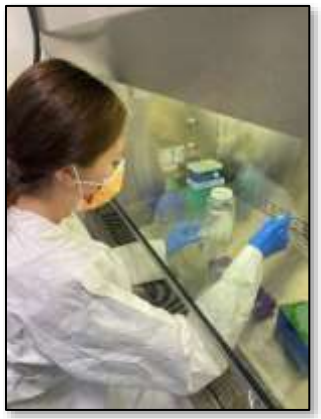

Novel Bench-To-Bedside Tools for Modeling Intrauterine Organs During Pregnancy

Drug testing during pregnancy is challenging as two patients, mother and fetus, must be evaluated. Current, *in-vitro*/*in-vivo* methods structurally nor functionally mimic the human feto-maternal interface (FMi) or the female genital-maternal uterine tract. To overcome these limitations, we have developed organ-on-chip (OOC) models that represent the structure, functions, and responses of intrauterine organs. Specifically, three devices have been established mimicking both FMi's, fetal membranes (FMi-OOC) and placenta (PLA-OOC), as well as the vaginal-cervix-decidua tract (VCD-OOC) to advance *in-vitro* testing. OOCs were fabricated in poly(dimethylsiloxane) (PDMS) using a two-step photolithography master mold, followed by soft lithography. The FMi-OOC contains four concentric circular chambers filled with cells and collagen matrix (decidua, chorion trophoblasts, amnion mesenchyme, and epithelium). The PLA-OOC is comprised of three rectangular chambers containing syncytiotrophoblasts, cytotrophoblasts, and umbilical cord endothelial cells. Both trophoblast layers formed natural 3D cell barriers to mimic placental barrier function. The VCD-OOC is composed of six culture chambers to mimic the lower female genital-uterine tract (vaginal epithelial cells, ectocervix, transformation zone, cervical stroma, endocervix, and decidua). Within each of these three devices, microchannels allow for individual treatment of chambers while promoting cell migration and communication between layers. Novel on-chip PDMS reservoir systems have been established for each OOC, allowing gravity-fed media to maintain long-term cell culture *in-vitro*. Each device has been developed and validated in animal models. These results describe platforms that can be used as novel tools to study physiological and pathological pregnancy conditions as well as to conduct preclinical trials and toxicology screening.

Undergraduate / In-progress / Poster 4

Presenter: Briana Ortiz

Mentor: Dr. Lauren Richardson

The University of Texas Medical Branch at Galveston, TX

The Menon Laboratory, Division of Basic & Translational Research,

Department of Obstetrics and Gynecology

Research in Obstetrics and Gynecology

Chlamydia infection induces TLR4-TAB1-mediated inflammation, but not cell death, in maternal decidua cells

During gestation, the maternal decidua is an essential layer of the maternal-feto interface, providing immune support and maintaining inflammatory homeostasis. Although Chlamydia Trachomatis (*Ct.*) infection during pregnancy is associated with reproductive tract cell death and inflammation, its effect on the decidua is not fully understood. To answer this question, this study examines how *Ct.* infection affects cell signaling, cell death, and inflammation in the decidua. Primary decidua cells (pDECs) from term, not-in-labor, fetal membranes were cultured using the following conditions: 1) control - standard cell culture conditions, 2) 100ng/mL of *Ct.* antigen to model chlamydia infection *in-vitro,* 3) 200ng/mL of *Ct.* antigen within 6 well plates. Toll-like receptor (TLR) 4, phosphorylated TGF-Beta Activated Kinase (PTAB1), TAB1, phosphorylated p38 mitogen-activated protein kinases (Pp38 MAPK), and p38 MAPK (western blot), apoptosis & necrosis (flow cytometry), and inflammation (ELISA) were determined in cells exposed to *Ct.* T-test was used to assess significance. *Ct.* significantly induced expression of TLR4 ($p=0.03$) and activation of TAB1 ($p=0.02$) when compared to controls; however, it did not induce p38 MAPK activation. pDECs also maintained their elongated morphology when introduced to *Ct.* infection and showed no signs of apoptosis and/or necrosis but did induce pro-inflammatory cytokine interleukin (IL)-6 (100ng/mL:$p=0.02$; 200ng/mL:$p=0.03$), in pDECs compared to controls. Prenatal *Ct.* infection can induce TLR4-TAB1 signaling and IL-6 inflammation without activating Pp38 MAPK and apoptosis & necrosis. This suggests that *Ct.* infection can affect cell signaling and inflammatory homeostasis within the decidua leading to dysfunction

Undergraduate / In-progress / Poster 5

Presenter: Ian Sisson

Mentor: Dr. Paul Bernazzani

Department of Chemistry and Biochemisty

Lamar University

Research in Polymers

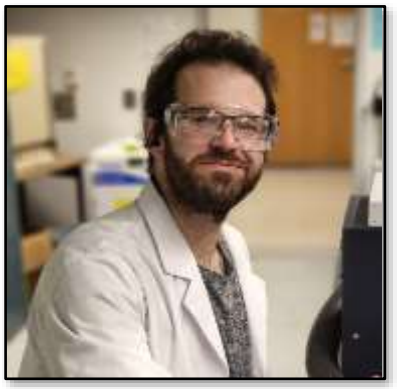

Iron-Cellulose Nanocomposites: A Potential Replacement for High Strength Plastics

Plastics are a useful and necessary material in modern society that are also a widespread non-renewable pollutant. Cellulose is a common renewable material and any attempt to strengthen its physical and thermal properties has merit. We propose that a cellulose bioplastic can be strengthened by selectively increasing the crystallinity of the material through insertion of ferromagnetic cations into a covalently bonded cellulose nanofiber matrix in an aqueous state and exposing the solution to a magnetic field during a crosslinking reaction, ordering the cations and therefore the nanofibers attracted or bonded to it along magnetic field lines.

Undergraduate / In-progress / Poster 6

Presenter: Jennifer Arredondo

Mentor: Dr. Robert Kelley Bradley

Department of Industrial Engineering

Lamar University

Research in Polymers

Silicone Nanocomposites Ferroelectrets

In this research, we were investigating ferroelectrets, a cellular polymer foam that can convert compressive and bending forces into electrical signals. Our objective was to engineer 'foam' by combining thin sheets of silicone that contain arrays of 'voids' or 'pockets' by stacking them on top of each other. Research questions included 1) can we control the movement of a ferroelectret by engineering the 'voids' or 'pockets' in the silicone? and 2) can an engineered silicone foam be made via this technique? A study of AC corona discharge treatment to improve adhesion between silicone sheets was conducted. Corona discharge will be investigated as a surface treatment to bond silicone based on a method of bonding used to combine molded layers and the alignment of the interconnections between layers. Samples were analyzed using a dielectric spectroscopy system and a piezometer to conclude if our engineered foam indeed acted as a ferroelectret.

Undergraduate / In Progress / Poster 7

Presenter: Kimberlie Travelstead

Co-authors: Brittney Brevell, Cody M. Cox,

Ashley N Kelahlyah, Juana Perez,

Jonathan Richards, Samana Shah

Mentors: Dr. Matthew Hoch[1] and Dr. Elizabeth Silvy[2]

[1]Department of Biology, Lamar University

[2]Department of Rangeland Wildlife and Fisheries Management,

600 John Kimbrough Blvd TAMU 2124 College Station TX 77843

Research in Ecology

Determining Baseline Fish Assemblage Composition for Pre-Restoration Efforts in North Pleasure Island, Sabine Lake, Texas

The loss of coastal ecosystems due to progressive erosion is an issue of concern in southeast Texas. The Coastal Sociological-Ecological Restoration Group (CSERG), supported by Lamar University's Center for Resiliency, has developed the North Pleasure Island Reconstruction pilot project to enhance the ecological benefits of planned restoration efforts to combat erosion in Sabine Lake. One component of this multifaceted project is a pre-restoration fish assemblage survey. Survey efforts provide important data on community dependence on the area for the economic value of fisheries, food security, tourism income, and land use. Fish sampling goals include a representative sampling of the species present and ascertaining their relative abundance and diversity. We conducted a multi gear survey to collect data on fish populations and assemblages using seines, otter trawls, and angling. The results of these monthly fish collection efforts from May through August 2022 suggest a lack of species richness in the fish communities at any given time. From preliminary seine data the predominant species captured are inland silverside (Menidia beryllina) and gizzard shad (Dorosoma cepedianum). Preliminary otter trawl data indicates that blue crabs (Callinectes sapidus) are present in abundance, with a higher incidence of males than females. Gulf menhaden (Brevoortia patronus) and pinfish (Lagodon rhomboides) were prevalent during trawls, but not simultaneously. Angling efforts indicated an abundance of hardhead (Arisopsis felis) with the largest fish captured being black drum (Pogonias cromis). These monthly summertime data are the first of our multi-season study for establishing a pre-restoration baseline inventory for use in assessing restoration effectiveness in enhancing fisheries.

Undergraduate / In-progress / Poster 8

Presenter: Landen Barrow[1,2]

Co-authors: Mubarak Adesina[1] and Saba Huriya Syeda[2]

Mentor: Dr. Nicholas Brake

[1]Department of Civil Engineering, Lamar University

[2]Center for Resiliency, Lamar University

Research in Resiliency

Reliability Assessment of a Flood Sensor Network

From June to November, Southeast Texas is prone to hurricanes and heavy thunderstorms. To help improve storm data collection and accessibility, Lamar University's Center for Resiliency in partnership with the Department of Homeland Security Science and Technology Directorate (S&T) and surrounding local government agencies has deployed 74 flood sensors across the Southeast Texas region. The flood network has 74 water level sensors across 7 counties. We use these sensors to help keep the public updated about rising waters in the region. As part of the project, we aim to understand further the performance and efficiency of the network of flood sensors which will aid in planning maintenance operations and data collection. To investigate the reliability of the flood network, data analysis is done using MATLAB and MS EXCEL to identify the frequency of non-responsive (timed out) periods over a 6-month timeline (March – September 2022). With these data, histograms were plotted to visualize the period and number of outages for all sites. These histograms illustrate the patterns within the outages and to help get a better understanding of the maintenance to keep the network running efficiently.

Undergraduate / In-progress / Poster 9

Presenter: Lac Nguyen

Mentor: Dr. Robert Kelley Bradley

Department of Industrial Engineering

Lamar University

Research in Nanotechnology

An Investigation of Environmentally Friendly Filler for Polymer Nanocomposites

Biodegradable filler reduces the impact of discarded plastic on the environment. We will investigate ball milling rice hulls to make biodegradable nanomaterial filler, and three roll milling to mix the nanomaterial with silicone polymer. We will analyze the samples using techniques for characterizing dispersion and change in physical properties. We will also study other environmentally friendly methods used in the plastic industry through literature review and interviews with experts at the Exxon Mobil Polyethylene Plant in Beaumont TX. Our study will include a tour for 10 students of the Exxon Mobil facility.

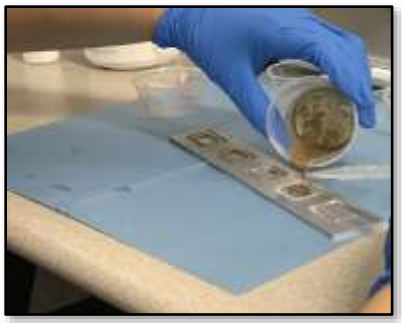

Master / In-progress / Poster 10

Presenter: Elizabeth Claire Alexander

Mentor: Dr. Maryam Vasefi

Department of Biology

Lamar University

Research in Biology

CBD Mechanisms of Action at the Human 5-HT1A Receptor

Cannabidiol (CBD) is a non-psychoactive phytocannabinoid with potential to treat psychiatric disorders. Recent literature has revealed that CBD has multiple molecular targets, including cannabinoid receptors and serotonin receptors. Many current treatments for common psychiatric disorders target the serotonin receptor subtype 1A (5-HT1AR). Several studies have also suggested that CBD produces anxiolytic and antidepressant effects by enhancing neuroplasticity and modulating the activity of the 5-HT1AR. Moreover, CBD may regulate neuronal survival via modulation of the ERK1/2 signaling pathway. The aim of this project is to investigate the molecular mechanisms of a unique CBD-mediated 5-HT1AR to ERK signaling pathway in human neurons. SH-SY5Y cells are treated with varying doses of CBD, then protein is extracted and analyzed by western blot. Following agonist-antagonist experiments, western blot analysis reveals the necessity of 5-HT1AR to CBD-mediated ERK1/2 signaling, while qRT-PCR demonstrates CBD-induced changes in 5-HT1AR and ERK1/2 gene expression. All data are normalized, and bar graphs will compare experimental results to that of the control condition. Our preliminary results reveal that CBD dose-dependently modulates the MAPK-ERK1/2 signaling pathway. Moreover, CBD's impact on ERK1/2 activity was altered by co-treatment with 5-HT1AR antagonist, WAY100135. These results suggest that CBD initiates a non-canonical 5-HT1AR signaling pathway. This project will delineate the mechanisms of CBD's antidepressant mechanism in human neurons.

Master / In-progress / Poster 11

Presenter: Kalen Baker

Co-author: Rahagir Ridwan Anik

Mentor: Dr. Ping He

Department of Mechanical Engineering, Lamar University

Research in Modeling Surfaces

Development of Gibbs Energy Model for Testing Hydrophobicity of Hierarchical Surface Structures

Superhydrophobic surface is an engineered material that causes water to bead up and separate from a surface of practical importance in protecting ship hulls, corrosion control, and self-cleaning surfaces. A Gibbs energy model utilizing the free energy thermodynamic analysis is developed to explain the wetting transitions between Cassie-Baxter and Wenzel state. For a set of reentrant pillars, the energy barriers between the two states were predicted by the Gibbs energy model and then compared with a continuum model. Continuum modeling was simulated in OpenFOAM using a 3-D wetting process with a 3-μL water droplet for three cases (1) droplet was simulated at zero gravity on the micropatterned surface either Cassie or Wenzel state and then allowed to stabilize. (2) In order calculate the energy barriers, a controlled body force was employed to pull the droplet from Wenzel to Cassie state or push it down from Cassie to Wenzel state. (3) Impact analysis was conducted by simulating the droplet on the micropatterned surfaces at specific initial velocities. After comparing the results between the thermodynamic model and the simulation, a good correlation was established. This model explains the technique for developing a strong Cassie state, opening the path to generate further designs for a more robust hydrophobic surface.

Master / Early Stage / Poster 12

Presenter: Aniket Kamthe

Co-authors: Matish Godambe and **Mahesh Nutakki**

Mentor: Dr. Robert Kelley Bradley

Department of Industrial and System Engineering

Lamar University

Research in Engineering Solutions for Visual Impairment

Smart Walking Stick for Vision-Impaired Users

The main aim of this system is to add functionality to the traditional cane used by visually impaired people. The device will issue an auditory alert via headphones if an obstacle is detected. We report the results of our systematic analysis of design alternatives and present the selected design, a stick that detects objects in front of the person and gives a response to the user either by vibrating or through sound. The smart walking stick detects objects with the help of a camera and measures the distance between objects by using an ultrasonic sensor. The product will aid in navigating unknown areas by providing voice output for obstacle avoidance and navigation using the ultrasonic sensor. The design includes voice IC, Arduino, vibrator, Moisture sensor, GPS, and GSM. The system can alert others, such as relatives, in an emergency. Manufacturing includes an aluminum stick with a water sensor at the bottom. The stick will be lightweight and will not get dented if it falls. The systems design process, including the identification of objectives and verification testing, will be presented.

Master / In-progress / Poster 13

Presenter: Huiling Liu

Co-author: Solomon Fensico Eugine

Mentor: Dr. Stefan Andrei

Department of Computer Sciences, Lamar University

Research in Solar Energy

Portable Solar Panels: Energy Maximization & Business Model

We have been relying on fossil fuels or major energy providers (e.g., Entergy) for centuries. Thus, when there is a power outage because of war, hurricane, or other factors, we do not have an alternative plan to help ourselves and others. However, reusable energy that can be collected in the household units could be the solution. It seems that solar energy is the one that is accessible to most of the household. Based on our experimental findings, we sketched a business model that may be applicable for more users to harness solar energy easily and efficiently as every individual's backup energy plan. Our idea mainly focuses on portable solar energy. Specifically, we proposed to add automated reflection(s) oriented to solar panel(s) and to adjust the optimal angles of solar panel(s)/reflection(s) according to the angle from the ground to the sun rays.

Additionally, we tested the running and surge power of different power-driven products to identify the required capacity of Portable Power Station and rechargeable battery chargers, which can be recharged by solar panel(s). Consequently, we researched and analyzed different rechargeable batteries (such as AA, AAA, AAAA, C, SC, and so on). Lastly, we concluded the project and mentioned some potential related future works.

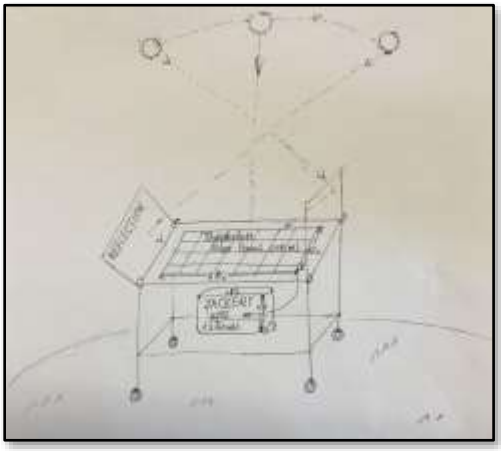

Doctoral / In-progress – Poster 14

Presenter: Rishi Bharadwaj[1]

Mentor: Dr. Cristian Bahrim[2]

[1]Phillip Drayer Department of Electrical Engineering

[1,2]Opto-Electronics Laboratory, Department of Physics

Lamar University

Research in Optoelectronics

Influence of an Isotropic Energy Background in the Interaction between a TEMoo Laser Beam and a Non-Conductive Surface

Interference Pattern between two Coherent TEMoo cw-laser beams is reported. In the experiment called Trial#1, a probe laser and a much stronger coupling laser of same wavelength, 532 nm, are incident on a 2 mm spot on a crown glass surface. At Brewster angle (which is 56.6 Degrees for our crown glass irradiated by the 532 nm green light from a diode laser beam) the parallel component of reflectance reaches nearly zero and the light reflected is 100% polarized. Around it we find a 2 degrees wide Brewster region, without a regular structure within as compared to the evenly spaced fringes observed in the outside wings. In our Trial#1 we observe a hump at the Brewster angle. This feature indicates that the stronger coupling laser takes over the weak probe laser completely. Outside the Brewster region, we observe a regular interference pattern with an even spacing of 0.6 degrees between maxima and minima of an almost perfect sinusoidal variation. We choose to place the crown glass between the plates of a capacitor in order to offer an isotropic energy background to the surface dipoles. At very low voltages, a regular interference pattern with even spacing of maxima-minima pairs is observed. At voltages higher than 0.3 volts this even distribution is altered and above 3 volts the pattern is uneven. This result is interpreted as due to an extra torque exerted on the surface dipoles by the electric field set up across the dielectric by the capacitor voltage. Finally, we report another Trial#2 of this coherent case experiment, but with a slightly different angular alignment and observe that no meaningful interference pattern emerges. This is because most of the experimental data points happen not lie on the points of inflection of a sinusoidal pattern. This study can lead to an interesting Opto-electronic switch and can also be used to generate Optical Bits.

Doctoral / Early Stage / Poster 15

Presenter: Md Mahbubur Rahman

Mentor: Dr. Robert Kelley Bradley

Department of Industrial Engineering

Lamar University

Research in Nanotechnology

Use of silicone micro-molds and UV-Curable Resin to Manufacture Single Wall Carbon Nanotube Carding Devices

Individual single-wall carbon nanotubes (SWCNTs) possess extremely high mechanical strength but individual SWCNTs cannot be utilized for most applications; they must be aligned to take full advantage of their properties. Our work focuses on a low-cost industrially viable method for aligning raw SWCNTs. Previously our group developed a technique similar to traditional textile carding utilizing a microfabricated carder array. We currently use a Nanoscribe Photonics Professional GT stereolithography system to create the carders, but the process is expensive for the large-scale production necessary to produce the samples we need for future research. We present a method utilizing silicone micromolds to replicate the carders in a way that is inexpensive, takes only minutes, and results in high-precision replicas. The process of mold making destroys the original carder, and the silicone mold produced has a limited life. To overcome this challenge, we report on a process to create a silicone master mold that is used to make a set of master patterns, that in turn are used to make a large number of working molds.

Master Pattern with two pyramids

Master Mold

Master Pattern with one pyramid

Doctoral / In-progress / Poster 16

Presenter: Daniel Quispe

Mentor: Dr. Mel Ulmer

Ulmer Research Group

Department of Physics and Astronomy.

Northwestern University, IL

Research in Material Sciences

A Concept for deployable Normal Incidence UV Mirror Based on Shape Memory Alloy Sheets

Based on the science case for the SMEX ESCAPE mission, a normal incidence EUV mirror mission would be an interesting follow-on. Our provisional SmallSat/CubeSat design has a 1 m diameter primary deployable mirror. The mirror would be coated with multilayers for normal incidence EUV reflectivity. The deployable mirror substrate is a shape memory alloy (SMA). The SMA needs to be over-coated with a material that can be polished to achieve a reflective surface finish. The combination that worked well on an aluminum cylinder is a high phosphorous content electroless nickel (eNiP) super-polished and then coated with carbon nitride (CNx). The multilayers were deposited on the eNiP+CNx stack. We report here our progress toward putting in place the pieces for a proof of concept. And discuss a scale-up of the previous return to shape on sheets of NiTi and the ray tracing results that demonstrate a sufficient return to shape of 1 micron. Furthermore, corrections post-deployment are possible if desired.

https://www.spiedigitallibrary.org/conference-proceedings-of-spie/12181/1218131/A-concept-for-a-deployable-normal-incidence-EUV-mirror-based/10.1117/12.2630153.full

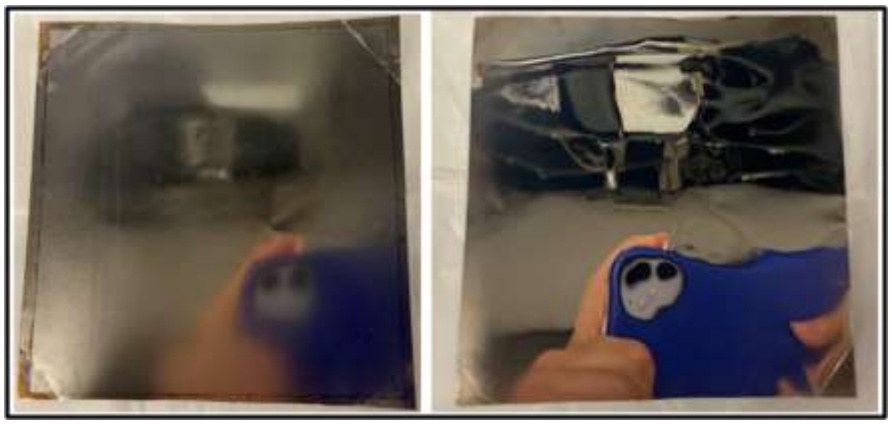

Doctoral / Early Stage / Poster 17

Presenter: Seyyed Saeed Vaezzadeh

Mentor: Dr. Robert Kelley Bradley

Department of Industrial and System Engineering

Center for Midstream Management and Science

Lamar University

Research in Plastic Composites

Creep-Resistant Thermoplastic Composites for Load-Bearing Applications

Injection molding is a common manufacturing technique for mass producing low-cost parts from thermoplastics. Due to their toughness, thermoplastic parts can be used in load-bearing applications. Their use as pipe support pads for corrosion prevention is a noteworthy instance. When load is initially applied there is an elastic deformation, however, under conditions of constant load time-dependent deformation (creep) will also occur. We use a custom aluminum mold made by CNC machining to create thermoplastic composite samples. Thermoplastics and filler materials are mixed and injected into the mold using a Galomb Mix-Molder system. Creep resistance of samples will be tested using a custom instrument similar to that described in the ASTM D2990 creep testing standard.

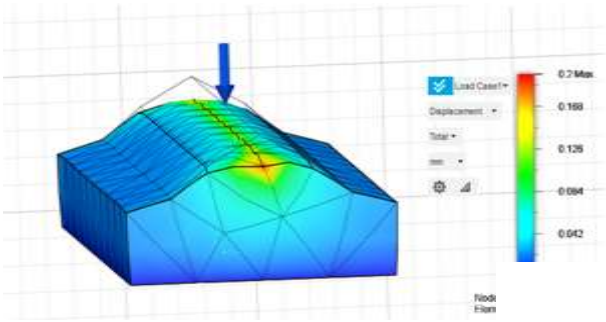

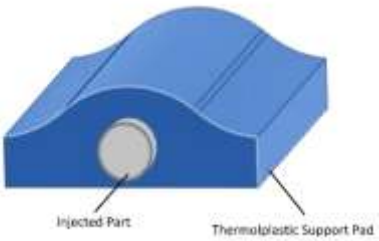

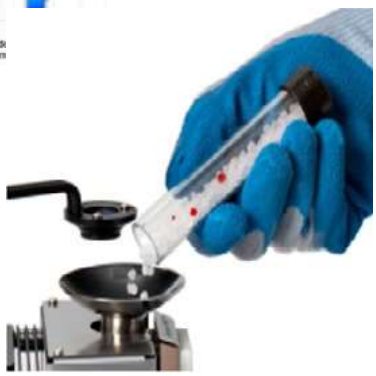

Undergraduate / Early Stage / Poster 18

Presenter: Tyler Stuck[1,2]

Mentor: Dr. Suaza[2] and Dr. Oraby[2]

Department of Mathematics, Lamar University

The University of Rio Grande Valley

Research in Fractional Differential Equations

Deep Learning and Solutions for Fractional ODEs

Fractional differential equations (FDEs) are useful as they can be used to model the spread of infectious diseases and rheological properties. These differential equations can be solved numerically, and their solutions simulated with multiple methods including neural networks. Do to the nature of the FDEs we are unable to just to take one point from the past to predict the future points. There must be three previous points considered before predicting the next point. The graph produced by the Neural Network is in good agreement with that produced by the Monte Carlo simulation. The mean squared error for the simulation when $\beta = 0.5$ was 3.9833e−10. The mean squared error for the simulation when $\beta = 0.9$ was 2.0942e − 9. We would like to continue to develop ways of plotting higher β order FDEs for future applications in disease modeling and rheological properties. In addition to furthering our ability to model fractional differential equations, we will work towards the inclusion of modeling fractional partial differential equations. This would allow us to simulate more complex situations.

Acknowledgements: This project was funded by the National Science Foundation – Research Experience for Undergraduates (REU) site at The University of Texas Rio Grande Valley.

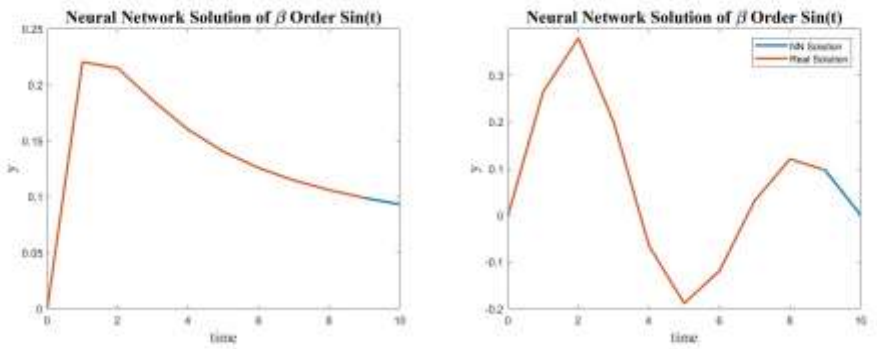

The graph on the left shows the β order FDE evaluated at $\beta = 0.5$, while the graph on the right is when the β order FDE is graphed at $\beta = 0.9$.

Undergraduate / Early Stage / Poster 19

Presenter: Tarin Hill

Co-author: Haley Snyder

Mentor: Dr. Ozge Gunaydin-Sen

Department of Chemistry and Biochemistry

Lamar University

Research in Chemistry

Exploiting the hydrogen storage properties of ammonia borane with the addition of polyacrylic acid and calcium chloride: Thermal and kinetic studies

Ammonia borane (AB) has a high capacity for hydrogen storage in a solid state, which the energy sector of the automotive industry can use as an efficient and effective fuel for the hydrogen fuel cell. To effectively use hydrogen as a clean fuel source, further studies are needed to expedite dehydration kinetics, increase efficiency, and reduce unwanted byproducts. The composites of AB blending with polyacrylic acid (PAA) were prepared using the sol-gel method. In addition to that, catalysts ($MgCl_2$ and $CaCl_2$) were added to AB:PAA composites to investigate any further improvement. The kinetic and thermal properties of the composites were then compared with pure ammonia borane. The preliminary experiments of kinetic studies were conducted using Differential Scanning Calorimeter (DSC). The AB:PAA results were shown to have a decreased activation energy when combined with $CaCl_2$ as a catalyst, these results show that there is a faster reaction meaning the kinetic property is improved through this combination of composites. Research is currently being done using different ratios of AB and PAA, different amounts of water, and possibly the use of different polymers or salts as a catalyst such as $BeCl_2$. Other studies include measuring the thermal decomposition of the composites via thermo-gravimetric analysis (TGA) and investigating the bonding properties, i.e. interaction between AB, PAA, and the catalysts using Fourier Transform Infrared spectroscopy (FTIR). These tests will further help to uncover the unwanted byproduct during the dehydrogenation using the TGA and give the ability to eradicate these gases from the processes in the future.

Breakout sessions

In alphabetical order and student academic ranking

Undergraduate / In-progress / Talk

Presenter: Angel Flowers[1]

Mentors: Latha Thomas[2], Kathy Jackson[3],

Matthew P. Hoch.[1], and William R. Miller[4]

[1]Department of Biology, Lamar University

[2]Department of Biology, University of Belize, Belmopan, Belize

[3]Department of Biology, McNeese State University, Lake Charles, LA

[4]Department of Biology and Chemistry, Baker University, Baldwin City, KS

Research in Ecology

Tardigrades of Belize

Tardigrades are aquatic invertebrates found in marine, freshwater, and moist terrestrial habitats across almost every ecosystem on earth. Most closely related to arthropods and onychophorans, the phylum Tardigrada encompasses over 1400 species to date. It is thought that only one-tenth of species have been discovered and described in the literature. The biogeographic relationships between North, South, and Central American tardigrades have received little attention due to the paucity of sampling in Central America. Based on limited collections mostly from Costa Rica, many tardigrade species from Central America appear unique and specific, while North and South America share some species, suggesting more complex biogeographic processes in Central America than explained by the Great American Biotic Interchange hypothesis alone. One country with no previous record of tardigrades is Belize, a beautiful, rich, tropical country situated on the Yucatan Peninsula facing the Caribbean Sea. This research serves to increase the knowledge of tardigrade biogeography in Central America and to further understand the drivers of species distributions.

Moss and lichen samples were collected in June 2022 from moist habitat types across Belize: cliff faces, waterfalls, cave entrances, and along forest trails. These were located within four different regions of Central Belize: Mountain Pine Ridge Forest Reserve, Chiquibul National Park, Cockscomb Basin Wildlife Sanctuary, and Monkey Bay Wildlife Sanctuary. Samples were obtained by scrapping the moss or lichen into a labeled paper

bag and allowed to dry thoroughly. Samples were prepared for processing by placing approximately one gram of dry sample into 20 mL of water and then soaking for 24 hours. Three, one- mL drops of water were placed in individual, black-backed dishes. These subsamples were observed using stereomicroscopes, and tardigrades extracted with an Irwin Loop were placed in double-stain before mounting to labeled slides in PVA medium, topping with a coverslip. The Coverslips were later sealed using clear nail polish to preserve the specimen. Tardigrades mounted to slides were later preliminarily identified to genus using light microscopy of morphological features. Target samples were then re-sorted for specimens to commit to DNA analysis and SEM imaging. Molecular analysis involved extracting single tardigrade DNA with Quick Extract (Lucigen), PCR amplification of COI and 28SrRNA genes, and both forward and reverse Sanger sequencing gene amplicons. Sequences obtained were compared to others in Genbank using NCBI BLASTn search tool to verify genus and species where possible.

Presently, 673 tardigrade specimens have been identified from Belize representing 18 species. Four species are in the Echiniscidae family of class Heterotardigrada. For class Eutardigrada, the numbers of species identified in four families were three Mlinesiidae, four Doryphoribiidae, five Macrobiotiidae, and two Hypsibiidae. This research project is presently still in progress, and samples and data are still being processed. It is believed the number of Tardigrade species from Belize will continue to climb as the remaining samples are processed. The results will be compared to prior studies of Central, South, and North America to support or offer new insights to current understanding for tardigrade biogeography across the Americas.

Acknowledgements- This work was supported by Lamar University, 2022 David J. Beck Fellowship awarded to A.M.F.

Undergraduate / Advanced / Talk

Presenter: Kayla Meyers

Co-authors: Cara L. Anderson and Adam A. Germain

Mentor: Dr. Young-Tae Kim

Department of Biomedical Engineering, College of Engineering

University of Texas at Arlington, Arlington, Texas

Research in Bioengineering

Melanoma Chemotherapy Treatment using Modified Cellulose-Based Injectable Hydrogels Combined with Temozolomide

Melanoma, the rarest form of skin cancer, is responsible for about 75% of all skin cancer deaths. A local delivery method of an injectable modified cellulose nanofiber hydrogel, DNCNF PAA 10%, loaded with the chemotherapy drug temozolomide, TMZ, was studied to investigate the most effective and safest therapy window on duke melanoma 6 (DM6) and human dermal fibroblast cells (HDF-α).

Loaded hydrogel concentrations of 25μM-1000μM were tested against the controls of no hydrogel, hydrogel alone, and free-drug TMZ. The treatments were administered inside PDMS microcurrent device for 72 hours, removed, cells stained, and quantified. For the long-term study, treatment was administered for 72 hours, treatment removed, and cells recovered for 72 hours. The data was quantified using a fluorescent live/dead cell assay and cells counted using ImageJ, Excel, and R/ANOVA with a significance of $p \leq 0.05$.

There was a plateau from 25μM-100μM, similar to hydrogel alone and a cell death dosage effect seen after the 250μM TMZ hydrogel treatment as the concentrations increased. The 500μM TMZ hydrogel had ~7-14% DM6 viability with ~50% HDF-α viability. Dosages higher than the 500μM TMZ hydrogel treatment and free 500μM TMZ had nonspecific killing of both cell types. The long-term melanoma recovery study showed surviving melanoma have possible TMZ resistance.

The most effective and safest therapy window was DNCNF PAA 10% 500μM-750μM TMZ. Currently, the treatment therapy window found is being studied further involving co-culturing of both cell types. Future studies recommended are TMZ resistance studies and in vivo animal studies.

Undergraduate / In-progress / Talk

Presenter: Zaid Mohammed[1]

Mentors: Dr. Ian Lian[1], Dr. Ryan Russell[2] and Zhihao Guo[2]

[1]Department of Biology, Lamar University

[2]Department of Cellular and Molecular Medicine, University of Ottawa, Ottawa, Canada

Medical Research

Role of Autophagy Receptors in Cancer

Autophagy is a self-digesting mechanism where damaged cellular components are sequestered by an autophagosome and fused with lysosomes for degradation. It serves as a natural recycling system as the nutrients gained from breaking down the old parts can be utilized to build new organelles. This is beneficial to a normally functioning cell as it removes cellular waste and maintains efficiency. However, research into the role of autophagy in cancer cells has shown that it could increase tumorigenesis. The autophagy pathway provides an alternative way for tumor cells to obtain nutrients in stressful conditions such as chemotherapy treatment. Thus, it is heavily linked to drug resistance in cancer cells. The pathway is regulated by a series of proteins, of which the Ulk complex is an upstream component, and inhibition of Ulk has been shown to shut down the pathway. However, not much is known about the specific roles that the other proteins in the pathway play in cancer cells. We are looking for any receptors which, if inhibited, have a similar effect as the Ulk complex inhibition in fighting drug resistance and tumorigenesis, but still allow the pathway to function and perform its normal activities. This would be most advantageous, as shutting down the entire process can lead to adverse complications. This project utilizes a drug resistant MB49 cell line that has been infected with Nluc and OVA virus, and we will inhibit 84 autophagy receptors to observe the effects that each of them have on tumorigenesis and drug resistance.

Doctoral / Advanced / Talk

Presenter: Rahagir Ridwan Anik

Co-Author: Kalen Baker

Mentor: Dr. Ping He

Department of Mechanical Engineering, Lamar University

Research in Mechanical Engineering

An Explanation of Wetting Transitions between Cassie-Baxter and Wenzel States on Reentrant Micropatterned Surfaces

Since the finding of multi-hierarchical microstructures in lotus leaves, the concept of robust superhydrophobic surfaces is being reinvestigated in a new direction toward the hierarchical design. To explore the wetting transitions between Cassie-Baxter and Wenzel states in hierarchical microstructures, a Gibbs energy model has been developed for a set of reentrant micropatterned surfaces. This theoretical model was used to calculate the energy barrier between the Cassie to Wenzel states and vice versa. Using OpenFOAM, a 3-D wetting process of a 3-μL water droplet was simulated in three approaches. In the first approach, the droplet was initiated in the Cassie or Wenzel state at zero gravity on the micropatterned surface and allowed to rest in a stable state. Second, to measure energy barriers, the droplet was pulled from the Wenzel to Cassie state or pushed from Cassie to Wenzel state using a controlled body force. Finally, at varied initial velocities, droplet impacts on the micropatterned surfaces were simulated. A good analogy was found when the data between the theory and simulation were compared. This research explains the mechanism behind the robustness of the Cassie state on the reentrant micropattern surfaces, and thus paves the way to design robust superhydrophobic surfaces.

Doctoral/ In-progress / Talk

Presenter: Rishi Bhradwaj[1]

Mentor: Dr. Cristian Bahrim[2]

[1]Phillip Drayer Department of Electrical Engineering

[2]Opto-Electronics Laboratory, Department of Physics

Lamar University

Research in Optoelectronics

Comparison of the Interference Patterns between Non-Coherent and Coherent Laser Beams Illuminating the Same Dielectric Surface

We analyze the interference patterns for two cases: two different lasers (non-coherent case) and two identical lasers (coherent case) illuminating the same dielectric surface. In the non-coherent case, a probe laser of 650 nm and a much stronger coupling laser of 532 nm illuminate the same 2 mm spot on a crown glass surface. When 650 nm laser is used, a minimum is observed in the parallel component of the reflectance (which shows a parabolic variation) at Brewster angle of 56.6 Degrees. In theory, at the Brewster angle the parallel component of the normalized reflectance becomes zero, and the light reflected is 100% polarized in the perpendicular direction to the plane of incidence. When using two lasers, a Brewster region 2 degrees wide around the Brewster Angle is now observed. Outside the Brewster region, evenly distributed oscillations are observed, and at 59 degrees, a dip forms as a signature of the destructive interference between the two non-coherent laser beams.

In the coherent case, both the lasers are of 532 nm wavelength but have different intensities, where the probe is much weaker than the second (coupling) laser beam. In this case we observe a prominent peak at the Brewster angle, which indicates that the stronger coupling laser has taken over completely the weak probe laser. In this second experiment, the Brewster region shows a less than 2% noise. Outside the Brewster region, a regular interference pattern with an even spacing of 0.6 degrees between adjacent maxima and minima of an almost perfect sinusoidal variation is clearly observed. The variation from maxima to minima is between 10 to 15% and is not affected by the experimental noise. Practical implementation of this research can be in the creation of new Opto-Electronic switches and formation of Optical Bits on dielectric surfaces.

Doctoral / Early stage / Talk

Presenter: Hari Lal Kharel

Mentor: Dr. Thinesh Selvaratnam

Department of Civil and Environmental Engineering

Lamar University

Research in Environmental Engineering

Bioremediation of Lead Using *Galdieria sulphuraria*

Microalgae are increasingly being used in the bioremediation of heavy metals due to their numerous advantages, such as their wide availability, low cost, superior metal removal effectiveness, and environmental friendliness. Lead (Pb), one of the heavy metals, is carcinogenic and poisonous even in lower concentrations and poses risks to humans and ecosystems. A thermoacidophile unicellular red alga, *Galdieria sulphuraria*, generally thrives close to sulfur springs and can withstand exceptionally high acidity, high temperatures, and heavy metal-rich environments. This research aims to evaluate how lead affects the growth of *Galdieria sulphuraria* and the potential of using this microalga as a bioremediation method to remove/recover lead. Different Lead (Pb) concentrations, ranging from 5mg/L-100 mg/L, were introduced into growth media, and experiments on biological growth were carried out in triplicate at varied lead concentrations for 6 days. Results indicated that the growth decreased on the first day and started to increase until the fourth day. The corresponding ammonia and phosphorus level in the growth media also went down in the system on the sixth day of the experiment. Further, ICP-AES was used to analyze the metals present in the supernatant to determine whether or not *Galdieria sulphuraria* could effectively bioremediate the Pb. Results showed that Pb was effectively sorbed by the *Galdieria sulphuraria* and showed considerable removal values over the course of the growth experiment. These initial results provided encouraging results for the bioremediation of Pb using *Galdieria sulphuraria*.

Experimental Setup Photo:

Doctoral / Advanced / Talk

Presenter: Nader Madkour[1]

Co-author: Dr. Reda Amer[2] and **Dr. Berna Eren Tokgoz[1]**

Mentor: Dr. Berna Eren Tokgoz[1]

[1]Department of Industrial and Systems Engineering

[2]Department of Earth and Space Sciences

Lamar University

Research in Soil Erosion

A Critical Approach Towards a Change Detection Framework for Assessing Soil Degradation Rates

Soil erosion in ports has been always a great challenge for the port's officials especially after the occurrence of a natural disaster event. It is one form of the soil degradation that occurs in almost all types of land. Soil erosion occurs due to the loss of soil texture which contain small grains or open structure, or when the slope of the plane level of the ground is steep, or when the intensity of rainfall increases. Soil erosion is a critical environmental hazard facing the world of construction and ports in the modern world. Soil erosion has serious threats to hydraulic structures, agriculture, and the world's ecosystem. The resilience of US ports is increasingly challenged by disruptive events especially in southeast Texas such as regulatory change, adverse weather, larger container ship sizes, changing patterns of trade and sea routes, and the still to be quantified effects of enlarging the capabilities and capacity of the port of Port Arthur which is most famous by the oil boom in the early 1900s. Port sustainability requires the port decision-makers to be resilient towards land degradation and natural caused disasters in their practices, to sustain existing performance levels and to develop market share when opportunity presents. To assist ports to successfully develop policies to improve resilience, this study aims to detect the soil erosion rates by using remote sensing techniques implemented on high resolution images obtained from the Texas Natural Resources Information System (TNRIS) with resolution between 60 cm to 1 meter.

Ph.D. candidate / In-progress / Talk

Presenter: Prasad Pawar[1,2]

Mentor: Dr. Clayton Jeffryes[1,2,3]

[1]Nanobiomaterials and Bioprocessing Laboratory (NABLAB),

Dan F. Smith Department of Chemical Engineering

[2]Center for Midstream Management and Science

[3]Center for Advances in Water & Air Quality

Lamar University

Research in Bioprocessing

Demulsification of Tight Crude Oil-Water Emulsions Under Microwave Radiation in Presence of Chemical Demulsifiers

The main objective of this study is to use microwaves to develop an energy efficient and economical separation method to demulsify stable crude oil and water emulsions. The crude oil emulsions are formed by high shear mixing of process water and crude oil during pumping, desalting and transportation. These highly stable tight crude oil emulsions often cause serious problems to the wellbores and pipelines such as clogging, corrosion, and pump failures. Chemical demulsification method is most commonly used by addition of chemicals called demulsifiers. The surface active demulsifiers move to the oil/water interface and weaken or break the rigid films present in the emulsion. Graphene oxide (GO) has oxygen containing functional groups like epoxide, hydroxyl, carbonyl, and carboxyl groups. Polyethylene glycol is a hydrophilic chemical demulsifier used for crude oil water separation. Here we have prepared a hydrophilic nanohybrid structure (GO-PEG) using graphene oxide and polyethylene glycol (PEG). To simulate field conditions, we mixed two crude oils to prepare samples with American Petroleum Institute (API) gravities between 28.9° and 46.0° and were mixed with water to create emulsions containing between 20% and 80% water. This array of Water-in-Oil (W/O) and Oil-in-Water (O/W) emulsions with different densities and viscosities were mixed at varying shear rates. A series of batch demulsification runs of these crude oil emulsions were done by exposure to microwaves for a set of parameters such as temperature, power, time, and salinity. For phase separation efficiency, final oil-phase water content was measured using Karl Fischer Titration.

Doctoral / In-progress / Talk

Presenter: Premkumar Ravishankar[1]

Co-Authors: Dr. Seokyon Hwang[3] and Dr. Jing Zhang[2]

Mentor: Dr. Berna Eren-Tokgoz[1]

[1]Department of Industrial and Systems Engineering

[2]Department of Computer Science

[3]Construction Management Program

Lamar University

Research in Oil Industry

Increasing The Oil and Gas Pipeline Resiliency

Using Image Processing Algorithm

Since the finding of multi-hierarchical microstructures in lotus leaves, the concept of robust superhydrophobic surfaces is being reinvestigated in a new direction toward the hierarchical design. To explore the wetting transitions between Cassie-Baxter and Wenzel states in hierarchical microstructures, a Gibbs energy model has been developed for a set of reentrant micropatterned surfaces. This theoretical model was used to calculate the energy barrier between the Cassie to Wenzel states and vice versa. Using OpenFOAM, a 3-D wetting process of a 3-μL water droplet was simulated in three approaches. In the first approach, the droplet was initiated in the Cassie or Wenzel state at zero gravity on the micropatterned surface and allowed to rest in a stable state. Second, to measure energy barriers, the droplet was pulled from the Wenzel to Cassie state or pushed from Cassie to Wenzel state using a controlled body force. Finally, at varied initial velocities, droplet impacts on the micropatterned surfaces were simulated. A good analogy was found when the data between the theory and simulation were compared. This research explains the mechanism behind the robustness of the Cassie state on the reentrant micropattern surfaces, and thus paves the way to design robust superhydrophobic surfaces.

Doctoral / In-progress / Talk

Presenter: Negar Saraei

Mentor: Thinesh Selvaratnam[1] and Dr. Berna Tokgoz[2]

[1]Department of Civil and Environmental Engineering

[2]Industrial and System Engineering

Lamar University

Research in Resiliency

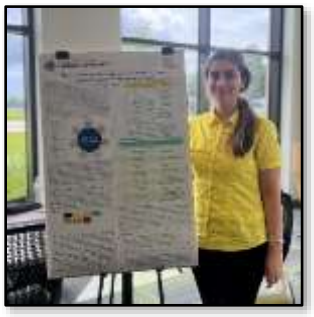

Developing a Resilience Framework for Jefferson County, Texas

Resilience is often defined as the capacity of a region to prepare for, respond to, and recover from hazards with the least possible harm to the general public's safety and health. This study focused on a literature review of all existing resilience frameworks and developing a tailored framework for Jefferson County. Based on the initial reviews of the frameworks, the data have been divided into geographical locations and further divided into five dimensions: infrastructure, environmental, economic, social, and health. For this study, we have focused only on the environmental dimension. We have analyzed all the literature and compiled a total of 127 environmental indicators in the environmental dimension. Regarding the environmental dimension, indicators measurement was quantitative, and weight allocation was used to measure the indicators. Among the 57 resilience frameworks collected during the literature review, the PEOPLES framework was chosen as the source of measurement, and the data was gathered from public databases. When evaluating the system's resilience, historical and ongoing data was analyzed through Geographic Information Systems (GIS). For calculation, a survey was set up statistically among the experts and was implemented to prepare the interdependency matrix. The resilience of the environmental dimension was determined by using the data from the GIS, along with the matrix's analysis, the weighting of the pertinent indicators, and the initial and post-disaster functionalities. Functionality before the occurrence of the disaster can be improved by understanding the degree of resilience in the area. Lastly, resilience planning reduces vulnerabilities to allow the communities to persist despite natural changes. Overall, this study provides the initial steps to developing a resilience framework for Jefferson County utilizing the existing frameworks.

2022-23 LURA Officers

President:

Zaid Mohammed

Major: Biology

Event Coordinator:

Tyler Stuck

Major: Physics and Math

Vice President:

Hannah Norwood

Major: Biology

Recruitment Director:

Tomisin Egbewale

Major: Computer Science

Treasurer:

Liam Gore

Major: Biology

Communications Director:

Morgan Luke

Major: Biochemistry

Secretary:

David Matherne

Major: Biology

OFFICE OF UNDERGRADUATE RESEARCH
LAMAR UNIVERSITY

Join our student organization:

Lamar University Undergraduate Research Association (LURA)

"LURA was founded in fall 2019 to fulfill the need for a community *by* and *for* undergraduate students to discuss, collaborate, and learn how effectively one can conduct research. The consistent quality and volume of research conducted by undergraduate students at Lamar University has made it clear that there is a need for an organization to act as a vital resource for building young researchers. Thus, LURA provides an academic forum that connects all level students from freshmen to seniors with their professors and mentors, and facilitates communication between Lamar undergraduates and their peers around the nation.

LURA is a platform for offering panel discussions about

- Research opportunities inside and outside Lamar,
- Better ways to deliver undergraduate research results in poster and oral presentations,
- Ways to perform peer-mentoring,
- Organizing workshops and panel discussions on various topics, including how to successfully apply to graduate schools.

LURA is the premier student organization at Lamar University for any undergraduate student interested in doing research. The Office of Undergraduate Research provides strong support and offers logistics to this student organization. Contact URALamar@gmail.com or visit the Office of Undergraduate Research—Chemistry 115D

For More Information about O.U.R. programs

DR. CRISTIAN BAHRIM - DIRECTOR OF O.U.R.
OFFICE: CHEMISTRY 115B, PHONE: 409-880-8290,
E-MAIL: CRISTIAN.BAHRIM@LAMAR.EDU

MS. JENNA ERWIN -
OFFICE - CHEMISTRY 115A, PHONE 409-880-8430,
E-MAIL: JERWIN6@LAMAR.EDU

Satellite Workshop 1

OFFICE OF UNDERGRADUATE RESEARCH
LAMAR UNIVERSITY

Join the O.U.R. workshop on

Planning for Graduate Studies

Come and meet our LU alumni



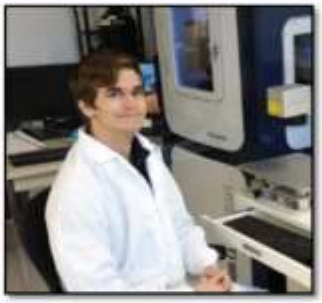

Alexus Locke Daniel Quispe Dylan Palmer

Alexus Locke — Clinical Research Coordinator, Atlanta; MS graduate from Cornell University.
Daniel Quispe— Ph.D. candidate at Northwestern University, Chicago.
Dylan Palmer — Ph.D. candidate at Colorado School of Mine, Denver.

Moderator: Dr. Chun-Wei Yao, Assoc. Prof. of Mechanical Engineering

Learn to be better prepared for a successful graduate school experience

November 4th — from 11 to 1:00pm

in the Landes Auditorium of Galloway bldg.

Pizza and beverages will be served!

FOR MORE INFORMATION PLEASE CONTACT:

Dr. Cristian Bahrim, Director of O.U.R. — cristian.bahrim@lamar.edu, 409-880-8290, Archer 100D
Ms. Jenna Erwin, Administrative Specialist — jerwin6@lamar.edu, 409-880-8430, Chemistry bldg., 115A

Satellite Workshop 2

OFFICE OF UNDERGRADUATE RESEARCH
LAMAR UNIVERSITY

Join the O.U.R. workshop on

Getting a Doctoral Degree in Electrical Engineering

Jay Prigmore

David Quispe

Dr. Jay Prigmore — Ph.D. in Electrical Engineering at Arizona State University —Electrical Quality Engineer—Technical Program Manager at Google Inc.

Mr. David Quispe— Ph.D. candidate at Arizona State University, Tempe.

Moderator: Dr. Gleb Tcheslavski, Assoc. Prof. of Electrical Engineering.

Learn About the Benefits of Pursuing Doctoral Studies

November 4th — from 1:30 to 2:30pm
in the Landes Auditorium of Galloway bldg.
Food and beverages will be served!

FOR MORE INFORMATION PLEASE CONTACT:
Dr. Cristian Bahrim, Director of O.U.R. – cristian.bahrim@lamar.edu, 409-880-8290, Archer 100D
Ms. Jenna Erwin, Administrative Specialist – jerwin6@lamar.edu, 409-880-8430, Chemistry bldg., 115A

Satellite Workshop 3

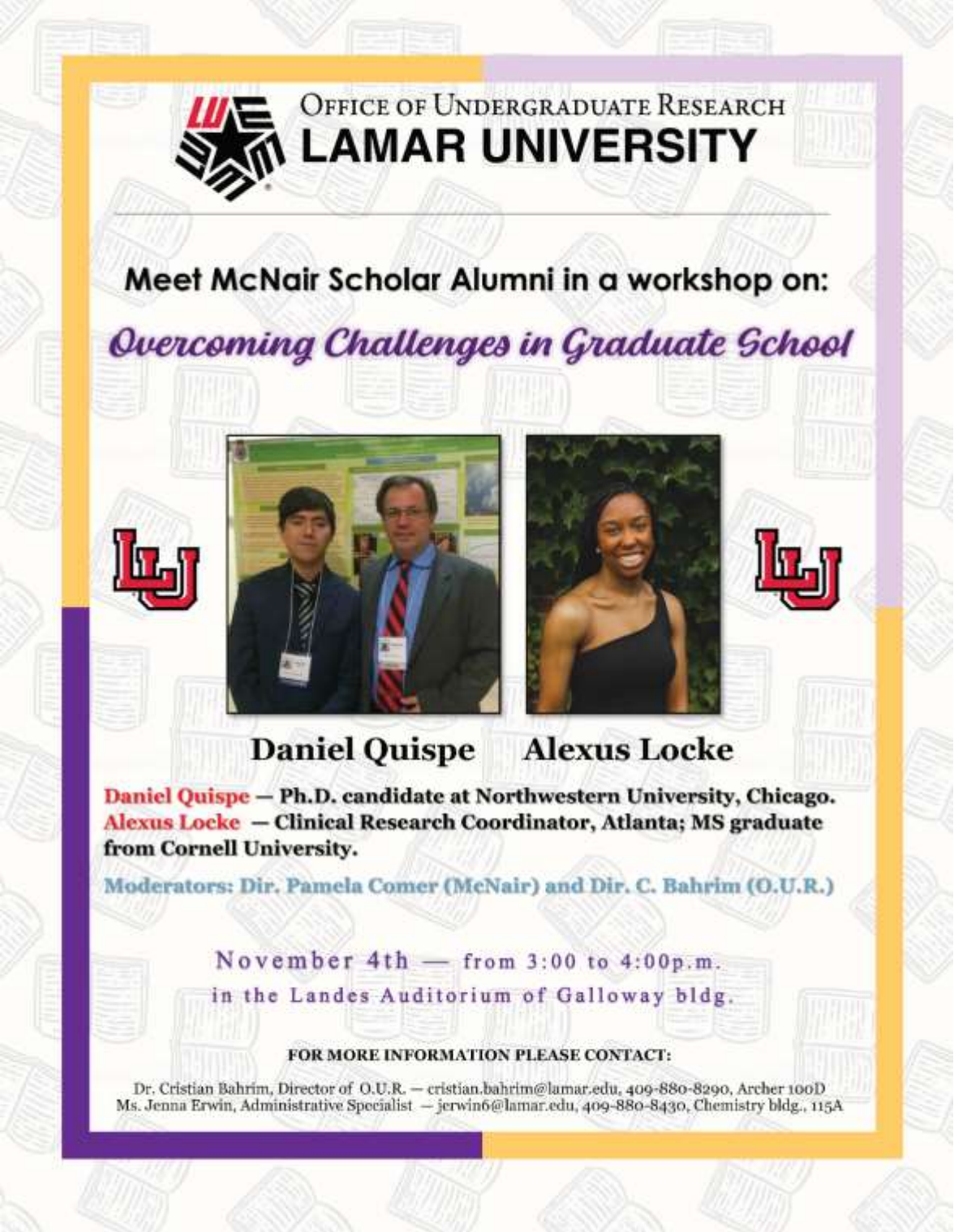

OFFICE OF UNDERGRADUATE RESEARCH
LAMAR UNIVERSITY

Please join us at our next STEM conferences

THE 10TH ANNUAL

Undergraduate Research & Creative Activity - Expo 2023

April 14, 2023 - Setzer Center

October 28, 2023

THE 11TH ANNUAL

Texas STEM Conference